

1999

Hydrogeology and Paleohydrology in the Williamson River Basin, Klamath County, Oregon

Jeffrey Scott Conaway
Portland State University

Follow this and additional works at: https://pdxscholar.library.pdx.edu/open_access_etds



Part of the [Geology Commons](#)

Let us know how access to this document benefits you.

Recommended Citation

Conaway, Jeffrey Scott, "Hydrogeology and Paleohydrology in the Williamson River Basin, Klamath County, Oregon" (1999). *Dissertations and Theses*. Paper 6378.

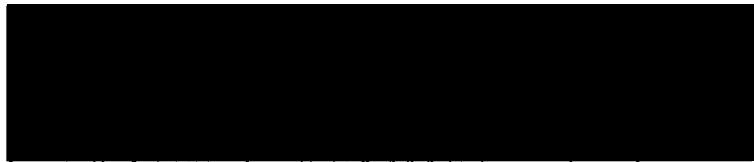
<https://doi.org/10.15760/etd.3524>

This Thesis is brought to you for free and open access. It has been accepted for inclusion in Dissertations and Theses by an authorized administrator of PDXScholar. Please contact us if we can make this document more accessible: pdxscholar@pdx.edu.

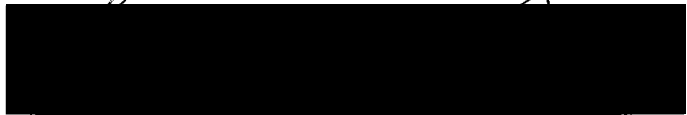
THESIS APPROVAL

The abstract and thesis of Jeffrey Scott Conaway for the Master of Science in Geology presented December 8, 1999, and accepted by the thesis committee and the department.

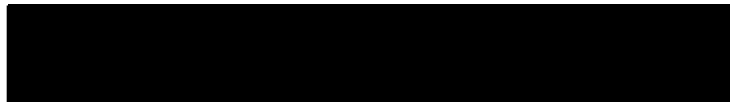
COMMITTEE APPROVALS:



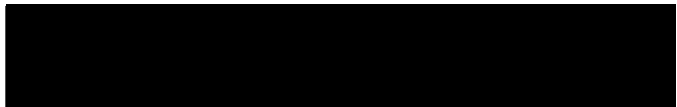
Michael L. Cummings, Chair



Jim E. O'Connor

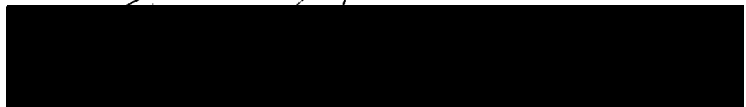


Kenneth M. Cruikshank



Roy W. Koch
Representative of the Office of Graduate Studies

DEPARTMENTAL APPROVAL:



Ansel G. Johnson, Chair
Department of Geology

Abstract

An abstract of the thesis of Jeffrey Scott Conaway for the Master of Science in Geology presented December 8, 1999.

Title: Hydrogeology and Paleohydrology in the Williamson River Basin, Klamath County, Oregon.

Stress on the water resources of the Williamson River basin has led to their regulation to protect important habitat. Quantification of this resource is required for accurate regulation. A portion of this study is a hydrogeologic reconnaissance that suggests directions for future work. Measured discharge and deuterium isotope data from points above and below the Williamson River canyon indicate that the river receives 99% of its discharge from ground water during periods of low flow. The principle aquifer of the southern Klamath Marsh is a fractured basalt, while continental sediments that are up to 200 m thick provide high artesian yields south of the canyon. The disparity between high precipitation on the basin's western margin and the low and variable discharge of the Williamson River at the Kirk Sill suggests either the presence of a fault zone that interrupts the flow of ground water or deep flow paths that do not surface within Klamath Marsh.

Three terraces line the eastern edge of Klamath Marsh at approximate elevations of 1380, 1385, and 1397 m. The lowest terrace is late Holocene and cut into marsh sediment and reworked deposits from the pyroclastic eruptions of Mount Mazama. The middle terrace is planed into bedrock and formed when Pleistocene Lake Chemult

occupied this basin. The upper terrace, a strand line, is delineated by a slope break that separates reworked pyroclastic deposits from undisturbed pyroclastic fall. Formation of this terrace occurred when pyroclastic flows from the cataclysmic eruption of Mount Mazama formed a blockage in the Williamson River canyon. Resultant backflooding reworked pyroclastic deposits and rafted pumice up to an approximate elevation of 1400 m. The blockage failed catastrophically from overtopping, draining $5.7 \times 10^9 \text{ m}^3$ of water, scouring the canyon and producing an erratic boulder deposit at the mouth of the canyon. Upstream evidence of rapid draining includes linear scour channels incised in pyroclastic-flow deposits and scouring of the broad Pleistocene terrace. Paleohydraulic reconstruction of down stream flooding using a flow-competence equation and a physically based dam-break model yield a peak discharge of $1.3 \times 10^4 \text{ m}^3 \text{ s}^{-1}$.

***HYDROGEOLOGY AND PALEOHYDROLOGY IN THE WILLIAMSON RIVER
BASIN, KLAMATH COUNTY, OREGON***

by

JEFFREY SCOTT CONAWAY

A thesis submitted in partial fulfillment of the
requirements for the degree of

MASTER OF SCIENCE
in
GEOLOGY

Portland State University
2000

Acknowledgments

This study was funded by a U.S. Geological Survey EDMap grant, and the Oregon Department of Geology and Mineral Industries. The Department of Geology kept me financially solvent with a teaching assistantship throughout my graduate work.

This research would not have been possible without the guidance and support from my advisor Michael Cummings. Grant writing, field visits, office visits, editing, and great discussions are some of the many contributions that he has made. His dedication to education is unsurpassed. Kenneth Cruikshank helped extensively with geostatistical analysis of geochemical data, GIS applications, and advice on structure. Jim O'Connor helped with the estimates of the magnitude of the downstream flooding. Marvin Beeson took time out of his retirement for my INAA work. GIS advice was also provided by David Percy. Paul Layer at the Geochronology Laboratory of the University of Alaska Fairbanks provided much needed age dating for the Wocus Bay quadrangle. Tom Douglas from the Earth Sciences Department at Dartmouth is acknowledged for his deuterium analysis. Winema National Forest provided maps and lent aerial photographs. My fellow students who listened to me talk about pumice for two years.

Field assistantship for the mapping project was dutifully provided by Charlie Palmer (Ponch). Ponch's hand augering, burrito recipes, and prowess with a Fat Cat are the modern legends of Klamath Marsh. Cynthia Restrepo assisted in the terrace surveys and boulder measurements. Stuart Cowburn and Heather Bragg helped gauge the mighty Williamson. Christy Lee provided information on the geology of Soloman Butte. Jason Hinkle swiftly elevated crew moral with ice cold Blitz, and a dozen donuts from Joe's. The Honda Corporation is acknowledged for producing the Fat Cat, the ultimate in central Oregon field transportation. The faithful service of my computer Ramona. Patricia Heiser provided helpful advice, a writing vacation at her farm, and fun visits. My parents have supported me morally and financially throughout my education.

Table of Contents

| | |
|--|----|
| Acknowledgments | i |
| Table of Contents | ii |
| List of Tables | iv |
| List of Figures | v |
| Chapter 1-Introduction | 8 |
| Climate | 11 |
| Geology | 12 |
| Chapter 2-Hydrogeology | 19 |
| Introduction | 19 |
| Previous Work | 22 |
| Methodology and Results | 23 |
| Williamson River discharge | 23 |
| Spring discharges | 25 |
| Deuterium analysis | 28 |
| Well logs | 28 |
| Discussion | 29 |
| Historic and measured discharge | 29 |
| Deuterium analysis | 38 |
| Well logs | 38 |
| Source and occurrence of ground water | 40 |
| Conceptual model A: No structural barrier | 42 |
| Conceptual model B: Structural barrier | 42 |
| Suggestions for further study | 44 |
| Hydrogeology Conclusions | 44 |
| Chapter 3-Paleohydrology | 47 |
| Introduction | 47 |
| Terraces levels | 48 |
| The middle terrace (late Pleistocene) | 52 |
| The upper terrace (middle Holocene) | 56 |
| Rafted pumice | 57 |
| Reworked pyroclastic-fall deposits | 59 |
| Scour channels | 62 |
| Scoured surfaces | 64 |
| Erratic boulders | 64 |
| The lower terrace (late Holocene) | 68 |
| Synopsis | 70 |
| Discussion | 72 |
| Rafted Pumice | 74 |
| Scour Channels | 74 |
| Catastrophic breaching of the pyroclastic flow dam | 75 |
| Magnitude of the outburst flood | 76 |
| Flow-competence | 77 |
| Empirically based dam-break analogy | 78 |

| | |
|--|-----|
| Physically based dam-break model | 78 |
| Evaluation of the discharge estimate techniques..... | 81 |
| Duration | 83 |
| Conclusions | 85 |
| References..... | 87 |
| Appendix A: Measured discharge data..... | 93 |
| Appendix B: Plots of Williamson River discharge and precipitaiton..... | 94 |
| Appendix C: Selected well logs | 102 |
| Appendix D: Projection of terrace levels..... | 113 |
| Appendix E: Soloman Butte hand auger descripitons..... | 116 |

List of Tables

| <i>Number</i> | <i>Page</i> |
|---|-------------|
| Table 1: Locaton (UTM Zone 10), discharge, and spring type for selected springs in the Wocus Bay and Soloman Butte quadrangles. | 27 |
| Table 2: δD values for water samples from the Wocus Bay and Soloman Butte quadrangles. | 28 |
| Table 3: Hydrologic units of the southern Klamath Marsh and their water-bearing properties. | 30 |
| Table 4: Hydrologic units of the Soloman Butte quadrangle and their water-bearing properties. | 31 |
| Table 5: Terrace elevations above prominent hydrophyllic vegetation and average elevations above sea level. | 49 |
| Table 6 : Area and volume of projected surface water elevations from terrace transect data. | 49 |
| Table 7: Pleistocene lakes of Oregon, modified from Dicken (1980). | 53 |
| Table 8: Location (UTM Zone 10), size, lithology, and velocity required for transport of measured boulders at the mouth of the Williamson River canyon. | 69 |
| Table 9: Summary of discharge estimates and variables. | 80 |

List of Figures

| <i>Number</i> | <i>Page</i> |
|--|-------------|
| Figure 1: Location of study with the Soloman Butte and Wocus Bay quadrangles, the Williamson River basin, and major water bodies highlighted. | 9 |
| Figure 2: Mean monthly precipitation and snow water equivalent with standard deviations from 1981-1998. Data are from USDA SNOTEL site Chemult Alternate (USDA, 1999). | 12 |
| Figure 3: Location of quadrangles, water bodies, and major water courses in the Williamson River basin. | 16 |
| Figure 4: Locations of discharge measurements within the Soloman Butte quadrangle. Coordinates are UTM Zone 10, contour interval 6 m. | 21 |
| Figure 5: Location of springs in the Wocus Bay quadrangle. Coordinates are UTM Zone 10, contour interval 6 m. | 26 |
| Figure 6: Annual mean discharge from 1955-1995 for the Williamson River with the three year moving average. Data are from U.S. Geological Survey stream gauge 11493500 (U.S. Geological Survey, 1999). | 33 |
| Figure 7: Discharge of the Williamson River at the Kirk Sill (U.S. Geological Survey, 1999) with cumulative snow water and precipitation (USDA, 1999) for 1993 | 34 |
| Figure 8: Discharge of the Williamson River at the Kirk Sill (U.S. Geological Survey, 1999) with cumulative snow water and precipitation (USDA, 1999) for 1995. | 35 |

- Figure 9: Annual mean discharge for the Williamson River at Kirk Sill (U.S. Geological Survey stream gauge 11493500) and annual precipitation from SNOWTEL sites Diamond Lake and Chemult Alternate. 36
- Figure 10: Proposed conceptual models for ground water flow in the southern Williamson River basin. Arrows indicate proposed ground water flow paths. Figure is not to scale. 43
- Figure 11: Locations of terrace transects (+), areas of rafted pumice (●), and scour channels in the Wocus Bay quadrangle. Coordinates are UTM Zone 10. 50
- Figure 12: Terrace transects. Elevation of Klamath Marsh is 1376 m. Vertical exaggeration is five times. 51
- Figure 13: Distribution of pyroclastic flows from the eruption of Mount Mazama (after Walker and MacLeod, 1992; Sherrod and Pickthorn, 1992; Conaway and Cummings, in preparation; and Lee and Cummings, in preparation) and the extent of backflooding (1400 m contour) that resulted from the blockage of the Williamson River. Dotted lines represent isopachs of pyroclastic fall from the eruptions of Mount Mazama. Thicknesses are in centimeters. 55
- Figure 14: Grain size analysis of samples collected from the middle Holocene terrace scarp at Hog Creek and Wocus Bay east. 60
- Figure 15: Thickness of pyroclastic-fall deposits on the middle Holocene terrace scarp at Hog Creek. Five times vertical exaggeration. 61
- Figure 16: Thickness of pyroclastic-fall deposits on the middle Holocene terrace scarp at Wocus Bay East. Five times vertical exaggeration. 62

- Figure 17: Scour channels and rafted pumice on the plateau west of the Williamson River canyon and location of the pyroclastic-flow blockage in the Soloman Butte quadrangle. Coordinates are UTM Zone 10, 6 m contour interval. 63
- Figure 18: Soloman Butte quadrangle with location of boulder deposit, wavy outcrop, and location of pyroclastic-flow blockage. Coordinates are UTM Zone 10, 6 m contour interval. 65
- Figure 19: Rounded boulder of the wavy textured basalt at the mouth of the Williamson River canyon. Boulder is 6.7 m in its longest dimension. 66
- Figure 20: Locations of rafted pumice (*), auger holes (+), gravel pit, and boulder deposit (stippled pattern) with average intermediate axis diameter of erratics. Coordinates are UTM Zone 10, 6 m contour interval. 67
- Figure 21: Three-stage development of terraces found along the eastern edge of southern Klamath Marsh. Figure is not to scale. 71
- Figure 22: Extent of backflooding that resulted from the pyroclastic-flow blockage in the Williamson River canyon. 73

CHAPTER 1: INTRODUCTION

The Klamath Basin is a large north-south-striking basin located in south-central Oregon and northwestern California. It occupies 14,700 km² in Oregon and lies in the transition zone between the Basin and Range and Cascade Range physiographic provinces. This basin contains the largest wetland complex in the western United States and is winter home to the largest concentration of migratory waterfowl in North America. This area also currently supports a \$200 million per year agriculturally based economy that includes over 100,000 head of cattle (Allen, 1999). Klamath Lake, which is located in the central portion of the basin, is the largest freshwater lake in Oregon. Two river systems flow into the lake: the Wood and the Williamson. The Williamson has the largest discharge and enters the lake from the north after flowing through Klamath Marsh. The Williamson River sub-basin covers 3,781 km² in the northwestern portion of the Klamath Basin (Figure 1). Illian (1970) delineated this sub-basin from topographic divides that he interpreted as groundwater boundaries.

Short-term variations in climate, issues related to water rights, and increases in consumptive uses of ground water resources in the Klamath Basin have prompted a detailed study of the hydrogeology. The first step in the overall study is to produce large-scale geologic maps to better understand the lithologies and structures that influence the movement of water. Portland State University mapped the Wocus Bay (Conaway and Cummings, in preparation) and Soloman Butte (Lee and Cummings, in

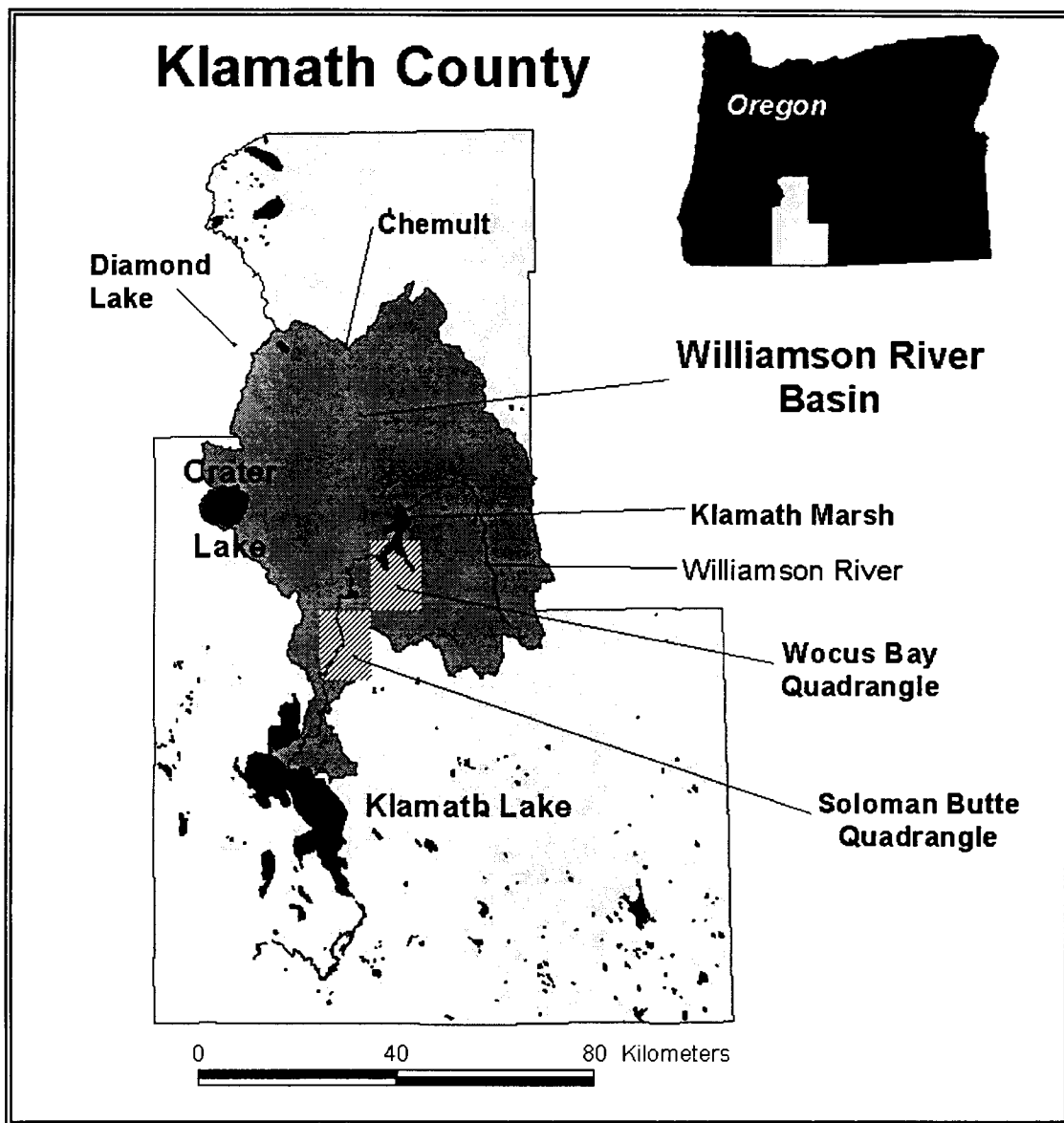


Figure 1: Location of study with the Soloman Butte and Wocus Bay quadrangles, the Williamson River basin, and major water bodies highlighted.

preparation) quadrangles. These data, as well as mapping done by the Oregon Department of Geology and Mineral Industries, will be incorporated into a basin-wide hydrologic assessment by the U.S. Geologic Survey Water Resources Division and Oregon Water Resources.

This thesis is the compilation of two studies, a hydrogeologic reconnaissance and an investigation of the basin's paleohydrology. The hydrogeology section, Chapter 2, is a preliminary investigation that can be used to provide direction for future work. The paleohydrology section, Chapter 3, concentrates on the geomorphic impacts of the cataclysmic eruption of Mount Mazama.

In Chapter 2 bedrock and surficial deposits, data on river and spring discharge, isotopic composition of surface and ground water, and water-well logs are examined to provide a preliminary view of the modern hydrology of the Williamson River basin. The objectives of this portion of the study are to:

1. Evaluate historic discharge data from the Williamson River at Kirk Sill
2. Determine the contribution from ground water to the flow of the Williamson River within the Williamson River canyon.
3. Define the principle aquifers in the southern Klamath Marsh and in the Soloman Butte quadrangle.
4. Develop preliminary conceptual models of ground water flow.

Chapter 3 investigates the record of water levels since the Pleistocene in the area that is currently occupied by Klamath Marsh. The objectives of this chapter are to:

1. Describe and define the process of formation for the terraces on the eastern edge of Klamath Marsh.
2. Describe the extent and affects of middle Holocene backflooding.
3. Evaluate the catastrophic failure of the blockage responsible for the middle Holocene backflooding.

Climate

The Klamath Basin has a semi-arid winter rainfall climate (Leonard and Harris, 1974). Precipitation data from 1981-1999 from the USDA SNOWTEL site Chemult Alternate at an elevation of 1450 m (USDA, 1999) indicate over seventy-five percent of the 68.15 cm ($\sigma \pm 23$ cm) of average annual precipitation in the Williamson River basin occurs during the months of October through March. The average snow water equivalent is 33 cm ($\sigma \pm 16$ cm) annually (Figure 2).

Large variations in temperature occur both seasonally and diurnally. The warm temperatures in summer (average high 26° C, temperatures in excess of 37° C are common) coupled with the reduced precipitation lead to high evapotranspiration rates. Orographic influences produce a humid alpine climate along the Cascade Range to the west while the basin remains semi-arid. The average annual precipitation 30 km to the west of Chemult at Diamond Lake (elevation 1620 m) (Figure 1) is 128 cm ($\sigma \pm 36$ cm).

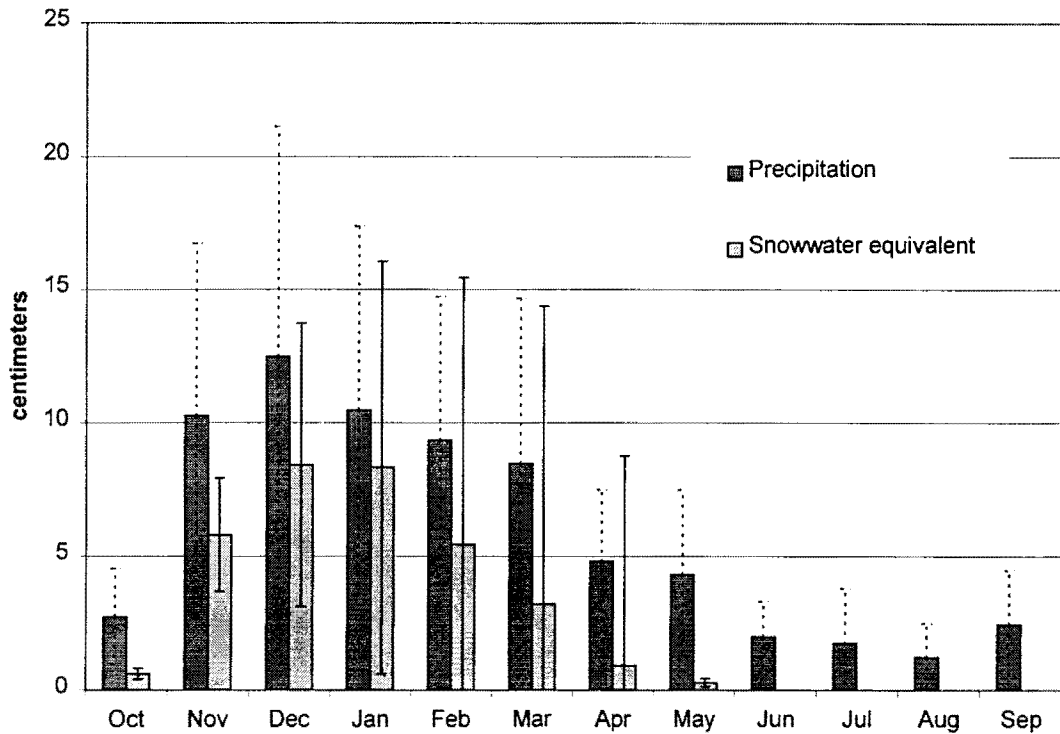


Figure 2: Mean monthly precipitation and snow water equivalent with standard deviations from 1981-1998. Data are from USDA SNOTEL site Chemult Alternate (USDA, 1999).

Geology

The Klamath Basin is the northwestern most extent of the Basin and Range province. The fault-block-mountains formed as a result of east-west crustal extension that began in the Miocene. In Oregon east of the Cascade Range and south of the Blue Mountains, this extension progressively decreases to the north as four right-lateral strike slip fault zones cross the province in an approximate west-northwest orientation (Lawrence, 1976).

The study area also lies partially within the Cascade Range province. The evolution of the Cascades is separated into five episodes of volcanism by Priest (1990).

1. (35-17 Ma) Local andesitic volcanism and voluminous eruptions of tholeiitic lava and silicic pyroclastic rocks.
2. (16.9-7.5 Ma) Volcanism preceded by a period of uplift and characterized by dacitic pyroclastic flows and pyroclastic falls, which began about 14 Ma, and voluminous eruptions of calc-alkaline two-pyroxene andesites and subordinate basaltic andesite and dacite.
3. (7.4-4.0 Ma) Eruption of voluminous basalt, basaltic andesite, and subordinate silicic pyroclastic flows and pyroclastic falls along a volcanic axis that is essentially coincident with the current High Cascades.
- 4 & 5. (3.9-0 Ma) The two episodes are separated at 0.735 Ma (beginning of the Brunhes normal magnetic polarity epoch) and have the same lithologies as episode 3, but the eruptions occurred over a narrower volcanic arc that was bound to the west by the uplifted Western Cascades and partially confined to the east by west-facing fault scarps.

This area is tectonically active as indicated by young fault scarps developed in alluvial fans and the occurrence of two moderate (M 5.9 and 6.0) earthquakes in 1993, which occurred approximately 30 km northwest of Klamath Falls in the West Klamath Lake fault zone. It has been estimated that this fault zone is capable of generating earthquakes as large as magnitude 7.25 (Lienau and Lund, 1993).

Sherrod and Pickthorn (1992) mapped the Williamson River basin at 1:250,000 scale. In this reconnaissance mapping the basalt and basaltic andesite flows, and vent deposits of the study area were assigned Pliocene to Pleistocene ages. The dominant surficial unit is pumiceous pyroclastic-fall lapilli and ash that are the product of the climactic eruption of Mount Mazama at $7,627 \pm 150$ cal yr B.P. (Zdanowicz et al., 1999). This cataclysmic eruption produced greater than 20 km^3 of tephra (dense-rock equivalent) that was distributed over 1.7 million km^2 in North America and had a plume height of 55 km during the Plinian phase of the eruption (Young, 1990; Gardner et al., 1998).

The geology of this basin is currently being mapped at a larger scale to be incorporated in a detailed hydrologic model. The Soloman Butte (Lee and Cummings, 1999), and Wocus Bay (Conaway and Cummings 1999) quadrangles have been mapped at a scale of 1:24000, and mapping of the Wildhorse Ridge quadrangle was conducted in 1999. The Wocus Bay and Soloman Butte quadrangles are investigated in this study because of proximity to Klamath Marsh, the course of the Williamson River, and the abundance of north-northwest-striking faults (Figure 1).

This mapping has furthered the understanding of the influences of structure on the geologic evolution of the basin. Volcanic centers are aligned along the north- and northwest-striking structural grain and are flanked by small sedimentary basins. The lithologies encountered are predominately basalt, basaltic andesite and andesite with interbedded sediment and pyroclastic deposits.

The stratigraphy and structure of the Wocus Bay quadrangle is described in Conaway and Cummings (in preparation). The following has been summarized from this source. The stratigraphy of the Wocus Bay quadrangle has been divided into four groups. Group 1 units are exposed predominately in the eastern half of the quadrangle and extend into adjacent quadrangles to the east (Buckhorn Springs), to the north (Military Crossing), and northeast (Wildhorse Ridge) (Figure 3). Deposition of these units occurred about 4 Ma. The predominate unit is a lithic-bearing, poorly welded rhyolitic tuff that is overlain by a sparsely phyrlic trachy andesite dated at 4.09 ± 0.05 Ma, and a basaltic andesite dated at 3.89 ± 0.08 . Also included in this stage are the trachyte, trachy andesite, and trachy dacite exposed at Little Wocus Butte, Wocus Butte, and the lower western flanks of Wocus Butte. The silica contents of these rocks are from 61 to 67 weight percent, the highest for bedrock units in the quadrangle.

Group 2 units are concentrated in the southeastern portion of the quadrangle and were deposited around 2 Ma. These basaltic andesite erupted from Soloman Butte to the southwest and from a local vent.

Group 3 is composed of high alumina olivine theoliite in the northwest portion of the Wocus Bay quadrangle and in the adjacent quadrangle to the north (Military Crossing). This unit has a characteristic diktytaxitic texture and is dated at 1.62 ± 0.47 Ma. The final group (4) includes pyroclastic-fall and pyroclastic-flow deposits from eruptions of Mount Mazama during the middle Holocene. These deposits overlie a well-developed paleosol and average approximately 3.5 m in thickness across the quadrangle.

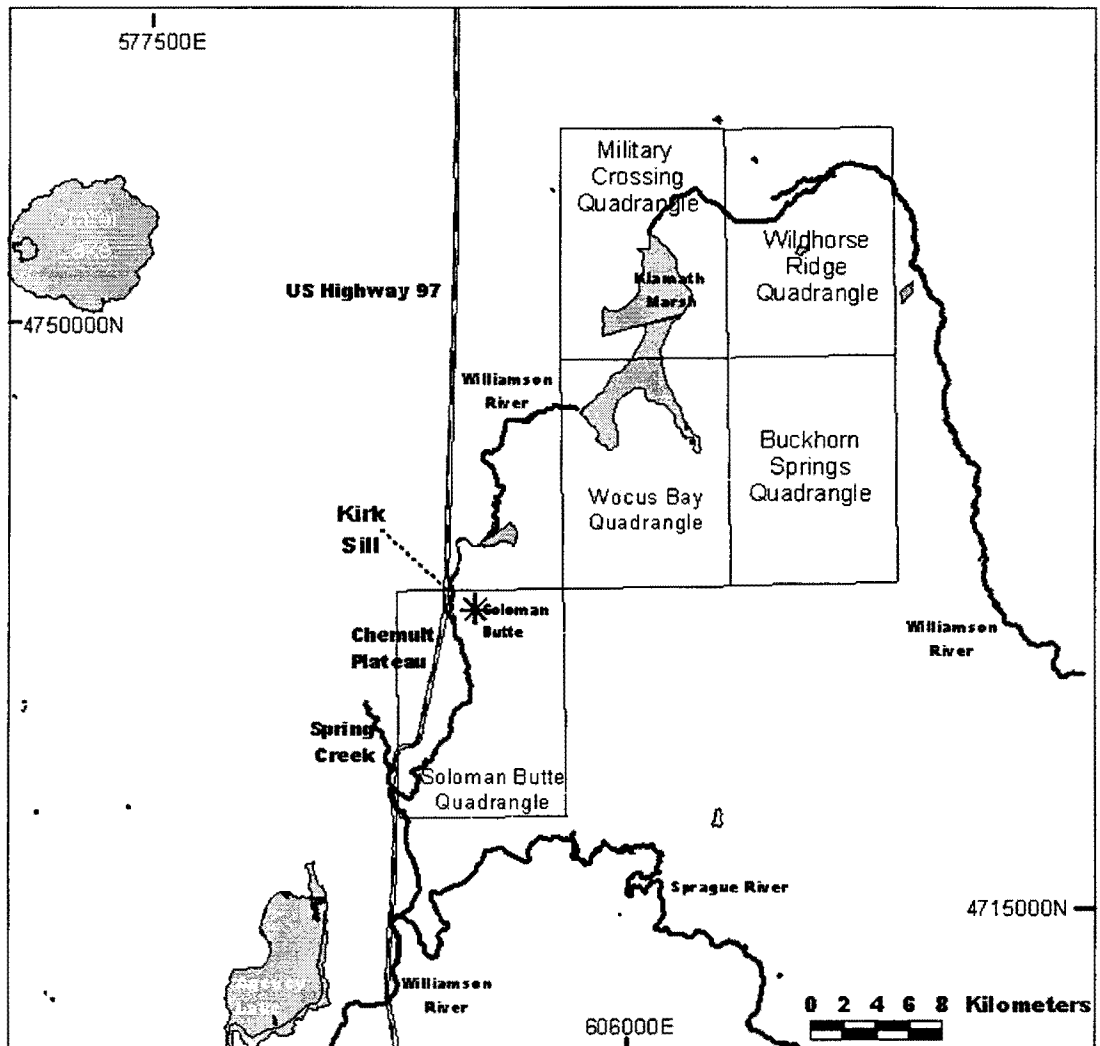


Figure 3: Location of quadrangles, water bodies, and major water courses in the Williamson River basin.

North-northwest striking, high-angle normal faults have dissected this quadrangle forming horsts, grabens, and tilted fault blocks. Deformation is thought to have occurred in two stages. Stage 1 deformation is recorded by ramping structures. Ramping structures are not found in units younger than those of group 1. Stage 2 deformation is characterized by dip-slip displacement that ranges from 15 m to 130 m and is thought to have occurred during the Pleistocene. Structure has influenced the extent of units and placement of volcanic centers in the quadrangle.

The source for at least some of the andesite flows of Group 2 appears to be Soloman Butte, a 300 m stratovolcano located in the northeastern corner of the Soloman Butte quadrangle. This correlation suggests that the Solomon Butte center is approximately two million years old, the age determination for one of the Group 2 flows in the Wocus Bay quadrangle. Lee and Cummings (in preparation) indicate that the Solomon Butte volcano overlies tholeiitic basalt flows that overlie basalt hydrovolcanic deposits and interfingered with fluvial/lacustrine siltstone and mudstone. The basalt flows and hydrovolcanic deposits line the canyon of the Williamson River west and southwest of Solomon Butte. West of the canyon of the Williamson River, a columnar jointed basaltic andesite flow caps the Chemult Plateau and overlies basalt hydrovolcanic deposits across an erosional unconformity. Pleistocene olivine-bearing andesite flows and cinder cones lie in the northwestern corner of the quadrangle and flows from one of these centers forms the bedrock barrier on the Williamson River at Kirk Sill. As in the Wocus Bay quadrangle, the Solomon Butte quadrangle is covered by a blanket of pyroclastic-fall deposits from Mount Mazama. Pyroclastic-flow deposits

cover the basaltic andesite flow of the Chemult Plateau and the upper reaches of the Williamson River in the Solomon Butte quadrangle (Lee and Cummings, in preparation). The modification to these deposits upstream from the Williamson River canyon, within the canyon, and near the mouth of the canyon are discussed in a later section of this study.

CHAPTER 2: HYDROGEOLOGY

Introduction

Ground water in the Klamath Basin is considered one of southern Oregon's most valuable resources (Illian, 1970). Demands for this resource have recently increased for uses other than irrigation and domestic use. In 1988, the U.S. Fish and Wildlife Service listed two endemic fish species, the Lost River Sucker (*Deltistes luxatus*) and the Shortnose Sucker (*Chasmistes brevirostris*) as endangered. To protect these species monthly minimum levels were designated for Upper Klamath Lake. To maintain these levels, upstream diversions of surface water for agricultural use must now be limited. Historical lake level records indicate that these required lake levels would not have been met 45 of the past 73 years without reductions in upstream diversions (Adams and Seong, 1998). Ground water resources will be called upon to compensate for decreased diversion and possibly to augment surface water levels. These issues have prompted a detailed study of the hydrogeology by the U.S. Geological Survey to develop a quantitative conceptual model and a numerical hydrologic model to test proposed use of ground water resources.

Surface and ground water enter Upper Klamath Lake from the Williamson River Basin, Sprague River Basin, and Upper Klamath Lake Basin. The Williamson River basin is bordered to the east and west by large volcanic peaks that are separated by a broad lowland. Klamath Marsh occupies 600 km² of this lowland and receives the

majority of its inflow from ground water that originates as precipitation on these volcanic uplands. The level of Klamath Marsh is controlled by the amount of ground water inflow, evapotranspiration, precipitation, surface water diversion, and consumptive uses of ground water. The level of the marsh is also limited by a topographic barrier. This barrier, the Kirk Sill (Figure 4), is a Quaternary basalt flow at the southern edge of the marsh. The lowland that contains Klamath Marsh is known as the Chemult Plateau and its southern boundary is located in the Soloman Butte quadrangle. The Williamson River, which originates from springs on the eastern edge of the basin (Figure 3), flows through the marsh then over Kirk Sill and through a 100-m deep canyon (Williamson River canyon). South of the canyon, the river is joined by Spring Creek, which also originates from springs. The river is then joined by the Sprague River and eventually empties into Upper Klamath Lake. The majority of the area of the Williamson River basin is upstream of Spring Creek, but the surface water contribution from this upper portion of the basin is only 17% of the total flow into Upper Klamath Lake (Gustafson, 1971). Approximately 28% of the total flow of the Williamson River into Upper Klamath Lake is from Spring Creek and during low flow months Spring Creek contributes almost the entire flow of the river (Gustafson, 1971). Spring Creek has a drainage basin of only 23 km².

This chapter synthesizes data gathered from the mapping of the Wocus Bay and Soloman Butte quadrangles, field investigations, water well logs, and climate records into a hydrogeologic reconnaissance of the southern portion of Klamath Marsh and the

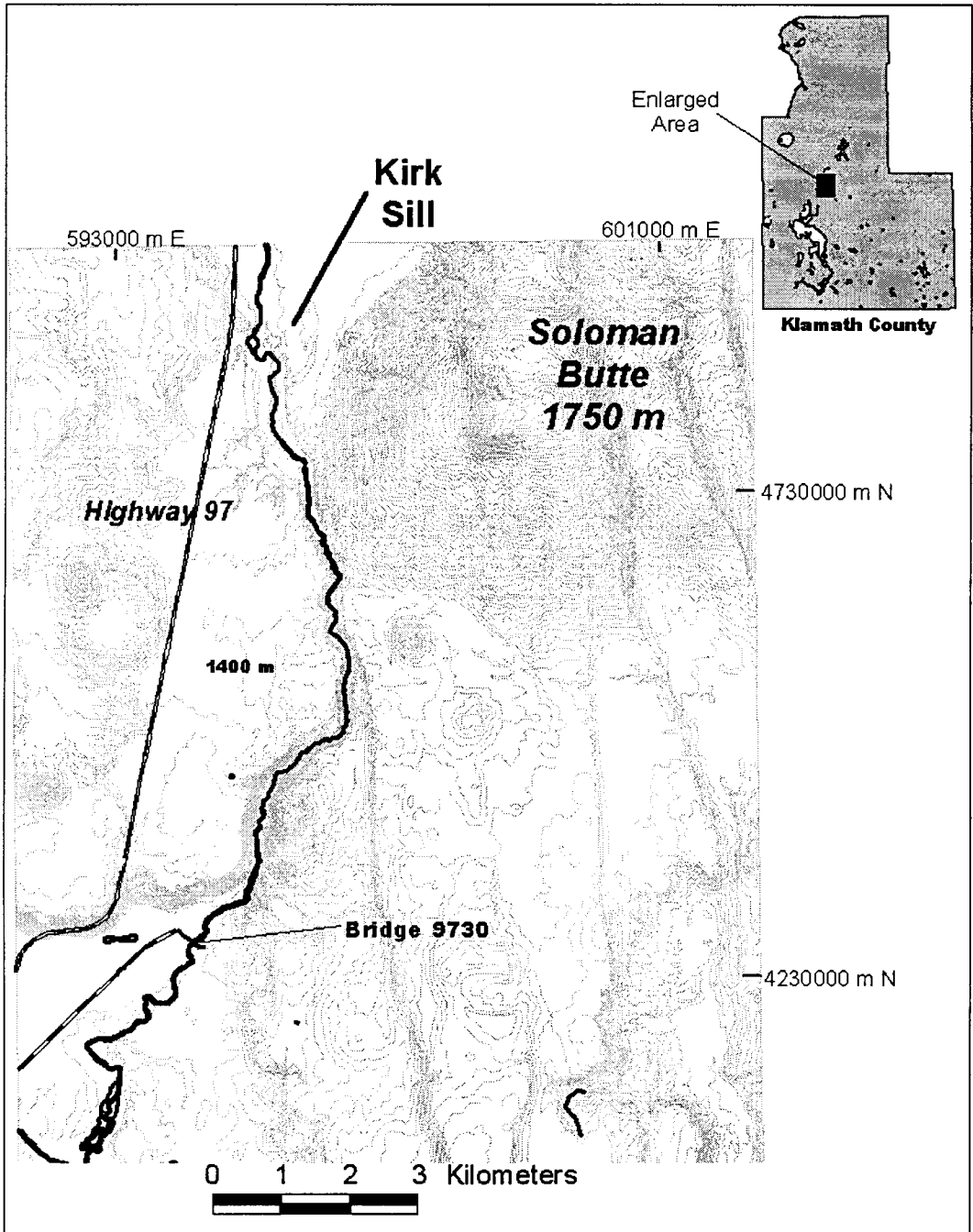


Figure 4: Locations of discharge measurements within the Soloman Butte quadrangle. Coordinates are UTM Zone 10, contour interval 6 m.

Soloman Butte quadrangle. Included in this chapter is a detailed study of the discharge history of the Williamson River at the Kirk Sill and the factors influencing this discharge.

Previous Work

The 3,781 km² drainage area of the Williamson River basin has been the subject of several reconnaissance studies. These studies have been limited to assessing the ground water potential of the area and a well-constrained water budget for this area has yet to be calculated.

Illian (1970) could not precisely identify the ground water boundaries of the basin within the larger Klamath basin because of the paucity of well logs in the mountainous areas. The basin was delineated from topographic divides that are thought to form ground water boundaries (Illian, 1970). Illian (1970) proposed a three-part flow system for the Klamath Basin that is separated into local, intermediate, and regional circulation. Local flow systems are present where discharge occurs close to the recharge source, flow paths are shallow and the residence times are short (Illian, 1970). The regional flow system has long deep flow paths with long residence times, the waters are enriched in solutes, and have geothermally elevated temperatures, which can reach 93° C in the Klamath Basin (Illian, 1970). This system receives recharge from the highest elevations in the basin (Cascades, Yamsay Mountain) and discharges in the lowest part of the ground water basin (Lower Klamath Lake) (Illian, 1970). The intermediate flow system has characteristics of both regional and local flow systems and Illian (1970) describes the flow from the Cascades to Klamath Marsh as intermediate.

Illian (1970) estimated that 9×10^5 ac-ft yr⁻¹ is recharged to the ground water system and of this 5×10^5 ac-ft yr⁻¹ resurfaces within the basin where it is lost to evapotranspiration, consumptive uses, and baseflow contribution to the Williamson River. The remaining recharge moves south out of the basin into the Upper Klamath Lake and Lost River sub-basins (Illian, 1970).

Leonard and Harris (1974) built upon previous work and defined the general geologic units of the Klamath Basin, described their water-bearing properties, and described the general movement and occurrence of ground water as well as the quality of this water. The path of water movement described in this report begins as precipitation and its subsequent infiltration on the slopes of the Cascades to the west and the volcanic centers surrounding Klamath Marsh, and discharge in the lowlands such as Beaver Marsh and Klamath Marsh (Leonard and Harris, 1974). Ground water in the Klamath Marsh area then moves south under a gradient of 0.2 m km^{-1} (Leonard and Harris, 1974).

Methodology and Results

Williamson River discharge

Discharge of the Williamson River at the Kirk Sill (Figure 4) was evaluated through historic stream gauge data and field measurements of discharge at the Kirk Sill and south of the Williamson River canyon at the bridge where Forest Service road 9730 crosses the Williamson River (bridge 9730).

Historic discharge values by stream gauge number are available for water years 1954-1995 and 1999 (U.S. Geological Survey, 1999). These data are daily flow rates

recorded in $\text{ft}^3 \text{s}^{-1}$ and were converted to $\text{m}^3 \text{s}^{-1}$ for this study. To complement these data, climate data are also examined. Temperature, rainfall, and snow water equivalent data for the water years from 1982-1999 are available for the USDA SNOWTEL site Chemult Alternate (USDA, 1999). Precipitation data for the Cascade Range at SNOWTEL site Diamond Lake (USDA, 1999) are also examined. This site lies just to the west of the basin boundary along the Cascade Range (Figure 1), but the precipitation values are thought to be representative for the Cascade Range in the Williamson River basin. The discharges and precipitation values from 1982-1995 and 1999 at the Kirk Sill were plotted separately for each water year to observe seasonal variations (Appendix B). The water year is defined as October 1st through September 30th of the following year.

Flow measurements were made with a flow meter on October 10, 1998 and on April 4, 1999. With the flow meter set to average velocity in m s^{-1} , eight readings were taken at approximately half the channel depth and at a distance interval that was relative to the channel width (Appendix A). These data were then integrated with the following equation to determine the total river discharge at each location:

$$Q = \sum_{i=1}^m q_i$$

where Q is the total discharge and q_i is the discharge at each point of measure, which is the product of the flow velocity from the flow meter, the channel depth, and the channel width (distance between measurements). The discharge values and channel dimensions are reported in Appendix A.

Spring discharges

Discharges for selected springs in the Wocus Bay and Solomon Butte quadrangles (Figure 5) were measured in June, 1998 and again in October, 1998. Discharges for Recovery, Wocus, and “Bat springs” were measured with the method outlined above for the calculation of the river discharge. Dice Crane spring flows into a reservoir that is drained by a pipe. The time taken to fill a one-liter container by this flow was recorded 10 times and averaged. These data are reported in Table 1.

Three types of springs were identified in the study area: contact, depression, and fault. Contact springs occur where a permeable unit overlies a unit with a hydraulic conductivity that is low enough to prevent transmission of all of the water that is moving through the upper unit (Bryan, 1919; Fetter, 1994). These springs occur along lava flow margins (Bat Spring) and at the interface between the pyroclastic-fall deposits and underlying bedrock units (Cabin Spring). Depression springs occur in topographic lows where the water table intersects the surface (Bryan, 1919; Fetter, 1994). These springs are commonly found within depressions that have been infilled with pyroclastic-fall deposits. It is thought that drainages existed within these depressions prior to the eruptions of Mount Mazama. The presence of phreatophytes in these paleodrainages suggests that water continues to move through these valleys, but not on the surface. The high permeability of the pyroclastic fall and the relatively low permeability of the underlying buried soil promote the lateral down slope movement of water through the pyroclastic-fall deposits. This hypothesis was supported where exploratory augering in several drainages revealed water-saturated pyroclastic-fall deposits near the surface. All

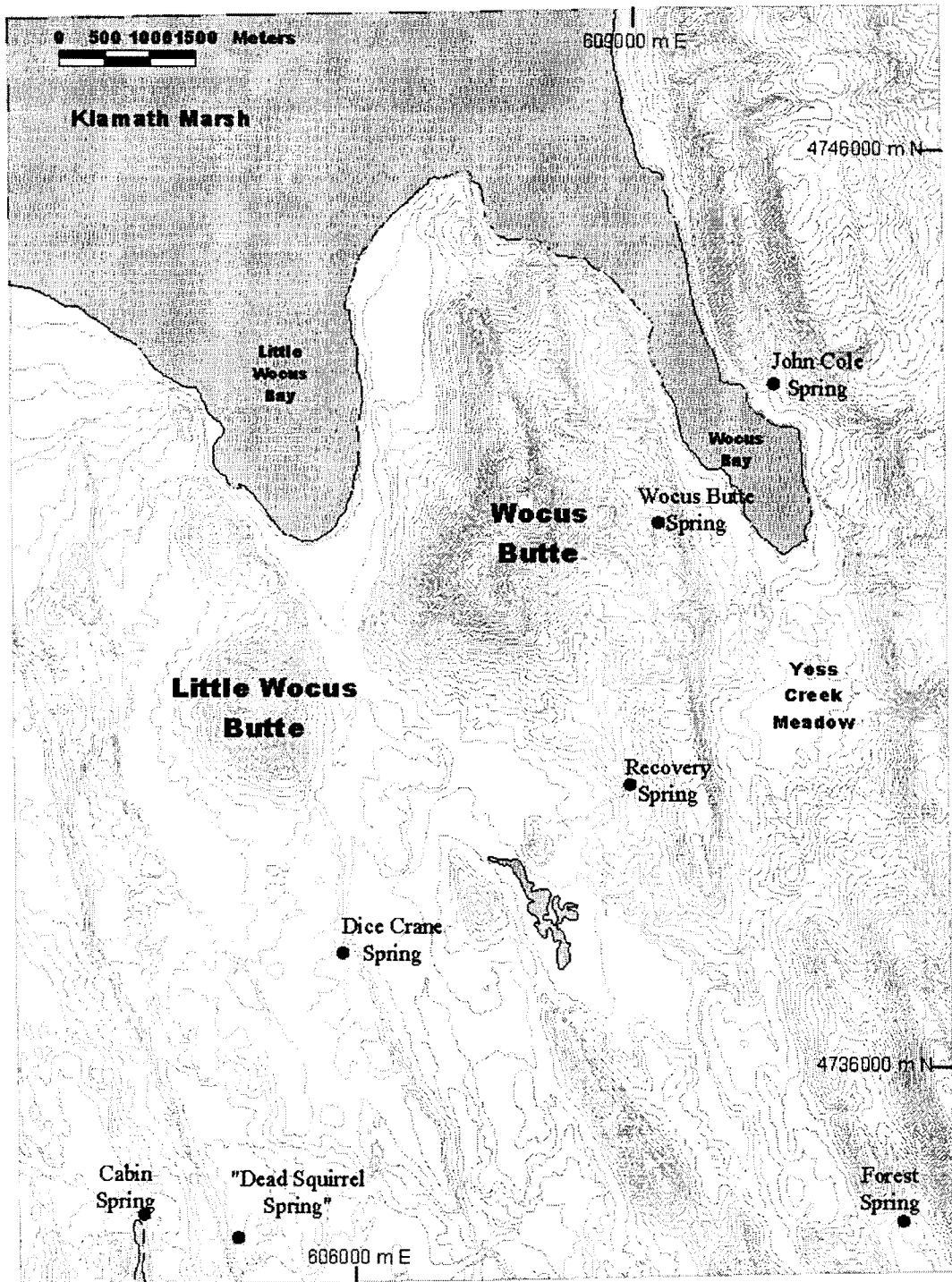


Figure 5: Location of springs in the Wocus Bay quadrangle. Coordinates are UTM Zone 10, contour interval 6 m.

of the depression springs in the Wocus Bay quadrangle are ephemeral and were dry or had significantly reduced discharges by mid-summer (Table 1).

Fault springs occur where interflow zones are offset or where fractures and porous zones are clogged with fault gouge thus creating a barrier to flow and forcing ground water to the surface. Dice Crane Springs is the only recognized fault spring in the Wocus Bay quadrangle with a measurable discharge. It occurs along a distinct northwest striking lineament and the topography upstream of the spring is insufficient to produce a depression type spring (Figure 5). The discharge of this spring only slightly decreased throughout the summer (Table 1). The relatively steady flow throughout the summer and the temperature of the water (7° C (June 98) and 8.5° C (October 1998)) suggest that this stream is being fed by intermediate flow described by Illian (1970).

Table 1: Location (UTM Zone 10), discharge, and spring type for selected springs in the Wocus Bay and Soloman Butte quadrangles.

| <i>Spring</i> | <i>Easting</i> | <i>Northing</i> | <i>June Discharge</i> | <i>October Discharge</i> | <i>Spring Type</i> |
|-----------------|----------------|-----------------|---------------------------------------|--------------------------------------|--------------------|
| Cabin Spring | 603670 | 4734230 | Channeled for stock use | | Fault |
| “Dead Squirrel” | 604684 | 4734062 | Not studied | | Depression |
| Forest Camp | 612000 | 4734010 | Not flowing | | Depression |
| Wocus Butte | 609250 | 4741940 | 0.0008 m ³ s ⁻¹ | Below detection | Depression |
| “Bat” | 595600 | 4732360 | .00001 m ³ s ⁻¹ | Dry | Contact |
| Recovery | 608970 | 4739100 | .003 m ³ s ⁻¹ | Dry | Depression |
| Dice Crane | 605800 | 4736890 | .0008 m ³ s ⁻¹ | .0005 m ³ s ⁻¹ | Fault |

Deuterium analysis

Water samples collected in October, 1999 from Kirk Sill, Bridge 9730, Cabin Spring, and Dice Crane Spring were analyzed for deuterium (^2H) by the Department of Earth Science at Dartmouth College. These samples were collected in 100-ml containers and completely filled to evacuate air from the container. The samples were then analyzed using a stable isotope mass spectrometer. The results are reported in the usual δ notation as per mil deviations from SMOW (standard mean ocean water) and presented in Table 2. Analytical precision for these values is estimated at ± 5 ‰.

Table 2: δD values for water samples from the Wocus Bay and Soloman Butte quadrangles.

| <i>Sample</i> | <i>δD</i> | <i>Standard deviation</i> |
|-------------------|------------------------------------|---------------------------|
| Kirk Sill | -106.147 | 0.324 |
| Bridge 9730 | -137.981 | 0.214 |
| Cabin Spring | -138.321 | 0.340 |
| Dice Crane Spring | -137.273 | 0.493 |

Well logs

Water-well logs for Klamath County were obtained from the Oregon Water Resources Department (158 12th Street NE, Salem, OR, 97310). These logs provide limited information on the lithologies encountered during the drilling of water wells for domestic, stock, and irrigation uses. Limited information exists on the few wells drilled in the Wocus Bay quadrangle so wells drilled north of this area in the Military Crossing

and Wildhorse Ridge quadrangles were included in this study. Well logs for the Soloman Butte quadrangle are plentiful, but are concentrated in the southwest. Representative well logs from these areas have been summarized in Appendix C.

The information available from geologic mapping, water-well logs, and work by Leonard and Harris (1974) were used to define the aquifers in the southern Klamath Marsh area (Table 3) and in the Soloman Butte quadrangle (Table 4).

Discussion

Historic and measured discharge

Analysis of historic discharge data provide information on basin characteristics and climate. A plot of the annual mean discharge of the Williamson River from 1955-1995 displays a high variability in discharge (Figure 6). A statistical measurement of variation is the coefficient of variation, which is defined simply as the ratio of the standard deviation of a variable, in this case annual mean discharge, to its mean. A value of zero describes no variation and values greater than one describe extreme variation. The value for the Williamson River is 0.59. When compared to reported values for North America by Riggs and Harvey (1990) this value is similar to those from the desert southwest of the United States. The variability of flow is related to the variability of precipitation, which is greatest in semiarid and arid regions (Riggs and Harvey, 1990). High variability is usually associated with low precipitation, but in areas with low precipitation and large ground water bodies or surface water storage, flow variability is

Table 3: Hydrologic units of the southern Klamath Marsh and their water-bearing properties.

| Age | Unit | Description | Water-bearing properties |
|--------------------------|---------------------------------|---|---|
| Holocene | Pyroclastic deposits | Widespread unconsolidated pumice and ash found mantling the topography. Thickness of reworked deposits in Klamath Marsh is up to 20 m. | High infiltration rate. Unconfined and generally above the water table. |
| Pleistocene and Holocene | Alluvium | Sands and gravels deposited by pre-Mazama eruption streams and rivers. Deposits underlying Klamath Marsh are up to 30 m in thickness. | Unconfined aquifer, recharge could move through these deposits off the Cascades. Generally low yield. |
| | Diktytaxitic basalt | Diktytaxitic texture with 20 % cavities. Thickness estimated at 10-20 m. Found in low lying areas around and under Klamath Marsh. | Unconfined unit with low yields. Used for domestic wells near Klamath Marsh. |
| Variable | Volcanic eruptive center facies | Basaltic andesite, dacite, cinder, and volcanic breccia. Small cones and larger shield volcanoes found throughout the basin. Thickness is variable. | Important source for recharge on the Cascade slopes and slopes of several buttes. Springs on the east slope of the Cascades discharge from this unit and it supplies wells on the western side of Klamath Marsh (Leonard and Harris, 1974). |
| Pliocene | Andesite and basaltic andesite | Basalt flows exposed along the eastern edge of Klamath Marsh. Platy jointing and flow brecciation are common in these units. | Generally low permeability units that supply low yield wells on the east side of Klamath Marsh. |
| Pliocene and older | Tuff and lapilli tuff | Lithic bearing and poorly welded tuff found only on the eastern edge of Klamath Marsh. | Low permeability confining layer. |
| | Continental Sediments | Coarse gravels and sands found on the eastern edge of Klamath Marsh. | Variable permeability, used for stock wells. |
| | Basalts | Fractured basalt and cinder facies identified from well logs. | Principle aquifer in Klamath Marsh. High yields, supplies most irrigation wells. |

Table 4: Hydrologic units of the Soloman Butte quadrangle and their water-bearing properties.

| Age | Unit | Description | Water-bearing properties |
|--------------------------|---------------------------------|---|--|
| Holocene | Gravel deposits | Boulders and gravels deposited at the mouth of the Williamson River Canyon by catastrophic flooding on the Williamson River. Thickness is no greater than 10 m. | High permeability, unconfined, with low yield. Supplies domestic wells. |
| Holocene | Pyroclastic deposits | Widespread unconsolidated pumice and ash found mantling the topography. Thickness of pyroclastic flows in the Soloman Butte area exceeds 10 m. | High infiltration rate. Unconfined and generally above the water table. |
| Pleistocene and Holocene | Alluvium | Sands and gravels deposited by pre-Mazama eruption streams and rivers including the Williamson River. | Unconfined aquifer, recharge could move through these deposits off the Cascades. Generally low yield. |
| Variable | Volcanic eruptive center facies | Basaltic andesite, dacite, cinder, and volcanic breccia. Small cones and larger shield volcanoes found throughout the basin. Thickness is variable. | Important source for recharge on the Cascade slopes and slopes of Soloman Butte. Supplies domestic and stock wells on the north side of Soloman Butte. |
| Pleistocene and older | Younger Continental sediments | Sandstone and diatomite sequences that are best exposed along Highway 97 at the Collier grade (> 120 m thick). Thickness is variable throughout the basin. | Serves mainly as a confining bed, but coarser beds do have small yields (Leonard and Harris, 1974). |
| Tertiary | Hydro-volcanics | Palagonitic rocks found at the mouth of the Williamson River Canyon and in the eastern portion of the Soloman Butte quadrangle. | Serves as a confining bed for the underlying older continental sediments. |
| | Older Continental sediments | Sandstone, diatomite, and clays that underlie the Collier State Park area and are over 200 m thick. | Alternating low permeability and high permeability sediment layers. High artesian yields. |

reduced (Riggs and Harvey, 1990). High infiltration rates and large aquifer storage in a basin result in runoff with little variability (Riggs and Harvey, 1990). The high infiltration rate of this basin and the high variability of the Williamson River discharge suggest low storage capability of the aquifers.

The annual hydrographs (1982-1995, and 1999) of discharge plotted separately with precipitation at Chemult (Appendix B) display the dependence of discharge on precipitation and the storage capabilities of aquifers in southern Klamath Marsh. On average, there is a large annual precipitation event usually as snowfall, between December and January. This does not produce an immediate response in discharge; there is a lag of approximately one-month. The usual crest in discharge is in either March or April. This lag between precipitation and discharge is attributed to snowmelt. The input from snowmelt is gradual due to variations in topography and slope aspect. The local snowpack is usually completely melted by mid-April to early May, while snow along the Cascade crest to the west is often present throughout the year. The snowpack provides temporary storage that sustains the system through periods of little or no precipitation in late spring and early summer. Variations in snow pack and the rate at which the snow pack melts have direct affects on the discharge of the river. Discharge in 1993 (Figure 7) is above average for the values observed from 1990-1995. Precipitation is also high for this year relative to other years, but the high discharge is partly the product of a large snow pack. The snow-water equivalent for this year was 16 cm above the average of 33 cm. The precipitation for 1995 was 63.5 cm, which is the

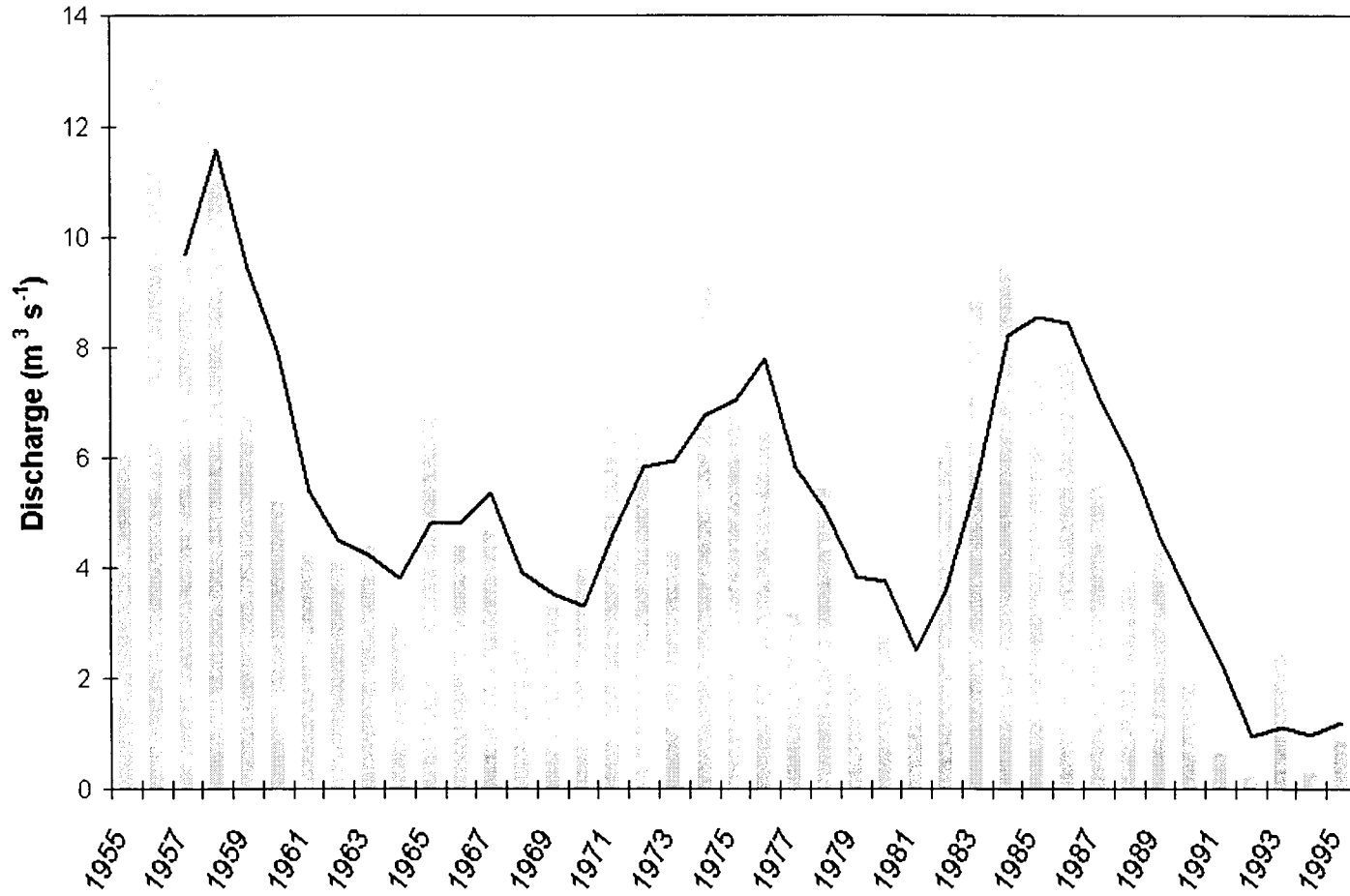


Figure 6: Annual mean discharge from 1955-1995 for the Williamson River with the three year moving average. Data are from U.S. Geological Survey stream gauge 11493500 (U.S. Geological Survey, 1999).

third largest in the fourteen-year span, but the total discharge for 1995 was the fourth lowest (Figure 8). This low discharge is partly the result of a snow-water equivalent of only 34 cm. The correlation coefficient between annual discharges and annual precipitations at Chemult is only 0.56 while the correlation between discharge and snow-water equivalent is 0.67. Another factor affecting discharge is the rate at which the snow melts. In 1993, it took 28 days for the snowpack at Chemult to decrease from 25 cm to 0 cm, while in 1995 it took 60 days for the same amount of snowmelt. This suggests that the faster the snow melts the more likely surface runoff will be achieved in the permeable pyroclastic deposits, which would lead to an increase in river discharge.

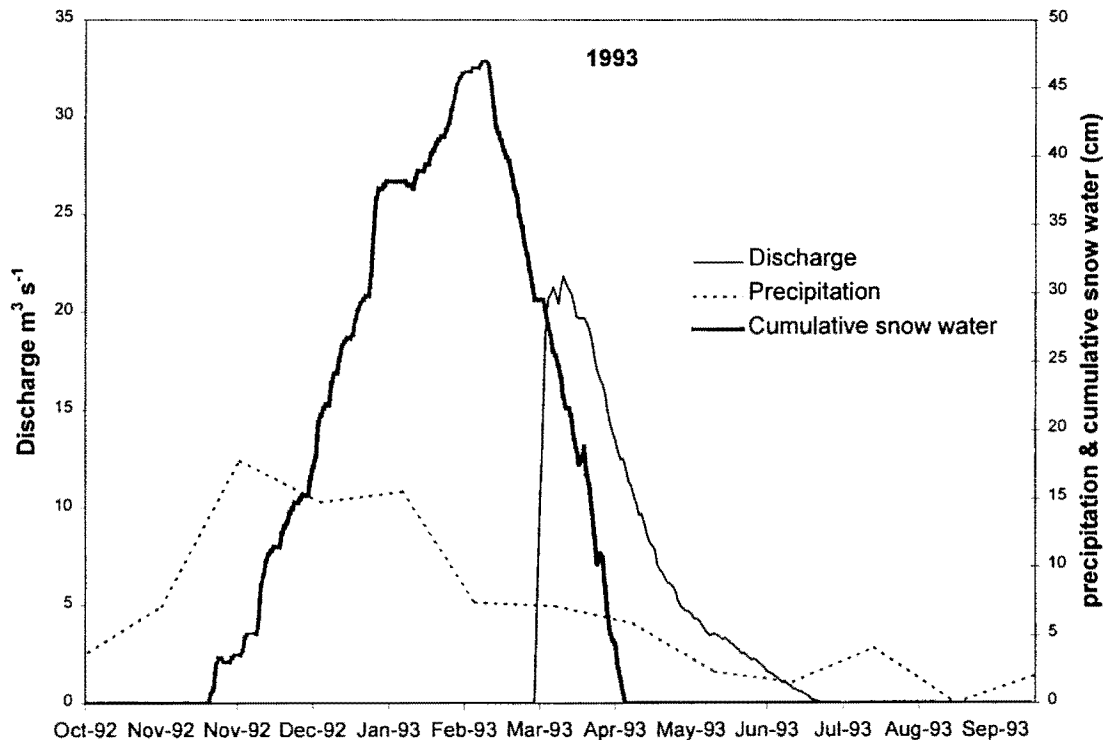


Figure 7: Discharge of the Williamson River at the Kirk Sill (U.S. Geological Survey, 1999) with precipitation and cumulative snow water (USDA, 1999) for 1993.

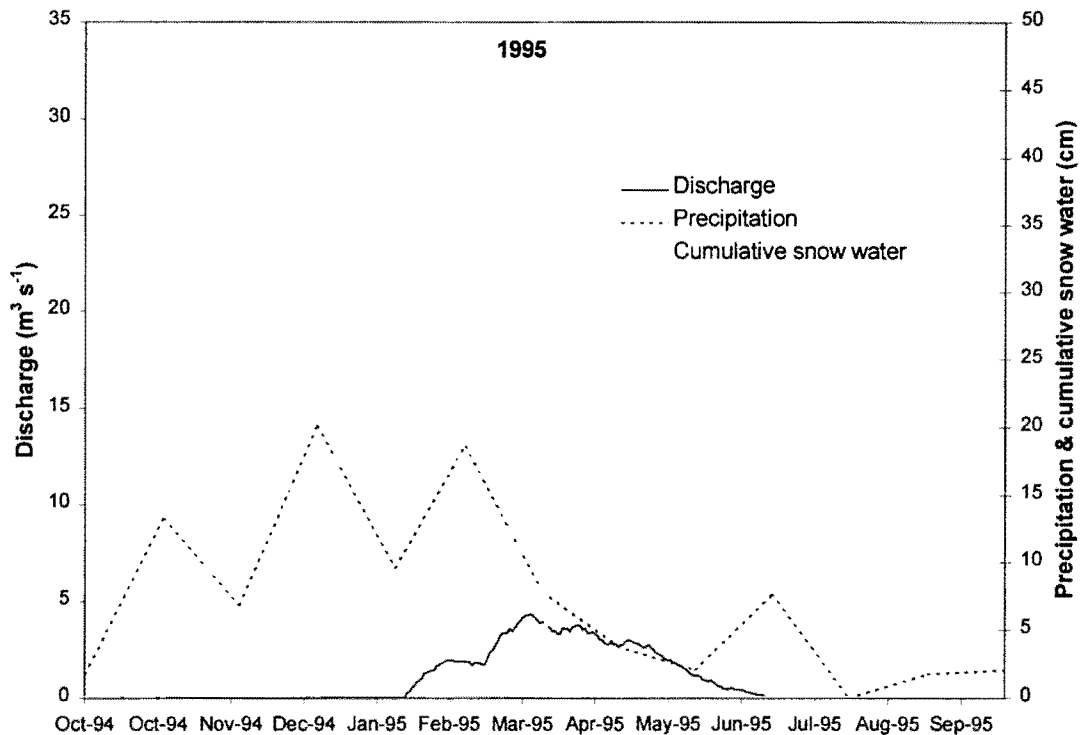


Figure 8: Discharge of the Williamson River at the Kirk Sill (U.S. Geological Survey, 1999) with cumulative snow water and precipitation (USDA, 1999) for 1995.

The low discharge in 1995 could also be the result of the preceding year's low precipitation (Figure 9). The precipitation value in 1994 was the lowest in the data set for both Chemult (34 cm) and Diamond Lake (68 cm). This indicates a dependence of discharge on preceding precipitation values.

The plot of annual mean discharge with precipitation from 1982-1995 (Figure 9) displays the response of the aquifer to low precipitation years. Precipitation was below the annual average for Chemult and Diamond Lake in 1981, 1985, 1987, 1988, 1989 (Diamond Lake only), 1990, 1991, 1992, and 1994. Discharge was below the average annual mean ($5 \text{ m}^3 \text{ s}^{-1}$) in 1981, and from 1988-1995. The low precipitation lead to less

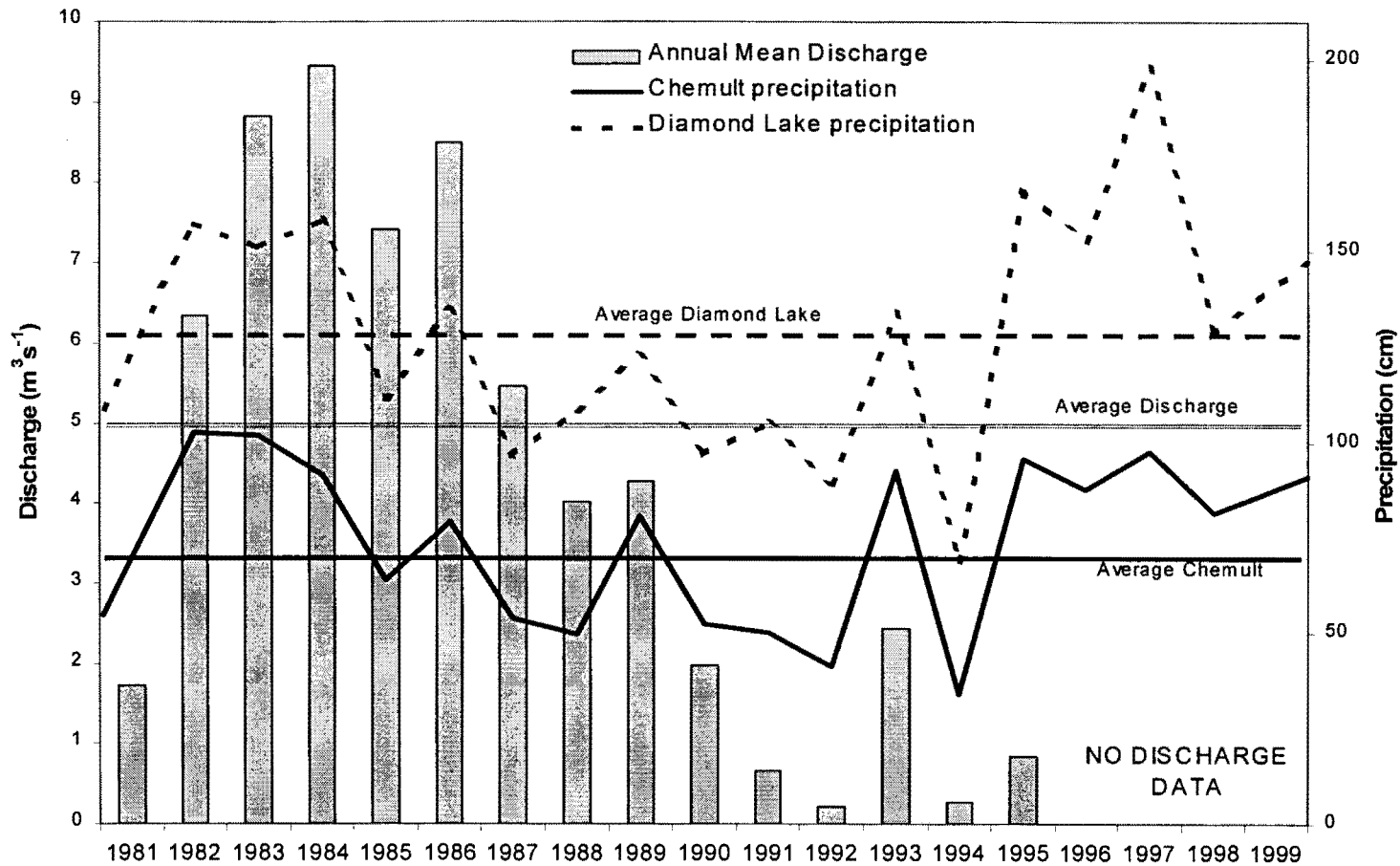


Figure 9: Annual mean discharge for the Williamson River at Kirk Sill (U.S. Geological Survey stream gauge 11493500) and annual precipitation from SNOWTEL sites Diamond Lake and Chemult Alternate.

recharge and to a depletion of water that was in storage in the southern Klamath Marsh aquifers. Less water in the aquifers resulted in decreased contribution to the Williamson River. Precipitation was above average for several years that the discharge was below average, but sufficient recharge to the aquifer had not taken place to increase the discharge of the Williamson River above Kirk Sill. The hydrographs from the years prior to 1990 are sustained throughout most of the season indicating sufficient ground water contribution to the river for discharge to occur at Kirk Sill (Appendix B). The depletion of storage was not immediate, it required three nonconsecutive years of precipitation below the annual average until the discharge of the river at Kirk Sill was below detectable limits for portions of the water year. Data are not available to determine how many years of average and above average precipitation are required for the replenishment of storage to the point that flow over the Kirk Sill was sustained throughout the water year. Precipitation was however above average in 1993, and 1995-1999. The discharge data available for a portion of 1999 and field observation of the discharge in August and October, 1999 indicate flow over the Kirk Sill for the entire water year. Unfortunately, the stream gauge was not operational from 1995-1998 so the time required for the aquifer to recover is unknown.

Discharge measurements made at the Kirk Sill ($0.013 \text{ m}^3\text{s}^{-1}$) and downstream at Bridge 9730 ($0.87 \text{ m}^3\text{s}^{-1}$) on 10 October, 1998 indicate that the discharge increases 66 times between the two points (Appendix A). There are no tributaries to the river along this stretch so the increase is the result of ground water contribution that is occurring between the two points of measure. This indicates that the upper Williamson River was

disconnected from the water table at and above the Kirk Sill, but then intersects the ground water table at a lower elevation in the canyon. The measurements taken on 04 April, 1999 show only a 19% increase between Kirk Sill ($21.98 \text{ m}^3\text{s}^{-1}$) and Bridge 9730 ($26.65 \text{ m}^3\text{s}^{-1}$). At this time of year, the percentage of ground water contribution to the discharge is less because of the high volume of water flowing over the Kirk Sill. The actual volumetric contribution from ground water was three times larger than the October, 1998 value. The high discharge at the Kirk Sill is attributed to contribution from snowmelt and ground water discharging in Klamath Marsh.

Deuterium analysis

The isotopic data from the Williamson River and springs in the Wocus Bay quadrangle support the information gathered from the October, 1998 discharge data. The Williamson River is enriched with deuterium at the end of summer as it leaves Klamath Marsh (Kirk Sill sample, Table 2). This enrichment occurs because the river and marsh are subject to large amounts of evaporation with little precipitation during the summer. These factors lead to high concentrations of deuterium because the ^1H is preferentially lost to evaporation and not replenished by precipitation. The sample from bridge 9730 has a value that is very similar to the ground water discharge at Cabin and Dice Crane Springs (Table 2). This indicates that when the sample was collected the Williamson River was intersecting the ground water table between the Kirk Sill and bridge 9730 and the discharge is ground water dominated.

Well logs

Wells on the west side of Klamath Marsh have high yields and often have artesian flow. Well 32S/8E-17ab (Appendix C) is drilled into a basalt aquifer at 100 m depth and

has a yield of 252 L s^{-1} (liters per second) (4000 gpm (gallons per minute)) with 24 m (79 ft) of drawdown. This basalt aquifer is the principle aquifer defined by Leonard and Harris (1974) for the Williamson River Basin and supplies most irrigation wells for Klamath Marsh. Recent geologic mapping in the Klamath Marsh area (Conaway and Cummings, in preparation) has shown that basalt, basaltic andesite, and andesite units are not laterally extensive. Therefore, the basalt aquifer of Leonard and Harris (1974) is likely comprised of several Pliocene and older basalt units throughout the basin. Lower yield wells around Klamath Marsh remove water from unconfined sands and gravels from the ancestral Williamson River channels. These deposits are over 100 m thick in well 32S/8E-30ab (Appendix C). Low yield wells drilled in areas with thick pyroclastic deposits are primarily for stock use because of their susceptibility to short term fluctuations from inflow. The primary confining layers in the eastern portion of southern Klamath Marsh are poorly welded Tertiary tuffs (Tt of Sherrod and Pickthorn, 1992, and Conaway and Cummings, in preparation) and cemented continental sediment. The confining layers in the western portion of southern Klamath Marsh are assorted basalt, basaltic andesite, and andesite with little jointing or vesiculation.

Wells in the southwest corner of the Soloman Butte quadrangle and the southeast corner of the Fort Klamath quadrangle are drilled into sands, diatomite, and clay and some have artesian yields. These deposits are over 200 m thick (well no. 34/7-4G). The well at Spring Creek Ranch Motel (well No. 34s/7e-4a) penetrates this aquifer of continental sediments to a depth of 79 m and has an artesian yield of 12 L s^{-1} (200 gpm). These high artesian flow rates are the result of a ground water mound that occurs at the

base of the Chemult Plateau and the confining layers of clays within the older continental sediments, and interfingering hydrovolcanics and overlying younger continental sediments. This ground water mound is topographically induced and is likely supplied by the high recharge from the east slopes of the Cascades. Several low yield domestic wells (33s/7e-35dc, 33/7-35) are located at the mouth of the Williamson River Canyon and are drawing water from ancestral Williamson River deposits.

Source and occurrence of ground water

The movement of ground water in the Williamson River basin is controlled by the areas of recharge and the geometry of the units through which the water is moving. Faults in this basin are thought to exert only local control over the movement and occurrence of ground water (Leonard and Harris, 1974). The area of greatest recharge is along the slopes of the Cascades to the west of Klamath Marsh with lesser amounts of recharge occurring on the volcanic centers bordering the marsh to the east and south. The high recharge along the slopes of the Cascades results from a combination of heavy precipitation and high infiltration through the pyroclastic deposits. Ground water then enters volcanic and sediment units and moves towards Klamath Marsh under a topographic gradient.

Two conceptual models for the movement of ground water in the Williamson River basin are presented. The preliminary analysis of climate data, water-well logs, historic hydrographs, measured discharges, isotope data, and data from geologic mapping must be considered in any conceptual models of ground water flow in the Williamson River basin.

Factors considered for conceptual models

1. Diamond Lake in the Cascade Range, receives approximately twice as much average annual precipitation as Chemult Alternate (128 cm versus 68 cm).
Figure 9 illustrates that there is little difference between the annual precipitation patterns at the two sites.
2. Despite the high precipitation values on the western edge of the basin, the Williamson River has periods of no flow at the Kirk Sill, and the variance in its discharge is similar to rivers in arid regions of the southwestern United States. Variations in discharge at the Kirk Sill illustrated by the hydrographs, high infiltration rates in the basin, and precipitation data suggest low storage capabilities in the aquifers.
3. High yield wells and large discharge springs are located on the west side of Klamath Marsh.
4. During periods of low flow, the Williamson River is ground water dominated and has an isotopic composition that is similar to perennial springs in the Wocus Bay quadrangle.
5. Spring Creek, which is spring fed, contributes approximately 28% of the total flow to the Williamson River into Upper Klamath Lake and contributes almost the entire discharge during low flow months.
6. The high infiltration rates of the pyroclastic deposits prohibit any surface water contribution to the river from the slopes to the west of the marsh. Therefore, any contribution to discharge of the Williamson River above Kirk Sill from the west must be made by ground water.

Conceptual model A – no structural barrier

The flow paths that originate in the Cascade Range and that are being supported by the high precipitation do not surface in Klamath Marsh to contribute to the river discharge (Figure 10). These flow paths occur at depths (intermediate flow path of Illian, 1970) that do not extend up into the unconfined aquifers of the marsh. The Pliocene basalt aquifer (Table 3), which supplies the high-yield agricultural wells on the west side of the lower marsh, could be recharged by these intermediate flow paths. The deuterium data and measured discharge on the river suggest contribution from a ground water source. The isotopic composition of these waters is similar to those of the perennial springs to the east of the river. These springs occur along faults that may be forming barriers to the intermediate flow paths. Another possibility is that the perennial springs are fed from the volcanic centers surrounding the marsh. Isotope work on waters from the Cascade Range would help to identify the source of the ground water feeding the springs and the Williamson River in the canyon.

Conceptual model B – structural barrier

Ground water flow from the Cascade Range encounters a structural barrier before it reaches Klamath Marsh and the river is supported only by inflow from the volcanic centers and lowlands surrounding the marsh (Figure 10). The springs and artesian wells on the western side of the marsh could indicate ground water being forced to the surface by such a structure. More significant are the voluminous cold springs that feed Spring Creek and the high-yield artesian wells near the headwaters of Spring Creek. They are a likely outlet of the ground water that originates in the Cascade Range. No large-scale faults have been mapped on the western edge of Klamath Marsh. However, Sherrod and

Pickthorn (1992) and Lee and Cummings (in preparation) show several small volcanic centers along the eastern front of the Cascade Range that could indicate the presence of such a structure.

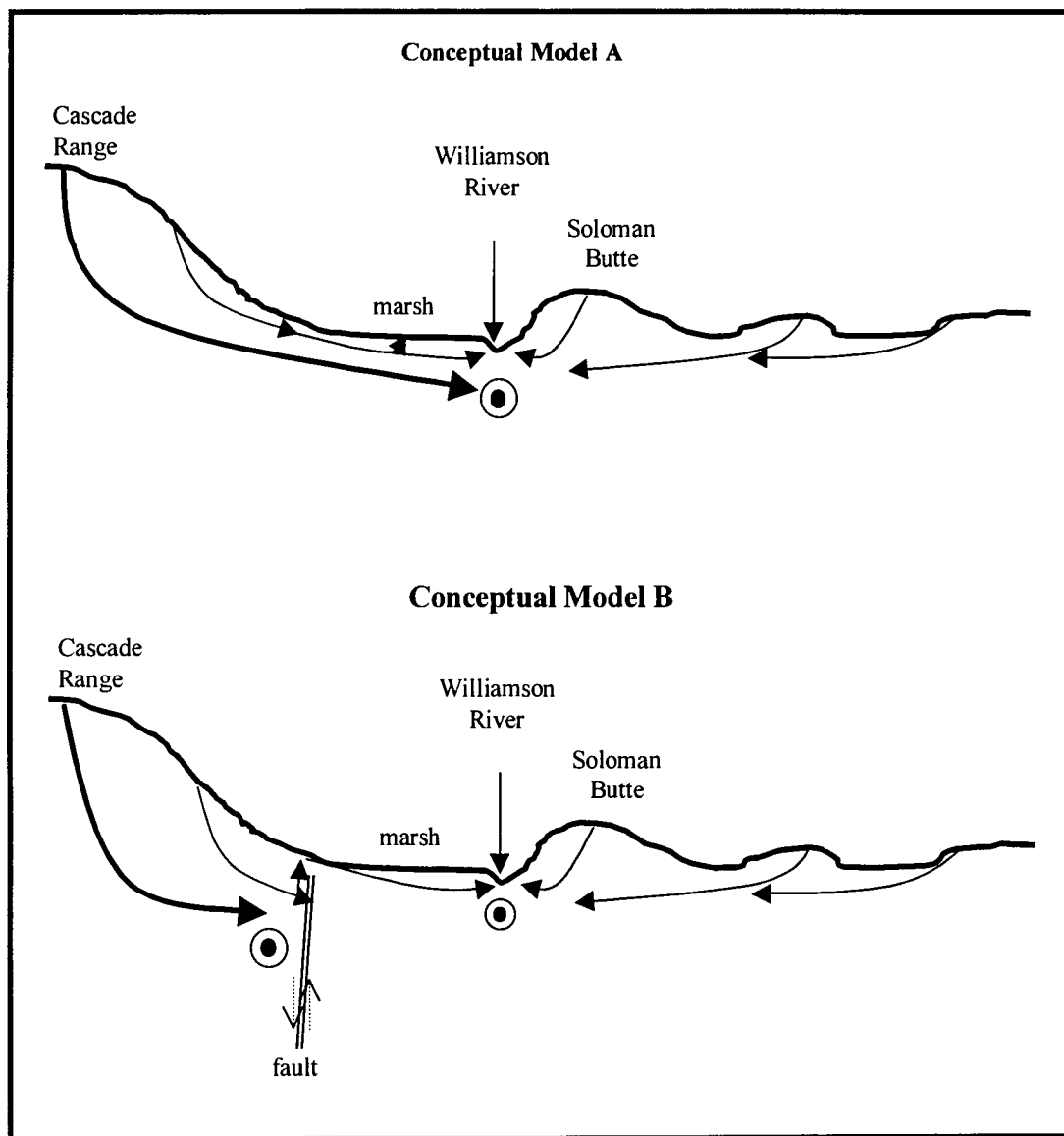


Figure 10: Proposed conceptual models for ground water flow in the southern Williamson River basin. Arrows indicate proposed ground water flow paths. Figure is not to scale.

Suggestions for future study

Future work should first be directed towards the development and testing of a conceptual model for ground water flow. The proposed preliminary conceptual models in this study could be tested easily with further stable isotope analysis. Once an isotopic signature for waters originating in the Cascade Range was established it could be compared to samples from Spring Creek, waters from the high yield wells in Klamath Marsh, and the data from this study. Age determinations of these waters would help identify the length of flow paths. Older age determinations from Spring Creek and the high yield wells would suggest a contribution from a more regional source.

Conclusions

Evaluation of historic discharge of the Williamson River from the Kirk Sill shows large variations in both annual and seasonal discharges. Seasonal variability is controlled by the magnitude and form of annual precipitation and the magnitude of historic precipitation. Greater discharge will occur at the Kirk Sill if the precipitation occurs locally as snow. The rate at which the snow melts also affects the discharge because the faster the snow melts the more likely that surface flow will be achieved in the permeable pyroclastic deposits. The below average annual precipitation years of 1985, 1987, 1988, and 1990 led to depletion of ground water stored in the shallow unconfined aquifers of southern Klamath Marsh and noncontinuous discharge over the Kirk Sill for the 1990-1995 water years. Precipitation was above average in 1995, and 1997-1999, but the stream gauge was deactivated from 1996-1998, so the time required to recharge the aquifer to the point of continuous flow over Kirk Sill is unknown. The

high infiltration rate of this basin and the high variability of the Williamson River discharge suggest low storage capability of the aquifers.

The measured discharge data quantify the ground water contribution to the Williamson River within the canyon. The discharge at Kirk Sill was only 1.5% of the flow south of the Williamson River canyon at bridge 9730 in October, 1998. The percentage of ground water contribution to the overall flow decreased in April, 1999 to only 18%, but the volumetric contribution was three times larger than the October, 1998 measurement.

Three types of springs were identified in the Wocus Bay quadrangle: contact, fault and depression. Depression springs are the most common and occur in topographic lows that are thought to be pre-Mazama drainages that were filled with pyroclastic deposits. The discharge from these springs is ephemeral and is the discharge point for local flow systems. The fault springs were the only springs that maintained consistent flow throughout the year. These springs are being recharged by intermediate flow systems.

Values of deuterium from the Williamson River at Kirk Sill and bridge 9730, and two springs in the Wocus Bay quadrangle support the conclusions from the measured discharge data. The deuterium enriched value from Kirk Sill and the similarity of the values from bridge 9730 and the springs indicate that the Williamson River discharge south of the canyon is ground water dominated.

Review of water-well logs and information gathered from geologic mapping defined the aquifers and their water-bearing properties for the southern Klamath Marsh and the Soloman Butte quadrangles (Tables 3 & 4). The primary aquifer with the

greatest yields in the southern Klamath Marsh is a basaltic unit that has only been identified from the well logs. The alluvial facies is also an important aquifer, but its extent is not as great as the basalt. Recharge to this aquifer is thought to occur on the east slopes of the Cascades and then flows through pyroclastic and pre-Mazama fluvial deposits to the Klamath Marsh. The aquifer with the greatest yield in the Soloman Butte quadrangle is an older continental sediment (Table 4) package that is over 200 m thick in some locations. Recharge to this aquifer and the basalt aquifer of southern Klamath Marsh is thought to occur in the volcanic eruptive center facies of the Cascades and the surrounding volcanic centers, and the alluvial facies.

Ground water in the Williamson River basin originates primarily as precipitation on the volcanic centers that surround Klamath Marsh. Ground water that originates in the Cascade Range to the west is thought to have little influence on the inflow to Klamath Marsh and the Williamson River. The ground water that originates in the Cascade Range is thought to either be prohibited from discharging in Klamath Marsh by a fault zone along the eastern slope of the Cascade Range or the flow paths are deep enough that discharge does not occur and the ground water moves south off of the Chemult plateau. The ground water from the Cascade Range is likely supplying the voluminous cold-spring-fed Spring Creek and many high yield artesian wells near the Spring Creek headwaters.

CHAPTER 3:PALEOHYDROLOGY

Introduction

Since the late Pleistocene, the extent and surface elevation of water bodies occupying what is now Klamath Marsh have experienced at least three major fluctuations. Each fluctuation produced geomorphic surfaces and surficial deposits that indicate extent and relative time of formation. Terraces along the eastern edge of Klamath Marsh provide the only record of all three fluctuations.

Terrace age is inferred from several lines of evidence that include recognized changes in climate, historical and anecdotal observations, terrace composition, and surficial deposits. The presence of undisturbed pyroclastic-fall deposits from Mount Mazama indicates that a surface is at least as old as the cataclysmic eruption. Reworked pyroclastic-fall deposits indicate establishment of the surface since the eruption. However, one surface does not conform to this thinking. The broad middle terrace is planed into bedrock and is either devoid of pyroclastic deposits or has these deposits significantly reworked. It is believed that this terrace, the Pleistocene terrace, developed during the late Pleistocene when Pleistocene Lake Chemult (this study) occupied the Klamath Marsh. The uppermost terrace, the middle Holocene terrace, has undisturbed pyroclastic-fall deposits on its tread and developed after the cataclysmic eruption of Mount Mazama as the result of backflooding from a pyroclastic-flow blockage in the Williamson River canyon. The lower terrace, the late Holocene terrace, developed possibly during agricultural expansion in the early nineteen hundreds.

Terrace levels

Terraces can form through both erosional and depositional processes. Erosional terraces are common along streams and rivers where they have incised through former valley fill or bedrock due to a change in base level, tectonic uplift, or climate change. They are also common along lake shorelines (Hamilton and Minor, 1993; Petty et al., 1994). Erosional terraces can form on alluvial or bedrock surfaces.

Three erosional terraces line the eastern edge of Klamath Marsh and are best developed in the Wocus Bay and Military Crossing quadrangles. The transects in the Wocus Bay quadrangle were surveyed in six locations (Figure 11). Each transect was measured from the elevation at which hydrophyllic vegetation was prominent around the marsh, approximately 1376 m. This elevation is considered an approximation due to the lack of accurate elevation control in the quadrangle. The error associated with these elevations is estimated to be ± 2 m. The approximate average elevations for the three terraces are 1380 m, 1385 m, and 1397 m (Table 5, Figure 12).

The elevation for each terrace was projected throughout the basin to determine the extent of the water bodies at each level (Appendix D). The elevation used for the upper terrace was 1400 m. This elevation was used because of the error associated with the upper terrace level and the 1400 m elevation of rafted clasts of pumice (see rafted pumice discussion). Using Arc View and digital elevation models of the basin the surface area of each water level and the volume for the current marsh, late Holocene, and the middle Holocene were calculated (Table 6). In this section the morphology, extent, and mode of formation for each terrace is outlined.

Table 5: Terrace elevations above prominent hydrophyllic vegetation and average elevations above sea level.

| <i>Survey Site</i> | <i>Lower (m)</i> | <i>Middle (m)</i> | <i>Upper (m)</i> |
|-----------------------------------|------------------------|------------------------|-------------------------|
| Wocus Bay West | 5.4 | 10.3 | 20.8 |
| Wocus Bay East | Not developed | 10.2 | Not developed |
| Wocus Butte North | Not developed | 9.5 | 21.2 |
| Little Wocus | 4.0 | 8.3 | 23.9 |
| Wocus Bay South | 4.2 | 8.7 | 22.3 |
| Hog Creek | Not developed | 8.6 | 17.2 |
| <i>Average Terrace Elevations</i> | | | |
| | Lower | Middle | Upper |
| Above Marsh | 4.5 m, $\delta\pm 0.8$ | 9.3 m, $\delta\pm 0.9$ | 21.0 m, $\delta\pm 2.5$ |
| Elevation (<i>m</i>) | 1380 | 1385 | 1397 |
| Elevation (<i>ft</i>) | 4529 | 4545 | 4583 |

Table 6 : Area and volume of projected surface water elevations from terrace transect data.

| <i>Water Level</i> | <i>Extent</i> | <i>Volume</i> |
|------------------------------|---------------------|--------------------------------------|
| Klamath Marsh | 99 km ² | 1.8 × 10 ⁸ m ³ |
| Late Holocene water body | 289 km ² | 8.1 × 10 ⁸ m ³ |
| Middle Holocene backflooding | 560 km ² | 6.5 × 10 ⁹ m ³ |
| Pleistocene Lake Chemult | 390 km ² | Not calculated |

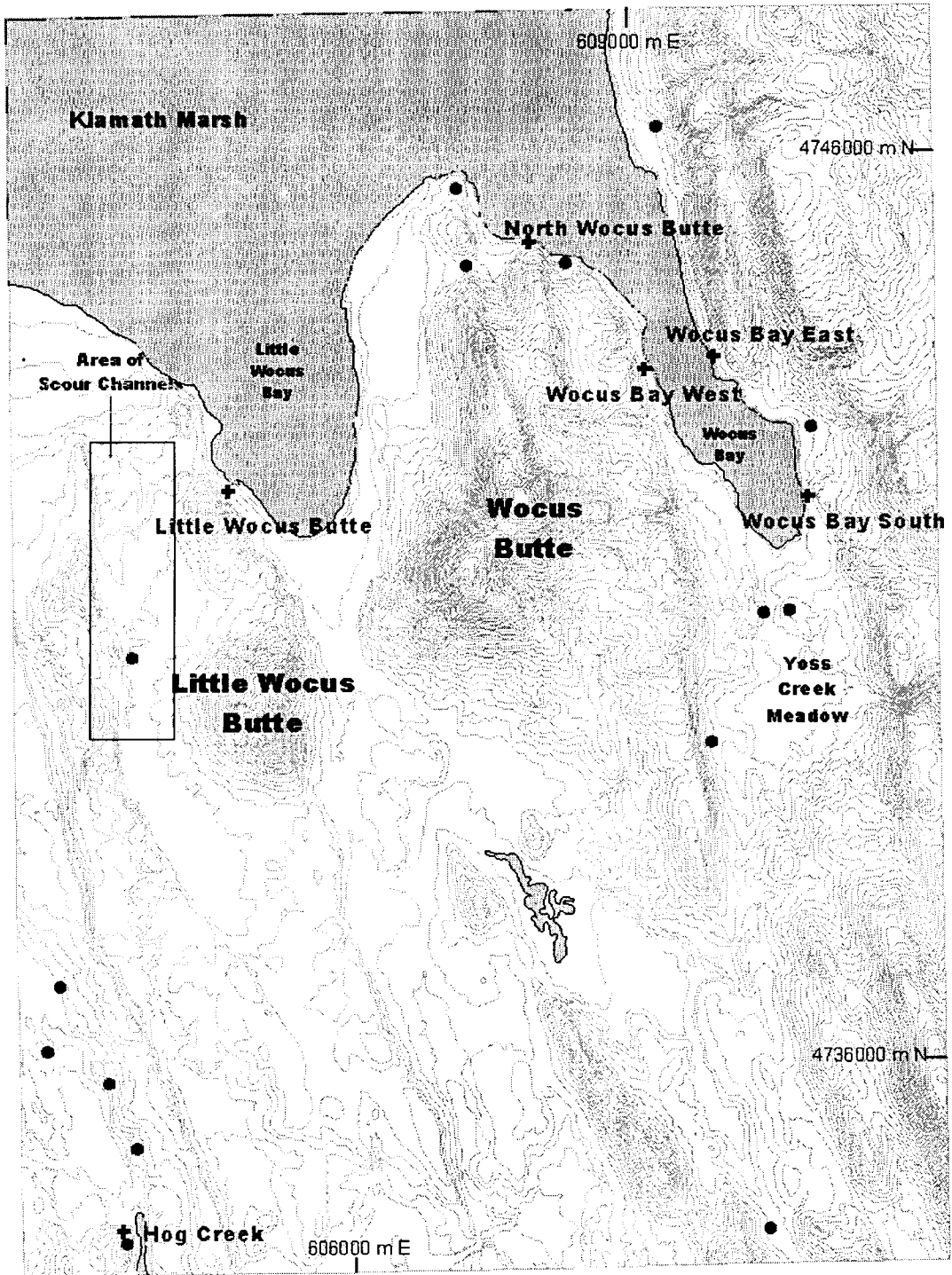


Figure 11: Locations of terrace transects (+), areas of rafted pumice (●), and scour channels in the Wocus Bay quadrangle. Coordinates are UTM Zone 10.

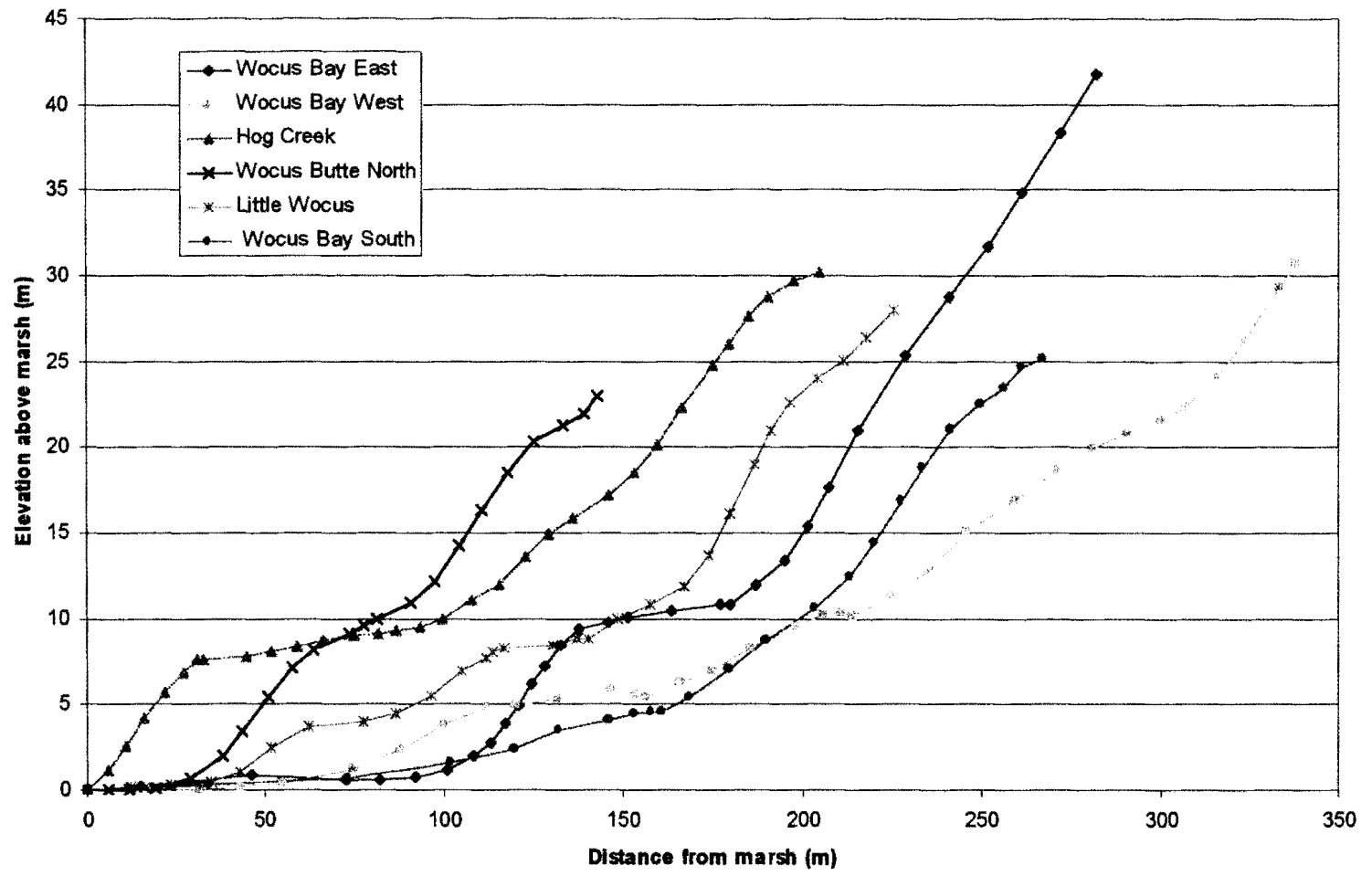


Figure 12: Terrace transects. Elevation of Klamath Marsh is 1376 m. Vertical exaggeration is five times.

The middle terrace (late Pleistocene)

The Pleistocene terrace is cut in bedrock approximately 9.3 m above the present marsh level. This is the most prominent terrace and is present in all six survey locations (Figure 12). The tread of the terrace ranges from 10-70 m. The tread surface is covered with thin deposits of reworked pyroclastic-fall deposits, and rounded water rafted clasts of pumice in some locations. Locally these deposits have been removed by erosion exposing the underlying bedrock units.

Late Pleistocene lakes were common throughout the Basin and Range province and have long been recognized (Russell, 1885; Gilbert, 1890; Meinzer, 1922; Feth, 1961; Snyder et al., 1964). These Pleistocene lakes occupied intermontane basins that filled with water due to the increased precipitation and cooler summer temperatures of the late Pleistocene. Several Pleistocene lakes have been recognized in Oregon (Table 7) and four have been studied in detail, Fort Rock (Forbes, 1972; Allison, 1979), Chewaucan (Allison, 1945; Allison, 1982), Malheur (Dugas, 1998) and Modoc (Dicken, 1980). Orr et al. (1992) recognized the existence of a Pleistocene lake in the Williamson River basin in a map of Oregon Pleistocene lakes developed after Allison (1982).

During the Pleistocene Mount Mazama and other central Cascade volcanoes had glaciers occupying their flanks. Several U-shaped valleys are exposed in cross section within the Crater Lake caldera and glacial tills are found interbedded with lava flows along the crater walls (Williams, 1942). The most prominent U-shaped valley that empties into the Williamson River basin is Kerr Valley. At its greatest extent the glacier that occupied this valley was 300 m thick and probably extended 12 km (Williams, 1942). The melt water from glaciers on the east side of Mount Mazama coupled with the

Table 7: Pleistocene lakes of Oregon, modified from Dicken (1980).

| <i>Pleistocene Lake</i> | <i>Location</i> | <i>Area</i> | <i>Comments</i> |
|-------------------------|--|-----------------------|---|
| Chemult (this study) | Northern Klamath County | 390 km ² | Included present day Klamath Marsh |
| Fort Rock | Northern Lake County | 1,510 km ² | Two lobes, in Fort Rock and Christmas Valleys. |
| Chewaucan | Central Lake County | 1,190 km ² | Included present day Summer and Abert Lakes |
| Goose | Southern Lake County and Modoc County, California | 953 km ² | Highest Pleistocene lake with highest shoreline at 1,524 m |
| Malheur | Harney County | 2,380 km ² | Included present day Harney and Malheur Lakes |
| Coleman | Southwestern Lake County | 1,250 km ² | Included present day Warner Lakes |
| Catlow | Harney County | 909 km ² | Drained into Pleistocene Lake Malheur |
| Alkali | Eastern Lake County | 549 km ² | Included present day Alkali Lake |
| Alvord | Harney County | 1,270 km ² | Over 160 km in length and only 16 km in width |
| Modoc | Klamath County and Modoc and Siskiyou Counties, CA | 2,839 km ² | Included present day Upper and Lower Klamath Lakes and Tule Lake |

reduced evaporation as a result of the lower Pleistocene temperatures lead to the development of a lake, herein called Lake Chemult, in the Williamson River basin.

The history of Lake Chemult is likely similar to other Pleistocene lakes in the Basin and Range province because their fluctuations for the most part were dependent on regional if not global climate. Fort Rock Lake, a closed Pleistocene lake that was located east of Pleistocene Lake Chemult, has five recognized levels that have been

correlated with glacial stages (Allison, 1979). Lake Chemult was located in an open basin, and therefore the surface elevation would have been controlled by discharge to the Williamson River. Lake Malheur, a basin whose lake elevation was also controlled by an outlet, reached its greatest extent between 32,000 yr B.P. and 29,300 yr B.P. (Dugas, 1998).

A trait that is common to all Pleistocene lakes is their size reduction in the late Pleistocene to early Holocene. This size reduction was the result of warmer drier climate that resulted in greater evaporation and the reduction of runoff, overland flow, and ground water flow to the Pleistocene lakes. In general, Pleistocene lakes in southeastern Oregon began to decrease in surface area between 13,000 and 11,000 yr B.P. (Allison, 1979; McDowell and Dugas, 1996). Fort Rock Lake was decreasing in size about 13 ka and was completely dry when pyroclastic fall from Mount Mazama was deposited (Allison, 1979). The sand dunes in the Catlow Valley were formed on Pleistocene lakebeds, stabilized, and eroded prior to the deposition of the Mazama pyroclastic fall (Mehring and Wigand, 1986).

The presence of a Pleistocene lake is further suggested by sand dunes located along the northeast margin of Klamath Marsh (Figure 13). Sand dunes are found along the margins of other former Pleistocene lakes in Oregon, most notable are the dune fields east of Summer Lake. Dunes are associated with Pleistocene lakebeds because the desiccation of the Pleistocene lakes provided for a short time an abundance of sediment that could be transported by wind. The largest dunes in the Williamson River basin are parabolic, up to 30 m high, and over 1 km in width from horn to horn. They are overlain

by pyroclastic fall from Mount Mazama and may be of similar age to the dunes described by Mehringer and Wigand (1986) in the Catlow Valley that were stabilized 7.2 ka.

Another line of evidence for Lake Chemult is the canyon of the Williamson River. The Williamson River is underfit relative to the canyon that it occupies in the Soloman Butte quadrangle (Figure 4). It flows south from Klamath Marsh into a canyon that has been eroded into basalt flows and hydrovolcanic deposits. This canyon is up to 100 m deep, 100 to 200 m wide at its base, and is about 8 km long. The volume of water that moves through this canyon currently seems insufficient to erode this size of a canyon into bedrock. Some of the basalt flows that the canyon has incised are early Pleistocene age. It is thought then that this canyon was formed during the Pleistocene when input to the river from the marsh was sufficient to form this canyon.

The upper terrace (middle Holocene)

The middle Holocene terrace (This feature is not actually a terrace, but a strand line. Terrace terminology is used to simplify the discussion.) is cut into pyroclastic-fall deposits from Mount Mazama and the upper elevation of its scarp averages 21 m above the current marsh level (Table 5). The terrace scarp begins as thinner than expected deposits of pyroclastic fall on the middle terrace. These deposits thicken up slope to the tread where the deposits are of uniform thickness. Identification of the terrace is made from a subtle slope break in the pyroclastic-fall deposits (Figure 12). This morphology is explained by the unique method of formation for this terrace.

Formation of the middle Holocene terrace occurred after the cataclysmic eruption of Mount Mazama. Pyroclastic-fall deposits from this eruption are reworked or removed up to the elevation of the middle Holocene terrace, but these deposits are undisturbed on the upper terrace tread. The middle Holocene terrace was not formed through planation as the lower terraces were; its formation was both erosional and depositional in origin.

Evidence of the middle Holocene terrace in the Wocus Bay, Military Crossing, Wildhorse Ridge, and Solomon Butte quadrangles includes rafted pumice and reworked pyroclastic-fall deposits. Scour channels, scoured surfaces, and rounded erratic boulders found in the Solomon Butte quadrangle suggest that the highest stand was accompanied by a rapid draining of Klamath Marsh.

Rafted Pumice

The pyroclastic-fall deposit from eruptions of Mount Mazama mantles the topography with up to 4.5 m of pumice, ash, and lithics in the Wocus Bay quadrangle. The description and distribution of this deposit in the Williamson River basin are presented by Young (1990) and for the Wocus Bay quadrangle by Conaway and Cummings (in preparation). The largest clasts of pumice that fell on the Wocus Bay quadrangle are 3-4 cm in diameter. Superimposed on these deposits at elevations below 1397 m and surrounding the Klamath Marsh are well-rounded clasts of pumice that are up to 40 cm in diameter. These large clasts of pumice are found in topographic depressions and constrictions, and resting on the middle terrace in the Wocus Bay quadrangle (Figure 11). West of Little Wocus Butte the rounded pumice is found in linear deposits that do not exceed an elevation of 1400 m. In the Solomon Butte

quadrangle the rounded clasts are found along the plateau to the west of the Williamson River canyon, and at the base of the Chemult plateau (Figure 17 and 18).

Williams (1942) first recognized the rafted pumice in Wocus Bay:

The water level in the marsh may have been higher than now, for at the head of Wocus Bay there are water-worn lumps of pumice between 20 and 30 feet above the present level. Of course the water level may not have been that much higher than at present, for the discharge of tremendous volumes of pumice into the marsh must temporarily have raised the level, and the flows, entering the water at great speed, must have caused powerful waves capable of carrying pumice lumps far up the opposite shore. Much of the pumice, after entering the marsh, escaped down the Williamson River, but most of it, after floating a short time, probably sank to the bottom.

The location that Williams (1942) describes at the head of Wocus Bay is the constriction between Wocus Bay and Yoss Creek Meadow.

In the Soloman Butte area, the rounded pumice on the plateau (west of the Williamson River, Figure 3) and south of the plateau was likely deposited as the waters overtopped the high point along the plateau. The pumice that is found in the scour channels was then deposited as the water receded and flowed down the canyon.

Isopleths of the climactic pumice fall (Young, 1990) indicate that clasts of pumice the size of those that are found rafted in the Wocus Bay area fell out of the plume within approximately 20 km of the vent. The inundation area for the highest stand of the marsh

overlapped this isopleth by 2 km, thus offering a possible source for the pumice of the size rafted into the Wocus Bay area. However, pumice clasts were also transported into the basin by the pyroclastic flows, which contain up to 10% pumice clasts in the deposits west of Little Wocus Butte and approximately 50% pumice clasts in the Military Crossing quadrangle to the north. The pyroclastic flows are the likely source for the rafted pumice because they would have transported the clasts well within reach of the backflooding on the western edge of Klamath Marsh. The clasts were then eroded from the pyroclastic flow and rafted throughout the basin. Some distinction can be made between the clasts of pumice that have been water transported versus those that have simply weathered from the pyroclastic flow. The clasts that are found within the pyroclastic-flow section and weathering from it are salmon pink, while those that have been rafted by water or are pyroclastic fall are buff. Roundness alone cannot be used to distinguish mode of transport because the clasts within the pyroclastic flows are also rounded. Where the large rounded clasts were found in linear deposits, in abundances greater than those in the pyroclastic-flow deposits, or in areas with no pyroclastic flow they were classified as rafted.

Reworked pyroclastic-fall deposits

Between the 1397 m elevation of the middle Holocene terrace and the modern marsh level, pumice-rich deposits lack the size distribution and sorting characteristics of the undisturbed pyroclastic-fall deposits. Samples of pyroclastic-fall deposits from

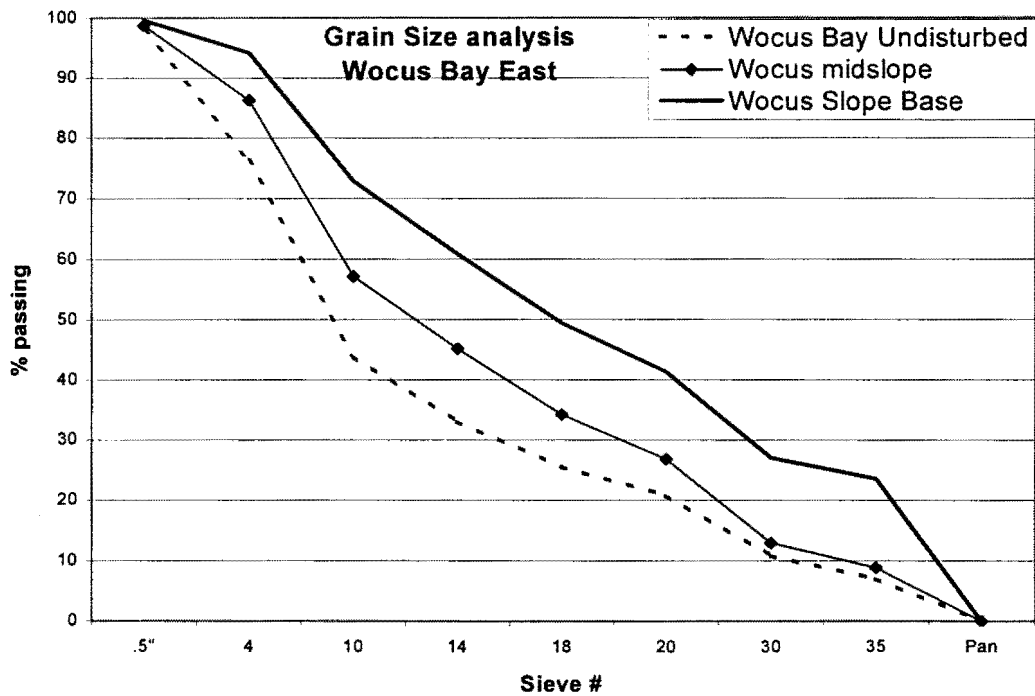
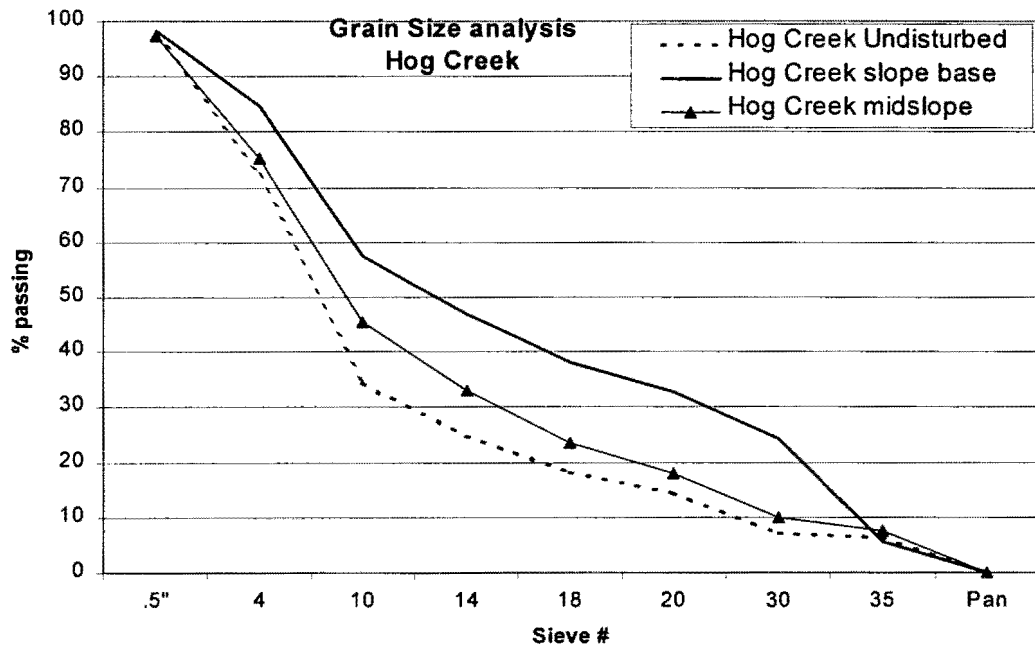


Figure 14: Grain size analysis of samples collected from the middle Holocene terrace scarp at Hog Creek and Wocus Bay east.

above and below 1397 m were collected from pits excavated along the survey transects Wocus Bay East and Hog Creek (Figure 11). The grain size of the pyroclastic-fall deposits decreases down slope from the tread of the middle Holocene terrace (Figure 14). The thickness of the pyroclastic-fall deposits also decreases from the tread. The decreases in grain size and thickness are a result of the backflooding eroding and floating the pyroclastic-fall deposits. The larger clasts of pumice float easier (Whitham and Sparks, 1986) and are therefore less prevalent on the middle Holocene terrace scarp than in the undisturbed section.

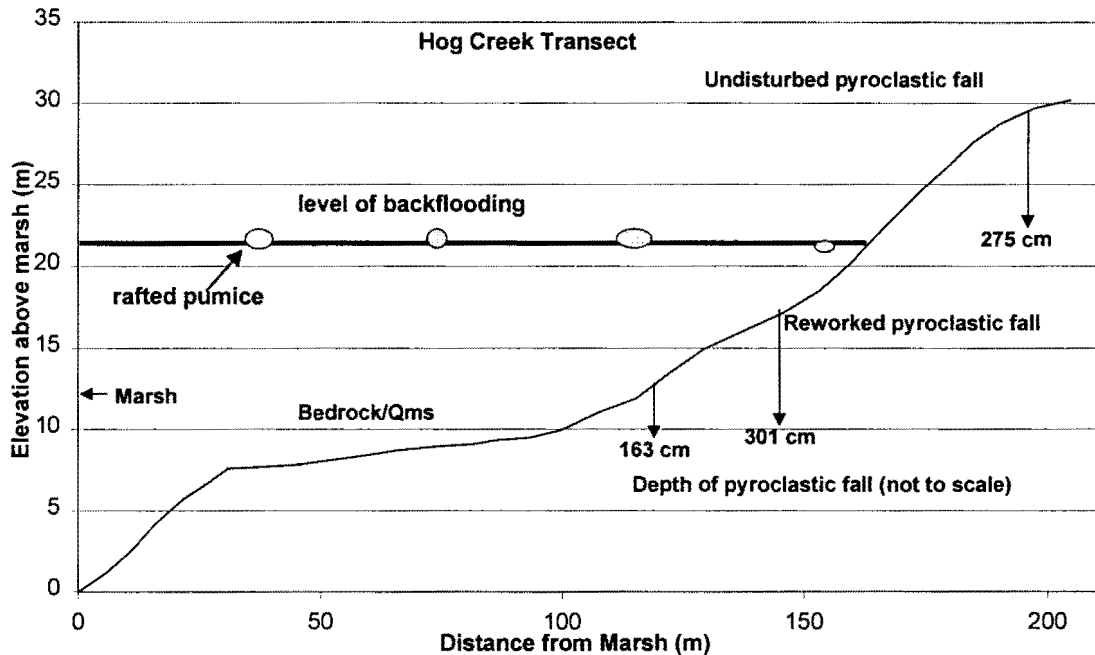


Figure 15: Thickness of pyroclastic-fall deposits on the middle Holocene terrace scarp at Hog Creek. Five times vertical exaggeration.

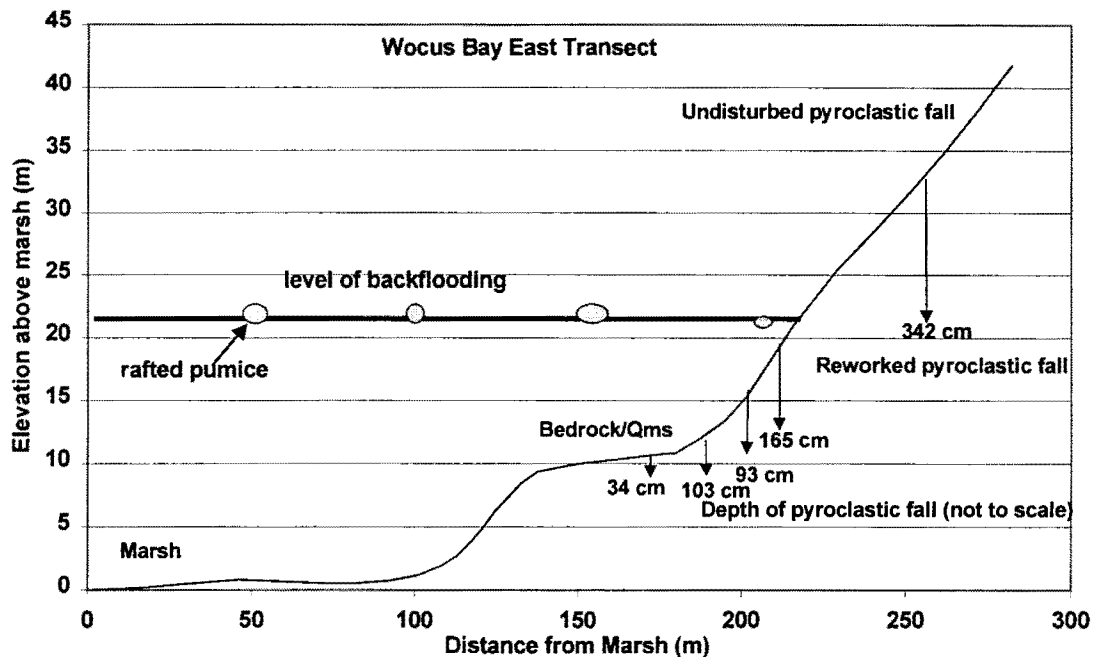


Figure 16: Thickness of pyroclastic-fall deposits on the middle Holocene terrace scarp at Wocus Bay East. Five times vertical exaggeration.

Scour channels

Several linear channels have been eroded into the pyroclastic-flow deposits in the Wocus Bay and Soloman Butte quadrangles. The channels in the Wocus Bay quadrangle are cut into a gently sloping plain underlain by pyroclastic-fall deposits (4.5 m) that dips toward the marsh on the west flank of Little Wocus Butte (Figure 11). These channels are about 1.5 to 2 m deep and 5 m wide. Rafted large clasts of pumice are found on the pyroclastic-flow deposits that these channels are incised into and within the channels. The channels in the Soloman Butte quadrangle are carved into a sloping plain west of the Williamson River canyon (Figure 17). Here, they are also eroded into pyroclastic-flow deposits and are up to 5 m deep and 10 m wide.

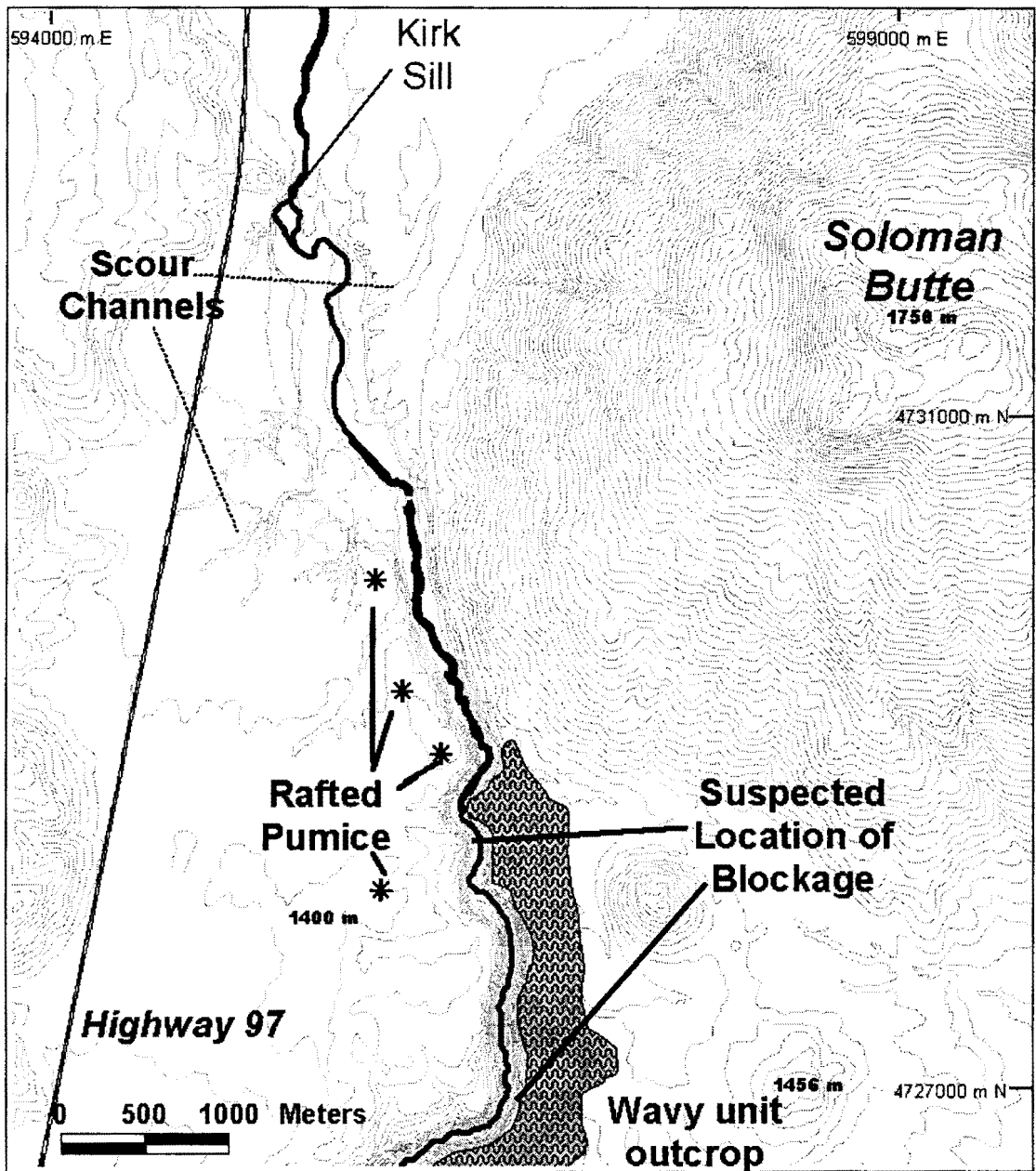


Figure 17: Scour channels and rafted pumice on the plateau west of the Williamson River canyon and location of the pyroclastic-flow blockage in the Soloman Butte quadrangle. Coordinates are UTM Zone 10, 6 m contour interval.

The thickness of the pyroclastic flows in this area is greater than 15 m (this minimum thickness was determined by hand augering within a 10 m deep scour channel in the pyroclastic flow to the 5 m limit of the auger). Rounded, large clasts of pumice are also found in these channels and on the pyroclastic flows that the channels are incised into. Channels in both locations are straight with no meanders. None of the channels shows evidence of recent stream occupation and all are forested with stands of Lodge Pole Pine.

Scoured surfaces

The eastern slope at the mouth of the Williamson River canyon is devoid of pyroclastic-fall deposits to an elevation of 15 m above the current channel. The pyroclastic-fall deposits in this area normally average 1.5 m in thickness. Well-rounded river cobbles have been deposited on this surface to the upper level of scouring.

Erratic boulders

The Williamson River canyon opens rapidly to a broad plain comprised of reworked pyroclastic deposits, gravels, and rounded boulders of three distinct lithologies (Figure 18). The lithologies found within the Williamson River canyon are thick palagonitic deposits produced from hydrovolcanic eruptions, distinctly wavy-textured basalt flows, and massive, diktytaxitic basaltic andesite flows (Lee and Cummings, in preparation). The palagonitic deposits crop out at the mouth of the canyon and in several locations south of the canyon mouth (Lee and Cummings, in preparation). The wavy-textured basalt flows crop out within the canyon approximately 6 km from the boulder deposit (Figure 18) and are also found along the canyon rim to the south.

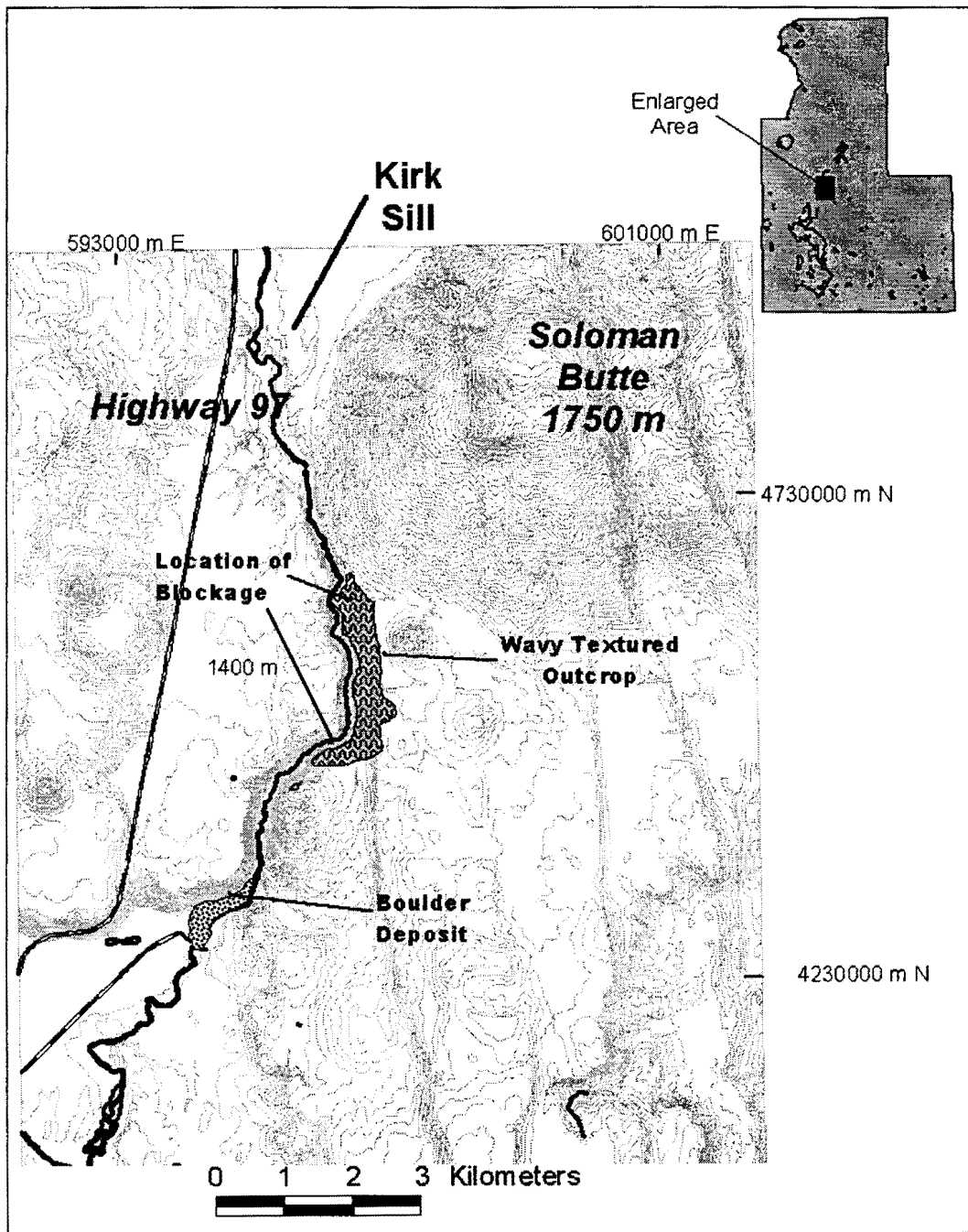


Figure 18: Soloman Butte quadrangle with location of boulder deposit, wavy outcrop, and location of pyroclastic-flow blockage. Coordinates are UTM Zone 10, 6 m contour interval.

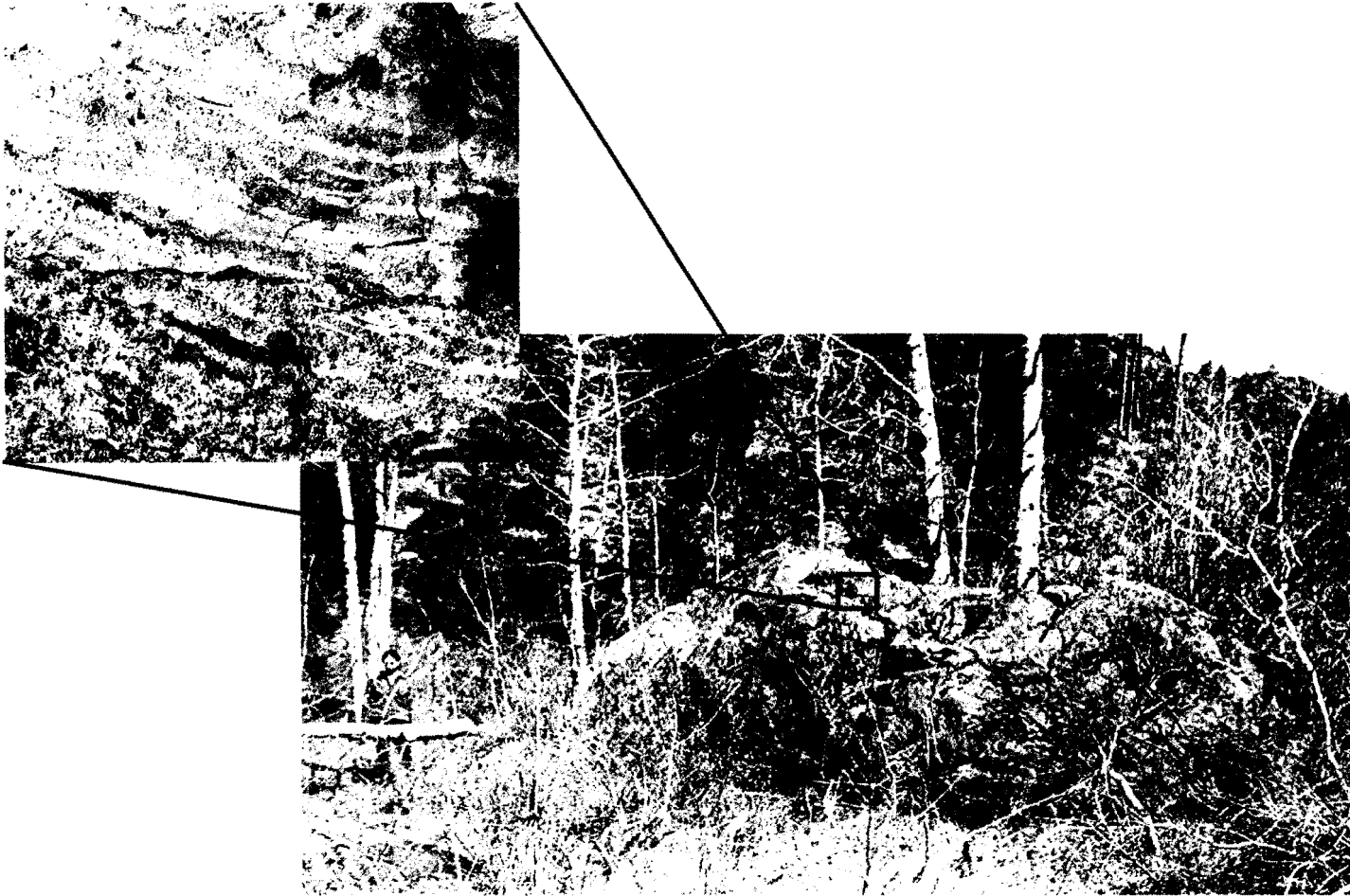


Figure 19: Rounded boulder of the wavy textured basalt at the mouth of the Williamson River canyon. Boulder is 6.7 m in its longest dimension.

The columnar jointed, diktytaxitic basaltic andesite crops out along the edge of the Chemult Plateau to the west.

The deposit contains boulders up to 6.7 m in the longest dimension (Figure 19) and grain size decreases away from the mouth of the canyon (Figure 20). The boulder deposit is bordered to the east by the current Williamson River channel and to the west by the Chemult Plateau (Figure 20). To the south, the boulder deposit grades to reworked pyroclastic-fall and pyroclastic-flow deposits. These deposits contain rounded clasts of pumice up to 7 cm in diameter with lenses of lithic rich sand (Appendix E).

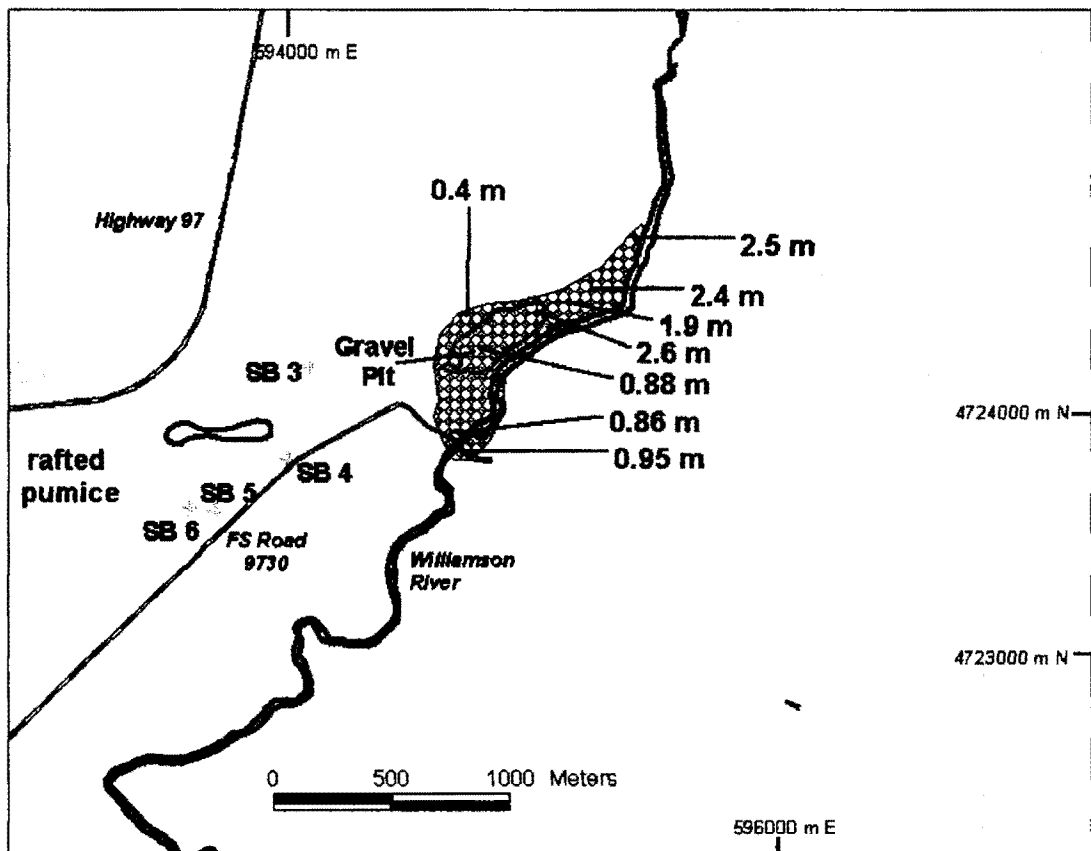


Figure 20: Locations of rafted pumice (*), auger holes (+), gravel pit, and boulder deposit (stippled pattern) with average intermediate axis diameter of erratics. Coordinates are UTM Zone 10, 6 m contour interval.

Portions of the deposit have been removed by quarrying, but the largest boulders were left behind. This has allowed for accurate measuring of the boulder diameters as well as the deposit thickness in these areas (Table 8).

The lower terrace (late Holocene)

The late Holocene terrace is cut into an organic-rich mixture of pumice and ash deposits at approximately 4.5 m above the current marsh. This terrace is only found in three of the locations surveyed (Figure 12) and has a tread that varies from 24 to 40 m in width.

The most recent fluctuations in the extent of Klamath Marsh are likely a combination of the redistribution of water for agricultural purposes, possible anthropogenic modification of a basalt flow, and climate change. Since the U.S. Bureau of Reclamation initiated the Klamath Reclamation Project in 1905 over 80% of the Klamath Basin's 1400 km² of wetlands have been converted to farm and cattle land (Allen, 1999). Agricultural needs have led to the diversion of the Williamson River before it reaches the marsh, which has likely reduced inflow affecting the surface elevation. The level of the marsh is controlled by input to the marsh and the base level is controlled by the Kirk Sill, a lava flow at the southern end of the marsh that water must first overtop before entering the Williamson River canyon. Anecdotal evidence reports that the Kirk Sill was blasted with dynamite at the turn of the century to lower the level of Klamath Marsh.

Early descriptions of Klamath Marsh by trappers and explorers provide evidence of the most recent fluctuations. Peter Skene Ogden was the first to describe Klamath Marsh when he visited it in November, 1826 (Davies, 1961; Dicken, 1980). His party

Table 8: Location (UTM Zone 10), size, lithology, and velocity required for transport of measured boulders at the mouth of the Williamson River canyon.

| Location (UTM) | | Distance From | Long (cm) | Intermediate (cm) | Intermediate | | Estimated | Estimated | Velocity (m/s) | Discharge m ³ /s |
|----------------|----------|---------------|---------------|-------------------|------------------|---------------|-------------------|-----------|---------------------|-----------------------------|
| Easting | Northing | breach (km) | Axis Diameter | Axis Diameter | Average (cm) | Lithology | Channel Width (m) | Depth (m) | $v=0.29 D_i^{0.60}$ | $Q=wdv$ |
| 594734 | 4724530 | 5.0 | 100 | 80 | | wavy | | | | |
| | | 5.0 | 100 | 80 | | hydrovolcanic | | | | |
| | | 5.0 | 124 | 80 | 88 | hydrovolcanic | 329 | 5 | 4.26 | 7003 |
| | | 5.0 | 110 | 60 | σ +/- 30 | hydrovolcanic | | | | |
| | | 4.9 | 200 | 140 | | hydrovolcanic | | | | |
| 594704 | 4724483 | 4.8 | 440 | 330 | 255 | wavy | 329 | 5 | 8.06 | 13258 |
| 594704 | 4724483 | 4.8 | 345 | 180 | σ +/- 106 | wavy | | | | |
| 594787 | 4724632 | 4.8 | 310 | 185 | | wavy | | | | |
| | | 4.8 | 140 | 75 | 153 | hydrovolcanic | 329 | 5 | 5.93 | 9758 |
| | | 4.8 | 235 | 200 | σ +/- 68 | wavy | | | | |
| 594856 | 4724708 | 4.7 | 330 | 240 | 257 | wavy | 329 | 5 | 8.10 | 13321 |
| | | 4.7 | 340 | 275 | σ +/- 24 | hydrovolcanic | | | | |
| 594865 | 4724728 | 4.7 | 90 | 30 | | wavy | 329 | | | |
| | | 4.7 | 46 | 26 | 35.3 | wavy | 329 | 5 | 2.46 | 4048 |
| | | 4.7 | 66 | 50 | σ +/- 3 | wavy | 329 | 5 | 3.03 | 4988 |
| 594802 | 4724749 | 4.7 | 150 | 110 | 110 | wavy | 329 | 5 | 4.87 | 8006 |
| 594714 | 4724685 | 4.7 | 69 | 49 | 49 | hydrovolcanic | 329 | 5 | 3.00 | 4928 |
| 594640 | 4723930 | 5.1 | 120 | 105 | | wavy | | | | |
| | | 5.1 | 84 | 77 | 86 | wavy | 670 | 2.7 | 4.18 | 7569 |
| | | 5.1 | 95 | 90 | σ +/- 15 | wavy | | | | |
| | | 5.1 | 93 | 70 | | wavy | | | | |
| 594690 | 4723910 | 5.1 | 132 | 93 | | wavy | | | | |
| | | 5.1 | 200 | 120 | 96 | wavy | 670 | 2.7 | 4.48 | 8101 |
| | | 5.1 | 100 | 80 | σ +/- 17 | wavy | | | | |
| | | 5.1 | 155 | 90 | | wavy | | | | |
| 595292 | 4724748 | 4.1 | 283 | 175 | | wavy | | | | |
| | | 4.1 | 410 | 290 | | wavy | | | | |
| | | 4.1 | 230 | 150 | 251 | wavy | 140 | 10 | 7.98 | 11172 |
| | | 4.1 | 450 | 230 | σ +/- 78 | wavy | | | | |
| | | 4.1 | 540 | 340 | | wavy | | | | |
| 4.1 | 670 | 320 | | wavy | | | | | | |

Note: Parameters based on flow-competence methods of O'Connor (1993).
Channel width was estimated from width of deposit
Channel depth was estimated from thickness of deposit and from elevation of scoured surfaces

visited a native village in the middle of Klamath Marsh that was surrounded by water too deep to be approached by foot or horseback. J.C. Frémont visited this same village in the summer of 1843 and found no difficulty in riding to the village (Frémont, 1856).

The fluctuations described by early visitors to the marsh were likely seasonally or climatically induced and would have formed the late Holocene terrace. The lowering of the Kirk Sill coupled with the diversion of the Williamson River have likely reduced the level of the marsh from the late Holocene terrace surface to its current elevation.

Synopsis

The formation of the terraces is separated into three stages (Figure 21):

Stage 1: During the Pleistocene, Pleistocene lake Chemult occupied the area now known as Klamath Marsh. Seasonal and more long-term climatic changes during the Pleistocene induced fluctuations in the extent of Lake Chemult. These fluctuations planed the Pleistocene terrace into bedrock and colluvium.

Stage 2a: Middle Holocene eruptions from Mount Mazama deposit an average of 3.5 m of pyroclastic fall on the Wocus Bay quadrangle.

Stage 2b: Pyroclastic flows from the eruption form a blockage in the Williamson River canyon. Backflooding inundates the marsh, and forms a lake with a shoreline at 1397 m rafting the ash and pumice from the recently deposited pyroclastic fall and flow.

Stage 2c: Catastrophic breaching of the blockage results in the rapid draining of the marsh, stranding water rafted clasts of pumice on the middle terrace.

Stage 3: Climatic fluctuations plane the late Holocene terrace and agricultural modifications lower the marsh to its present elevation of 1376 m.

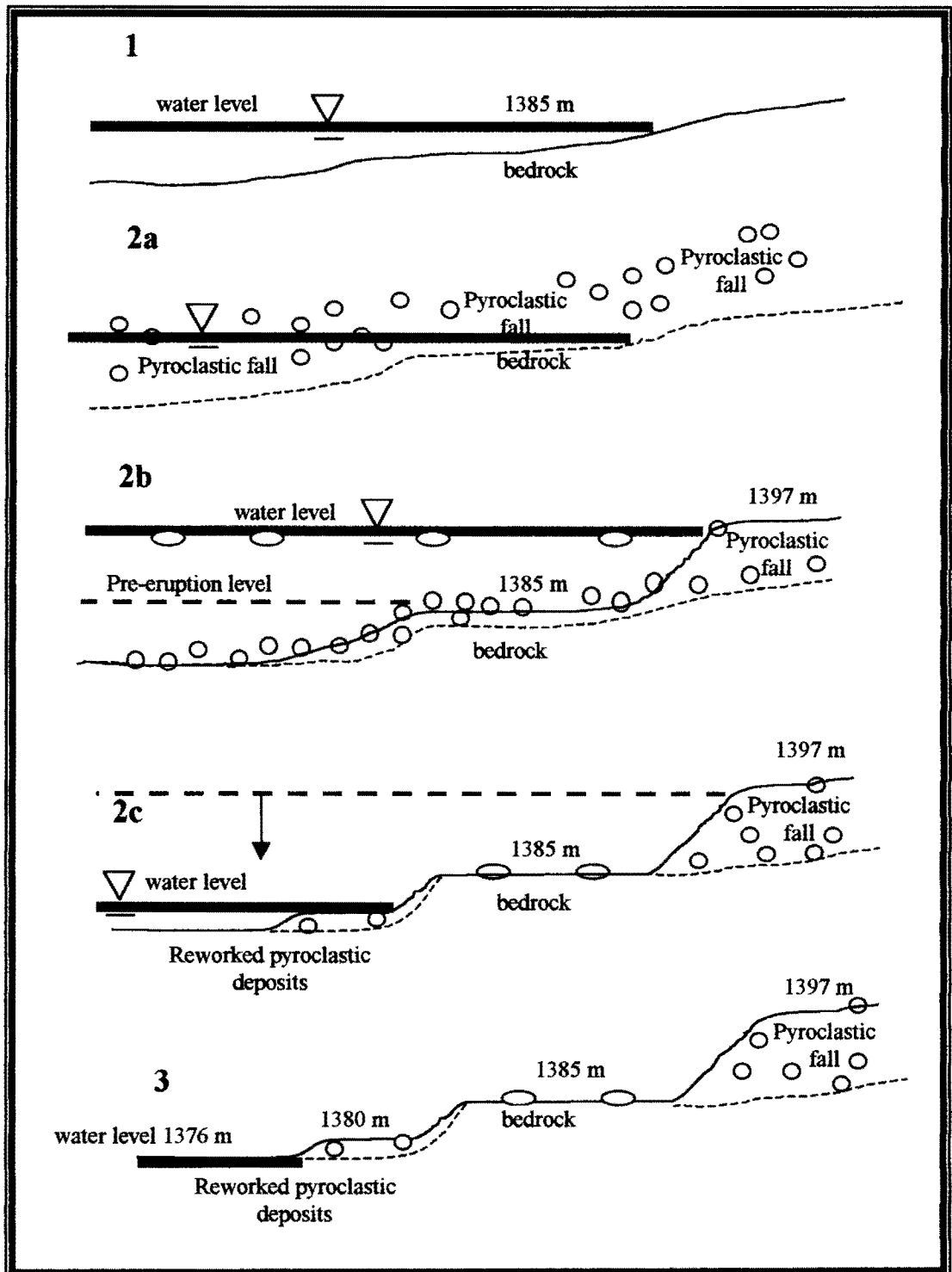


Figure 21: Three-stage development of terraces found along the eastern edge of southern Klamath Marsh. Figure is not to scale.

Discussion

To backflood the Klamath Marsh to the 1397 m elevation of the middle Holocene terrace a blockage of the basin's only outlet is required. The logical place for this blockage is in the canyon west of Soloman Butte (Figure 22). The river is confined to a slightly sinuous bedrock canyon that is only 75 to 100 m wide. Following the eruptions of Mount Mazama the basin was inundated with pyroclastic fall and pyroclastic flows. The pyroclastic flows were confined to drainages as they traveled off the eastern flanks of Mount Mazama en route to the Klamath Marsh where they were directed by the topography towards the Williamson River canyon. Within the canyon the flows likely became constricted and formed a blockage. The blockage is believed to have occurred at the point where the canyon begins to narrow and meanders slightly (Figure 17 and 18). The size of a blockage in this location was estimated from the topographic map to be 38 m high. Water entering the basin then backed up behind this constriction to the elevation of the middle Holocene terrace slope break at approximately 1397 m. The upper elevation of the plateau west of the Williamson River canyon coincides with that of the middle Holocene terrace slope break. Thus, the elevation of the plateau was a limiting factor for the extent of the backflooding caused by the pyroclastic flow constriction. This also suggests that the water was overtopping both the constriction and the plateau. Rafted pumice found across the plateau support this interpretation (Figure 17).

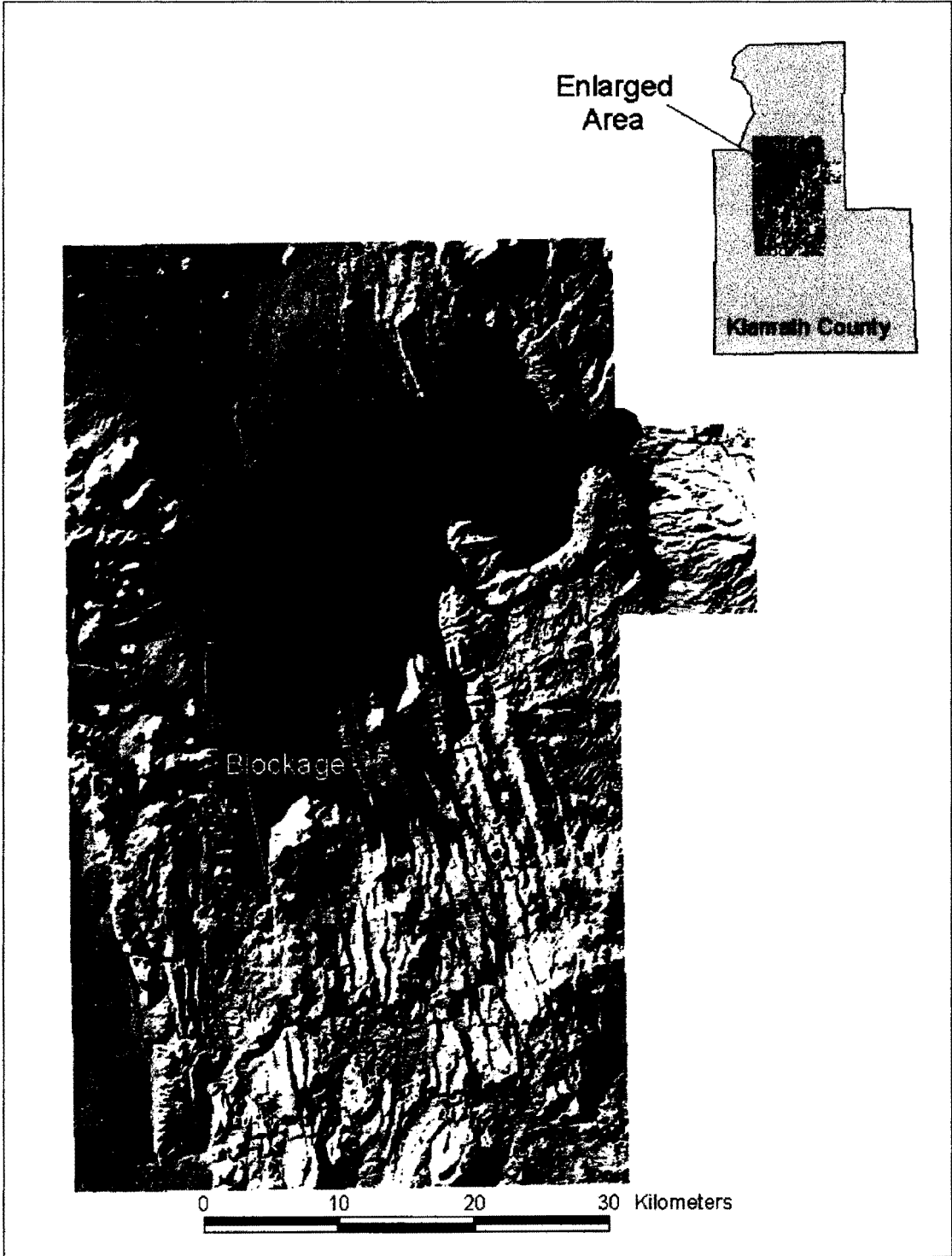


Figure 22: Extent of backflooding that resulted from the pyroclastic-flow blockage in the Williamson River canyon.

Rafted Pumice

The rounded clasts of pumice found in the Wocus Bay area were water transported to their current location when the damming of the Williamson River backflooded the Klamath Marsh. The clasts are found at the 1397 m upper limit of the floodwaters in only a few locations. The deposits are also found in constrictions such as Skellock Draw in the Wildhorse Ridge quadrangle, and the constriction between Yoss Creek Meadow and Wocus Bay, where Williams (1942) first described the rounded pumice. In these locations, the pumice-laden floodwaters would have backed up in these hydraulic constrictions as the area was being drained. This resulted in the high concentration of rounded pumice clasts in these areas. The clasts are also commonly found on the broad Pleistocene terrace in the Wocus Bay quadrangle. Deposition on this surface is also thought to have occurred as the water receded stranding the larger clasts on the broad terrace as the impounded water rapidly receded. The linear deposits that are found to the west of Little Wocus Butte are interpreted as shorelines of the temporary lake.

Scour Channels

Formation of the scour channels is thought to have occurred when the backflooding rapidly receded. The water saturated ash would have been easily eroded as the level of backflooding dropped. The channels in the Soloman Butte quadrangle are larger than those in the Wocus Bay area. The channel size is likely the result of the steeper gradient of the surface in the Soloman Butte area. Incision of the channels occurred as the impounded water was evacuated down the canyon after failure of the blockage. The presence of these channels in both areas and their linear morphology suggests that the draining of the marsh was rapid (Figures 15 and 16).

Catastrophic breaching of the pyroclastic flow dam

The presence of rounded erratic boulders, scoured surfaces, deposition of river cobbles above the current channel, and the scour channels, all in the Soloman Butte quadrangle indicate a catastrophic breaching of the pyroclastic flow constriction within the Williamson River canyon. The coinciding elevation of the middle Holocene terrace and the plateau as well as the presence of rafted pumice on the plateau south of the constriction indicate that the impounded water overtopped the pyroclastic flow constriction. Overtopping leads to rapid dam failure by the headward erosion of channels in the downstream side of the dam.

Boulders that are found on the outwash plain are a conglomeration of material that was in the channel prior to the flood and material that was plucked from the outcrops lining the canyon. The wavy textured basalt boulders crop out in the canyon at the location of the suspected blockage. This lithology is also found south of the blockage along the canyon rim, but these outcrops would have been above the level of scouring in the canyon. Talus from these outcrops likely contributed to the boulders that were entrained by the downstream flooding. The boulders of hydrovolcanic deposits found in the outwash plain were transported less than 1 km, but their presence is significant. This lithology is quite susceptible to physical weathering and would not have withstood typical stream transport to its present position. It can then be inferred that these boulders were plucked from the hydrovolcanic outcrop near the mouth of the canyon and deposited in their present position in a single event.

The velocity of the flood and size of the material transported rapidly decreased as the flood left the canyon. Beyond the delineated boulder deposit are deposits of rounded

pumice, sand, and ash. Hand auger SB4 (Figure 20, Appendix E) encountered 74 cm of reworked pyroclastic deposits that were underlain by cobbles. These cobbles could be river deposits or flood deposits, but since undisturbed pyroclastic fall was not encountered in this section, the underlying cobbles are likely part of the flood deposits. This stratigraphy indicates that the flood velocities were decreasing and deposition of finer grained material was taking place. The lenses of sand intermixed with rounded clasts of pumice in auger SB5 suggest either pulses in the waning flood discharge or primitive channel migration.

The current Williamson River channel flows along the eastern edge of the boulder deposit and then crosses the deposit about 1 km from the mouth of the canyon (Figure 20). The concentration of the boulder deposit to the west of the current channel is the product of hydraulic routing of the outburst flood. Two factors likely influenced this routing. The paleochannel of the Williamson River could have occupied a channel west of its current position. The outburst flood upon exiting the canyon would have been directed by the channel to the west. Another possibility is that as the floodwaters left the canyon, they would have been deflected to the west by a westward bend in the canyon at its mouth. This is the more likely scenario given that the water was scouring surfaces approximately 15 m above the current channel at the mouth of the canyon. The paleochannel of the river likely had little influence on a flood of this magnitude.

Magnitude of the outburst flood

The paleohydrologic reconstruction of the outburst flood is based on upstream and downstream geomorphic evidence and hydraulic principles. Estimates of the peak-discharge of the outburst flood were determined with three methods:

1. Flow-competence
2. Empirically based dam-break model
3. Physically based dam-break model

Flow-Competence

Flow competence equations are based upon empirical correlations and theoretical formulas relating the largest clasts transported by a flood to velocity, shear stress, and stream power (Baker and Ritter, 1975; Costa, 1983; Komar, 1989; O'Connor, 1993). For this study the regression relation for velocity developed by O'Connor (1993) in a study of the Bonneville flood is used. O'Connor (1993) used geologic evidence coupled with the step-backwater method to develop regressions for velocity, stream power, and shear stress. This regression is particularly useful for this study where the deposit has been quarried because it is based upon the largest clasts transported rather than a median grain size. The following equation (O'Connor, 1993) was used to estimate velocity:

$$v = 0.29D_i^{0.60}$$

where D_i is the intermediate axis diameter (cm), and v is the flow velocity (m s^{-1}). The results of the flow-competence calculations and their averages at each site are given in Table 8. The discharge (Q) was then estimated by the relation $Q=wdv$, where w is the flow width and d is the flow depth. The flow width was estimated from the width of the boulder deposit and the depth was estimated from the elevation of the scour surface at the mouth of the canyon and the depth of the boulder deposit elsewhere (Table 8). The maximum discharge estimate with this method is $1.5 \times 10^4 \text{ m}^3\text{s}^{-1}$. An average discharge of $1.3 \times 10^4 \text{ m}^3\text{s}^{-1}$ was calculated for two sites (Table 8).

Empirically based dam-break analogy

Costa and Schuster (1988) used a regression analysis with potential energy as the independent variable to derive equations for landslide, glacier, moraine, and earth- and rock-fill dam-break discharges. The data used to construct the equations are gathered from historic dam-failures where good estimates of potential energy of the back-flooded area and resultant discharges were available. For this study, the equation for a landslide dam-break is used. This equation was chosen because landslide dams are typically wide at their base, comprised of large volumes of material, and are usually easily eroded (Costa and Schuster, 1988). These characteristics make them most analogous to a pyroclastic flow dam in the Williamson River canyon. The empirical relation for peak discharge (Q_p) from the failure of a landslide dam (Costa and Schuster, 1988) is:

$$Q_p = 0.0158E_p^{0.41}$$

where the potential energy of the lake (E_p) = $\rho_w g d V_0$. For the lake formed by the pyroclastic flow constriction, $d = 17$ m (drop in water from elevation of middle Holocene terrace at 1397 m to the elevation of the late Holocene terrace at 1380 m), and $V_0 = 5.7 \times 10^9$ m³ (volume drained from the lake). Using $\rho_w = 10^3$ kg m⁻³ (density of water) and $g = 9.8$ m s⁻² (acceleration due to gravity), this equation yields a peak discharge of 2.2×10^4 m³s⁻¹.

Physically based dam-break model

Walder and O'Connor (1997) evaluated regression relations that are used for predicting peak discharge and determined that factors not used in these relations actually provided the greatest influence on the discharge. These factors are the erosion rate of the dam (k), and the morphology of the dam and basin.

Walder and O'Connor (1997) outline “benchmark” predictive relations that are based on mean values from typical natural dams and can be used for hazard-assessment purposes. Fundamental to these relations is the dimensionless parameter η , that is defined as

$$\eta = k V_0 g^{-0.5} d^{-3.5}$$

where k is the erosion rate of the dam (m s^{-1}), V_0 is the volume of water drained by the breach (m^3), g is the acceleration due to gravity (m s^{-2}), and d is the drop in water level during down stream flooding (m). If this parameter is significantly greater than 1, then the following equation is justified for determining peak discharge

$$Q_p = 1.94 g^{0.5} d^{2.5} (D_c d^{-1})^{0.75}$$

where Q_p is peak discharge, and D_c is height of dam crest relative to dam base (Table 9).

The value 1.94 is a multiplier derived from the morphology of the breach. For the pyroclastic flow dam on the Williamson River the erosion rate (k) is unknown. Data compiled by Froehlich (1987) show that k for constructed earthen dams are between 1 and 10^3 m hr^{-1} . The compaction of a pyroclastic flow dam is likely less than that of a constructed earthen dam, but values from 1 to 10^4 m hr^{-1} were used to determine η and the results are all significantly greater than 1 (Table 9). The erosion rate is actually not significant for lakes that have large volumes for a given depth because erosion of the dam will be complete before any significant decrease in volume has occurred. If the dimensionless parameter V^*_0 ($V^*_0 = V_0 / d^3$) is greater than 10^4 , erosion rate has little affect on peak discharge (Walder and O'Connor, 1997). For the flooded area behind this blockage that was drained V^*_0 equals 1.2×10^6 .

The peak discharge that was determined with the physically based dam-break model of Walder and O'Connor (1997) is $1.3 \times 10^4 \text{ m}^3 \text{ s}^{-1}$. A summary of estimated discharges and their associated variables is found in Table 9.

Table 9: Summary of discharge estimates and variables.

| Variable | Parameter | Value |
|----------|---|--|
| | Flow Competence (O'Connor, 1994) | $1.3 \times 10^4 \text{ m}^3 \text{ s}^{-1}$ |
| Q_p | Peak discharge | |
| | Empirically based dam-break model (Costa and Schuster, 1988) | $2.2 \times 10^4 \text{ m}^3 \text{ s}^{-1}$ |
| | Physically based dam-break model (Walder and O'Connor, 1997) | $1.3 \times 10^4 \text{ m}^3 \text{ s}^{-1}$ |
| d | Drop in water level (1397 m – 1380 m (level of Late Holocene lake)) | 17 m |
| D_c | Height of dam crest relative to base (determined from topographic map) | 38 m |
| k | Erosion rate (unknown, but determined to be insignificant to Q_p) | $1-10^4 \text{ m s}^{-1}$ |
| E_p | Potential energy of lake = $\rho_w g d V_0$ | $9.5 \times 10^{14} \text{ joules}$ |
| ρ_w | Density of water | 10^3 kg m^{-3} |
| V_0 | Volume of water drained from lake | $5.7 \times 10^9 \text{ m}^3$ |
| V^*_0 | Dimensionless measure of total volume drained from the lake = V_0^3/d^3 | 1.2×10^6 |
| g | Acceleration due to gravity | 9.81 m s^{-2} |

Evaluation of the discharge estimate techniques

The highest discharges determined using the flow-competence equation and the channel dimensions (Table 8) were for boulders in the gravel pit located in the middle of the deposit. The intermediate axis of these boulders was smaller than the measured intermediate axis of the boulders at the mouth of the canyon that were not excavated. This discrepancy in discharge is the result of overestimation of the channel width and/or depth at the gravel pit. The channel width was determined from the width of the boulder deposit and assumes that the deposit was emplaced in one event. The deposit is likely more of a fan that had channels migrating across its width as the flood stage decreased. The estimation of channel width and depth at the mouth of the canyon is thought to be more accurate because it is constrained by the river to the east and the plateau to the west. The maximum estimated discharge for this location is $1.07 \times 10^4 \text{ m}^3 \text{ s}^{-1}$. However, the velocity estimates for these boulders is likely conservative because they were not excavated and their complete dimensions could be concealed by overburden.

The flow-competence equation is also likely a conservative estimate of the peak discharge because it is based on boulders found ~6 km from the suspected dam location. The discharge likely decreased over this distance, but the decrease would have been small because the flow was confined to the canyon across this distance. Material that is currently found in the canyon was not used in the flow competence equation because it is difficult to distinguish the material associated with the dam-break from colluvium. Another factor that leads to the underestimation of discharge with this method is the size of the material that was available for transport. Columnar jointed basalt would produce boulders with a size limitation dependent on the jointing

pattern. The wavy textured basalt is a massive unit and the material derived from its outcrops would not have these limitations.

The empirically based dam-break model is limited in its estimate of the discharge because it only uses the volume of water impounded by the blockage and the drop in the level of this water. This method would provide the same discharge estimation for a dam that was several kilometers in width as it would for a dam that was only a few meters in width, provided that the volume and drop in water level of the flooded areas was equal. This equation must also be used with caution because it is derived from data supplied by a variety of sources at different locations. This method is based on discharges gathered downstream of the breach with no consideration of energy losses or translation of the flood wave and is therefore an underestimation of discharge in most situations (Walder and O'Connor, 1997; Waythomas et al., 1996). The most significant limit to this method is that most discharges are controlled by factors other than the volume and drop in lake level (Walder and O'Connor, 1997). The factors that are usually the primary influences on peak discharge are erosion rate of the impoundment and to a lesser extent the geometry of the breach and basin (Walder and O'Connor, 1997).

The physically based model is considered to be the most accurate estimate of discharge at the breach. Uncertainties in this method lie with the calculation of shape multiplier. This factor is based on average shape parameters (channel size and morphology) from historic dam-breaks and these parameters are not exactly known for the constriction on the Williamson River. Variances in these parameters would not

however greatly affect the estimated peak discharge.

Duration

Rough estimates for the duration of the backflooding from the pyroclastic flow dam can be made indirectly from comparison to landslide dams, geologic evidence, and hydrologic characteristics of the basin.

The three factors that control the stability of natural dams are the rate of inflow to the impoundment, the size and shape of the dam, and the geotechnical characteristics of the dam (Costa and Schuster, 1988). Rate of inflow to the impoundment is difficult to estimate, but the existence of landslide dams is short when a small slide blocks a stream with a large drainage area (Swanson et al., 1986). Since the dam and the plateau were overtopped by floodwaters, it can be concluded that the rate of inflow was greater than the rates of seepage through the impoundment and evaporation. The relatively uniform grain size of this impoundment would have prevented extensive piping through the dam. The dam was likely thicker than typical constructed earthen dams, because the pyroclastic flows were utilizing the channel as well as flowing into it from the west creating a long constriction in the canyon. This thickness would have contributed to the stability of the impoundment. Landslide dams that are composed of large or cohesive materials are more stable than those composed of soils or loose rock (Costa and Schuster, 1988). Ash, although fine grained, is quite cohesive when moist. The factors controlling the failure of the dam after its overtopping would have been the erosion rate of the ash on the downstream side and the length of the impoundment within the canyon. Failure likely occurred shortly after the overtopping of the dam, so the

longevity of the pyroclastic flow impoundment was primarily controlled by the rate of inflow to the impoundment.

To fill the basin with water to an elevation of 1397 m from the late Holocene elevation of Klamath Marsh requires the addition of $5.7 \times 10^9 \text{ m}^3$ of water. To achieve this with the highest recorded discharge from the gauging station along the Williamson River at the Kirk Sill would require 4.75 years. This is a likely overestimate for several reasons. At the time of the cataclysmic eruption, glaciers perhaps 60 m thick occupied the Sun and Kerr Valleys (Williams, 1942). The eruption would have caused extensive melting of these glaciers and the resultant meltwater from Kerr Valley would have contributed to the flooding of Klamath Marsh. Water that was present in the marsh at the time of the eruption would have been displaced by the sinking of pyroclastic fall and the emplacement of pyroclastic flows. The depth of these deposits in Klamath Marsh is over 20 m in some locations.

The rafted clasts of pumice found in Wocus Bay can be loosely used to infer the longevity of the lake. A simple experiment consisting of a bucket of water and rafted clasts of pumice retrieved from Wocus Bay revealed that these clasts would currently float no longer than 5 days. These samples weathered since they were erupted and certainly were able to float for a longer period prior to this weathering. Rafted pumice for the 1952 eruption of Volcan Barcena on Isla San Benedicto, Mexico produced pumice rafts that were sighted floating in the Pacific Ocean for a minimum of three years following the eruption (Richards, 1958). Eruptions from the Rabaul Caldera,

Papua New Guinea in 1878 and 1937 produced pumice rafts several meters thick that hampered shipping for several months after the eruptions (McKee et al., 1985).

An estimate of the time to drain the lake can be made by assuming that a hydrograph of the discharge is triangular and dividing twice the volume by the peak discharge. Using this method, it would have taken 2.5 days to drain the flooded area impounded by the dam.

Conclusions

The extensive Pleistocene terrace that has been planed into bedrock and colluvium is the product of climate fluctuations during the Pleistocene. Pleistocene lake Chemult, which covered an area of 390 km², likely occupied this basin between about 32 ka and 11 ka. The increased inflow to the basin lead to the development of the Williamson River canyon. Desiccation of this lake exposed fine grained lake sediments that were then easily eroded and transported by winds forming the parabolic dunes found in the northeast corner of the basin

The cataclysmic eruption of Mount Mazama (7627±150 cal yr B.P.; Zdanowicz et al., 1999) and resultant pyroclastic flows were responsible for backflooding that rose 22 m above the current level of Klamath Marsh to an elevation of approximately 1400 m. This large-scale backflooding was the result of a pyroclastic flow constriction along the Williamson River in the Soloman Butte quadrangle. Failure of the pyroclastic flow constriction was catastrophic and resulted from overtopping by the impounded water. Discharges generated by the dam failure are estimated to have been $1.3 \times 10^4 \text{ m}^3\text{s}^{-1}$. The resultant downstream flooding transported boulders up to 6.7 m in length approximately

6 km. The boulder deposit rapidly grades to clasts 1 m in diameter in 1 km. The flood deposits have confined the current Williamson River channel to the east at the mouth of the canyon. The upstream effects of the dam include terrace formation, channels scoured into pyroclastic-flow deposits, reworking of pyroclastic-fall and pyroclastic-flow deposits, and the inundation of $5.6 \times 10^8 \text{ m}^2$.

The most recent fluctuation in the extent of Klamath Marsh is attributed to the agricultural redistribution of water resources in the Williamson River basin. The diversion of inflow to the basin and the purported lowering of the Kirk Sill are the likely mechanisms behind the lowering of Klamath Marsh to its current level.

References

- Adams, R. M., and Seong, H. C., 1998, Agriculture and endangered species: An analysis of trade-offs in the Klamath Basin, Oregon: *Water Resources Research*, v. 34, no. 10, p. 2741-2749.
- Allen, L., 1999, Klamath's troubled Basin-Replacing the missing pieces: *Nature Conservancy*, v. 49, no. 2, p. 19-23.
- Allison, I. S., 1945, Pumice beds at Summer Lake, Oregon: *Geological Society of America Bulletin*, v. 56, no. 8, p. 789-807.
- Allison, I. S., 1979, Pluvial Fort Rock Lake, Lake County, Oregon: Oregon Department of Geology and Mineral Industries Special Paper 7, p. 72.
- Allison, I. S., 1982, Geology of Pluvial Lake Chewaucan, Lake County, Oregon: *Oregon State University Studies in Geology*, 11, 78 p.
- Baker, V. R., and Ritter, D. F., 1975, Competence of rivers to transport coarse bed-load material: *Geological Society of America Bulletin*, v. 86, p. 975-978.
- Bryan, K., 1919, Classification of springs: *Journal of Geology*, v. 27, p. 522-61.
- Conaway, J. S., and Cummings, M. L., in preparation, Geologic Map of the Wocus Bay quadrangle, Klamath County, Oregon: Oregon Department of Geology and Mineral Industries, scale 1:24000.
- Costa, J. E., 1983, Paleohydraulic reconstruction of flash-flood peaks from boulder deposits in the Colorado Front Range: *Geological Society of America Bulletin*, v. 94, p. 986-1004.
- Costa, J. E., and Schuster, R. L., 1988, The formation and failure of natural dams: *Geological Society of America Bulletin*, v. 100, p. 1054-1068.
- Davies, K. G., 1961, Peter Skene Ogden's Snake Country Journal 1826-1827: London, England, The Hudson Bay Record Society, p. 31-57.

- Dicken, S. N., 1980, Pluvial Lake Modoc, Klamath County, Oregon, and Modoc and Siskiyou Counties, California: *Oregon Geology*, v. 42, no. 11, p. 179-187.
- Dugas, D. P., 1998, Late Quaternary variations in the level of paleo-lake Malheur, Eastern Oregon: *Quaternary Research*, v. 50, p. 276-282.
- ESRI, 1998. Arc View GIS, Version 3.1. Environmental Systems Research Systems, Inc., Redlands, CA
- Feth, J. H., 1961, A new map of western conterminous United States showing the maximum known or inferred extent of Pleistocene lakes: U.S. Geological Survey Professional Paper 424-B, p. B110-B112.
- Fetter, C. W., 1994, *Applied Hydrogeology*, 3rd edition: New York, NY, Macmillan College Publishing, 691 p.
- Forbes, C. F., 1972, Pleistocene shoreline morphology of the Fort Rock Basin, Oregon [Ph.D. dissertation]: University of Oregon, 203 p.
- Frémont, J. C., 1856, *Memoirs of my life*: Chicago, Ill., Longman, Green, and Company, 507 p.
- Froehlich, D.C., 1987, Embankment-dam breach parameters, *in* R.M. Ragan, editor, *Proceedings of 1987 National Conference on Hydraulic Engineering*, American Society of Civil Engineers, New York, p. 570-575
- Gardner, J. E., Carey, S., and Haraldur, S., 1998, Plinian eruptions at Glacier Peak and Newberry volcanoes, United States: Implications for volcanic hazards in the Cascade Range: *Geological Society of America Bulletin*, v. 110, no. 2, p. 173-187.
- Gilbert, G. K., 1890, *Lake Bonneville*: U.S. Geological Survey Monograph 1, 438. p.
- Gustafson, F., 1971, *The Klamath Basin*: Oregon Water Resources Board, 288 p.
- Hamilton, W. L., and Minor, D. R., 1993, Progress in identifying lake and river terraces to measure Holocene deformation at Yellowstone caldera, *in* *Eos, Transactions, American Geophysical Union*, AGU 1993 Fall Meeting, San Francisco, CA, p. 592.

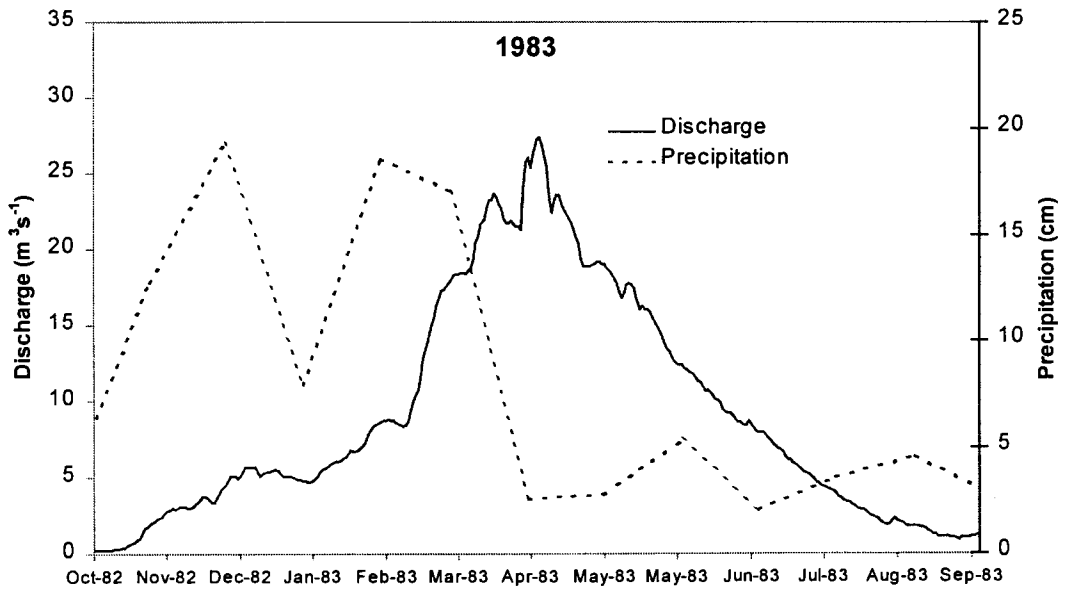
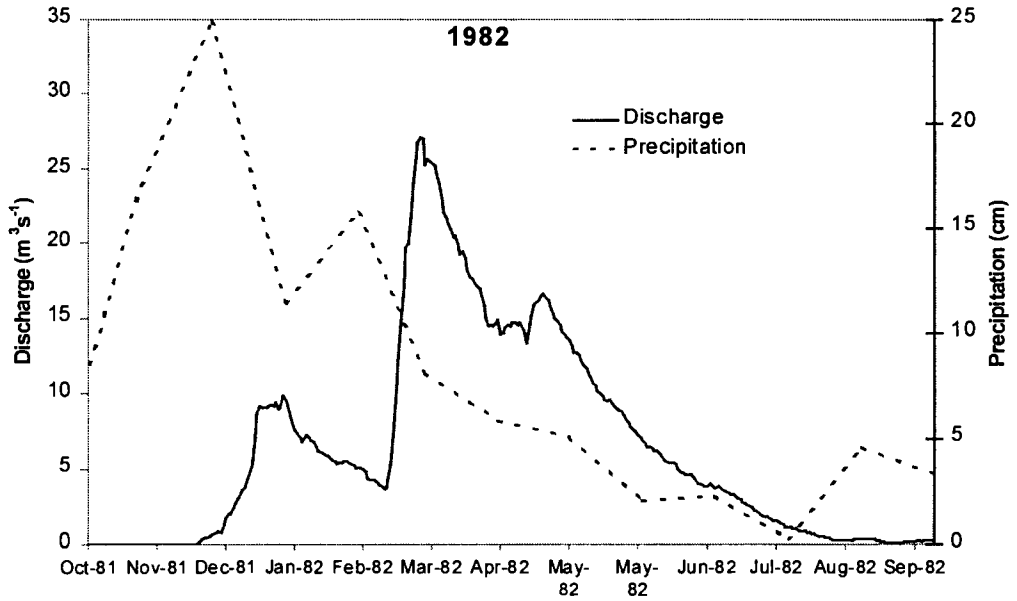
- Illian, J. R., 1970, Interim report on the ground water in the Klamath Basin Oregon: State Engineer, 110p.
- Komar, P. D., 1989, Flow-competence evaluations of the hydraulic parameters of floods: An assessment of the technique, *in* Beven, K., and Carling, P., eds., *Floods-Hydrological, sedimentological, and geomorphological implications*: Chichester, England, John Wiley and Sons, p. 107-134.
- Lawrence, R. D., 1976, Strike-slip faulting terminates the Basin and Range province in Oregon: *Geological Society of America Bulletin*, v. 87, p. 846-850.
- Lee, C. L., and Cummings, M. L., in preparation, *Geologic Map of the Soloman Butte quadrangle, Klamath County, Oregon*: Oregon Department of Geology and Mineral Industries, scale 1:24000.
- Lienau, P. J., and Lund, J. W., 1993, Groundwater anomalies associated with the Klamath Basin earthquakes of September 20-24, 1993: *Geo-Heat Center Quarterly Bulletin*, v. 15, no. 2, p. 17-19
- Leonard, A. R., and Harris, A. B., 1974, Ground water in selected areas in the Klamath Basin, Oregon: *Oregon State Engineer Ground Water Report no. 21*, 104 p.
- McDowell, P. F., and Dugas, D. P., 1996, Holocene eolian and lake level variations in the Oregon Great Basin., *in* Benson, L., ed., *Ongoing Paleoclimatic Studies in the Northern Great Basin*, U.S. Geological Survey Water Resources Investigation Circular 1119, p. 53-54.
- McKee, C. O., Johnson, R. W., Lowenstein, P. L., Riley, S. J., Blong, R. J., De Saint Ours, P., and Talai, B., 1985, Rabaul Caldera, Papua New Guinea: Volcanic hazards, surveillance, and eruption contingency planning: *Journal of Volcanology and Geothermal Research*, no. 23, p. 195-237.
- Mehring, P. J., Jr, and Wigand, P. E., 1986, Holocene history of Skull Creek dunes, Catlow Valley, southeastern Oregon, U.S.A.: *Journal of Arid Environments*, v. 11, p. 117-138.

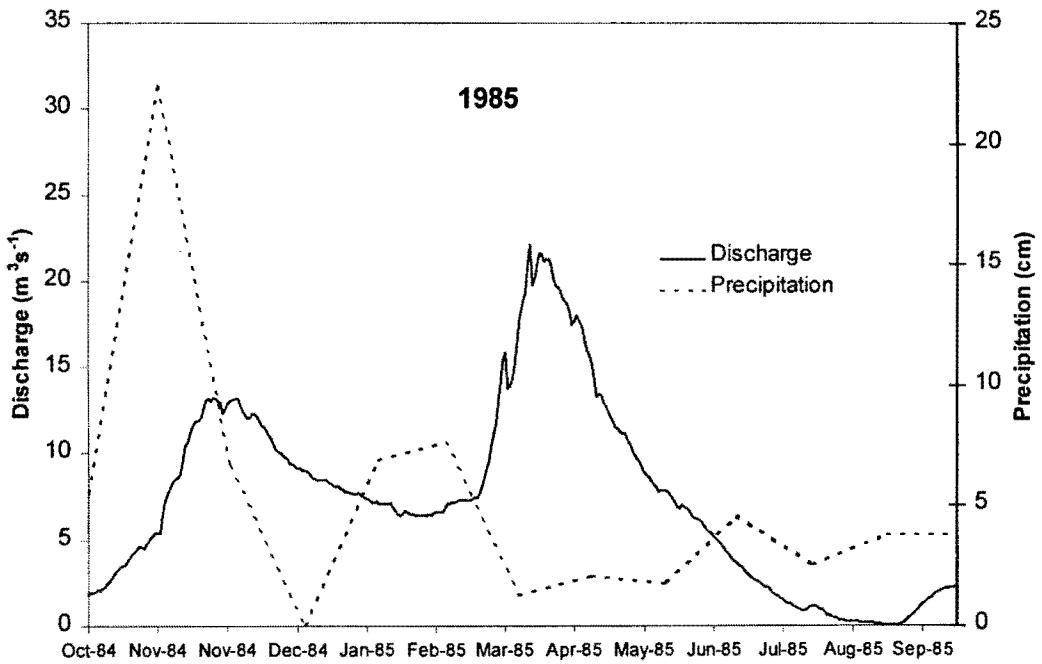
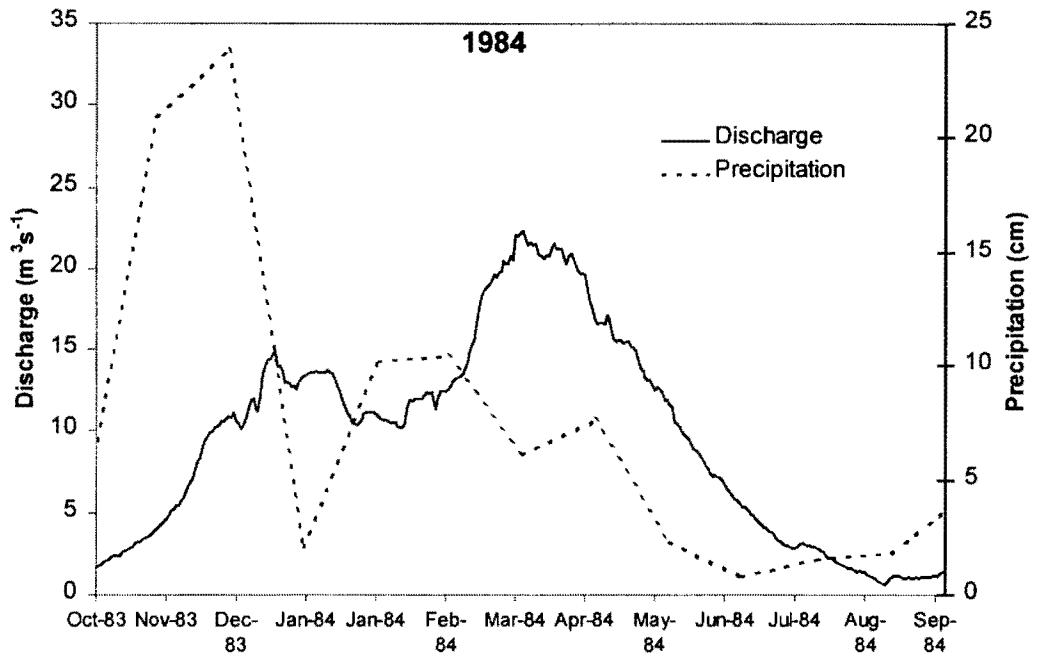
- Meinzer, D. E., 1922, Map of Pleistocene lakes of the Basin and Range Province and its significance: Geological Society of America Bulletin, v. 33, p. 541-542.
- O'Connor, J. E., 1993, Hydrology, hydraulics, and geomorphology of the Bonneville flood: Geological Society of America Special Paper 274, 83 p.
- Orr, E. L., Orr, W. N., and Baldwin, E. M., 1992, Geology of Oregon: Dubuque, Iowa, Kendall/Hunt, 254 p.
- Petty, W. H., Delcourt, P. A., and Delcourt, H. R., 1994, Holocene lake-level fluctuations and beach-ridge development along the northern shore of Lake Michigan, USA, *in* AMQUA special issue; II, Journal of Paleolimnology, Minneapolis, MN, p. 147-169.
- Priest, G. R., 1990, Volcanic and tectonic evolution of the Cascade volcanic Arc, Central Oregon: Journal of Geophysical Research, v. 95, no. B12, p. 19,583-19,599.
- Richards, A. F., 1958, Transpacific distribution of floating pumice from Isla San Benedicto, Mexico: Deep-Sea Research, v. 5, no. 1, p. 29-35.
- Riggs, H. C., and Harvey, K. D., 1990, Temporal and spatial variability of streamflow, *in* Wolman, M. G., and Riggs, H. C., eds., Surface Water Hydrology: The Geology of North America v. O-1: Boulder, Colorado, Geological Society of America, p. 81-96
- Russell, I. C., 1885, Geological history of Lake Lahontan, a Quaternary lake of northwestern Nevada: U.S. Geological Survey Monograph 11, 288 p.
- Sherrod, D. R., and Pickthorn, L. B. G., 1992, Geologic map of the west half of the Kamath Falls 1° by 2° quadrangle, south-central Oregon: U. S. Geological Survey Miscellaneous Investigation Series Map I-2182, scale 1:250,000.
- Snyder, C. T., Hardman, G., and Zdeneck, F. F., 1964, Pleistocene lakes in the Great Basin: U.S. Geological Survey Miscellaneous Geologic Investigations Map I-416, scale 1:1,000,000.

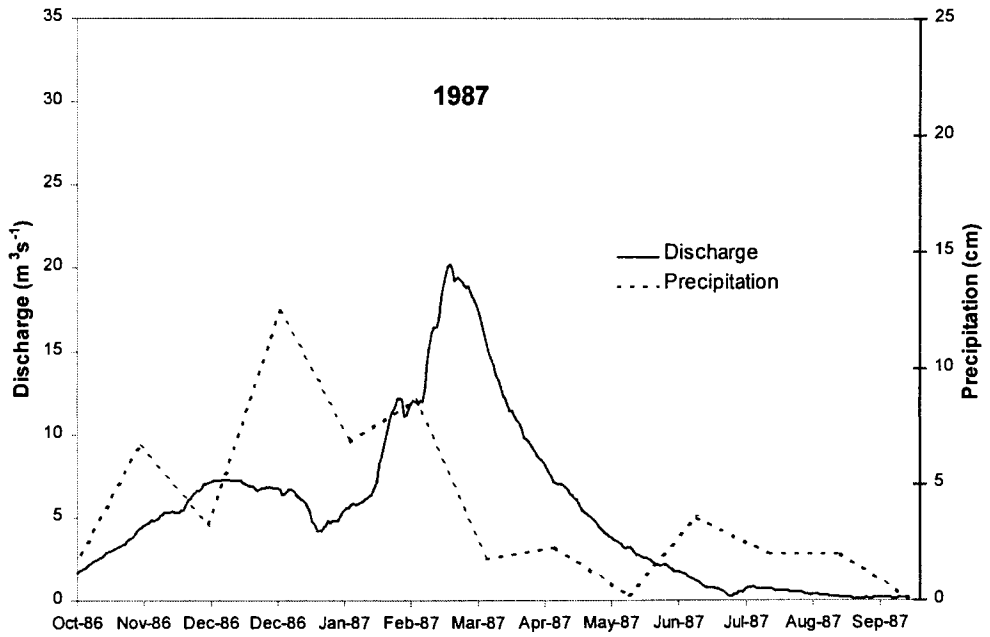
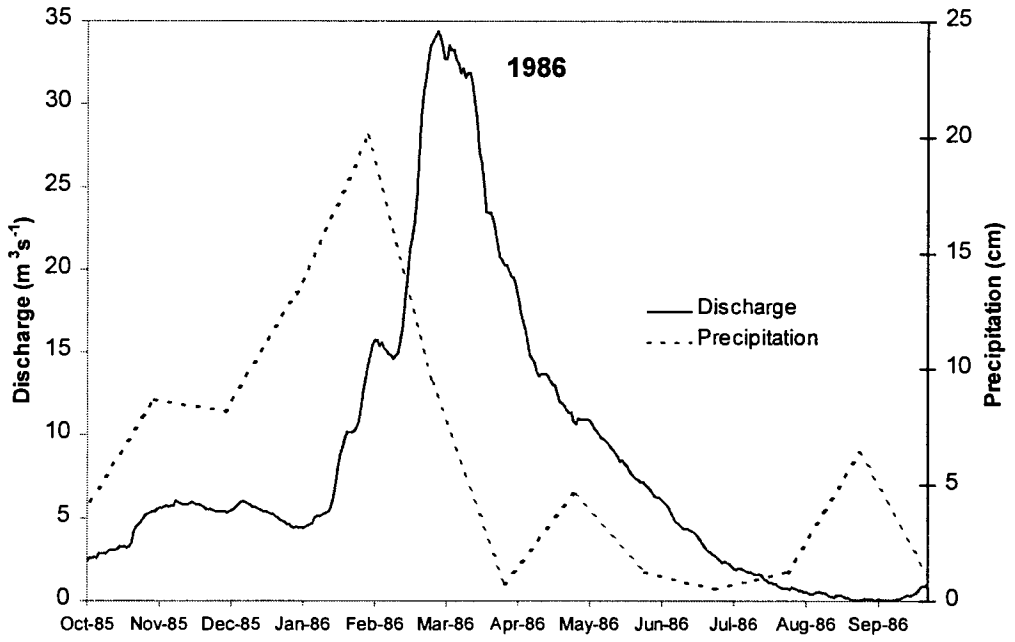
- Stilwell, K. B., 1995, Quaternary glacial geology, shoreline morphology, and tephrochronology of the Iliamna/Naknek/Brooks Lake area, Southwestern Alaska [Masters thesis]: Utah State, 176 p.
- Swanson, F. J., Oyagi, N., and Tominaga, M., 1986, Landslide dams in Japan, *in* Schuster, R. L., ed., Landslide dams-Processes, risk, and mitigation, American Society of Civil Engineers Geotechnical Special Publication 3, p. 131-145.
- USDA, 1999. SNOWTEL data site. <http://crystal.or.nrcs.usda.gov/snowsurveys/>, accessed 03 November 1999. A copy is available from the author.
- U.S. Geological Survey, 1999, Stream gauge data. <http://waterdata.usgs.gov/nwis-/OR/data.components/hist.cgi?statnum=11493500>, accessed 03 November 1999. A copy is available from the author
- Walder, J. S., and O'Connor, J. E., 1997, Methods for predicting peak discharge of floods caused by failure of natural and constructed earthen dams: *Water Resources Research*, v. 33, no. 10, p. 2337-2348.
- Walker, G. W., and MacLeod, N. S., 1991, Geologic map of Oregon, 92-38134: U.S. Geological Survey, scale 1:500,000.
- Waythomas, C. E., Walder, J. S., McGimsey, R. G., and Neal, C. A., 1996, A catastrophic flood caused by drainage of a caldera lake at Aniakchak Volcano, Alaska, and implications for volcanic hazards assessment: *Geological Society of America Bulletin*, v. 108, no. 7, p. 861-871.
- Whitham, A. G., and Sparks, R. S. J., 1986, Pumice: *Bulletin of Volcanology*, v. 48, p. 209-223
- Williams, H., 1942, The geology of Crater Lake National Park, Oregon: Carnegie Institute of Washington, Publication no. 540, 162 p.
- Young, S. R., 1990, Physical volcanology of Holocene airfall deposits from Mount Mazama, Crater Lake, Oregon [Ph.D. Dissertation]: University of Lancaster, 307 p.

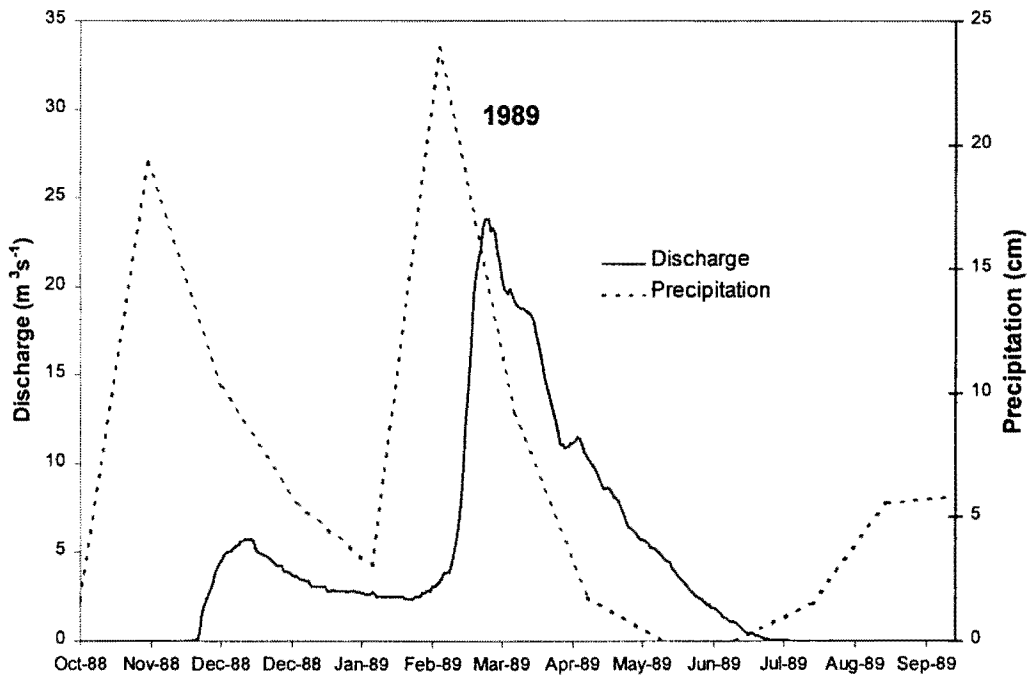
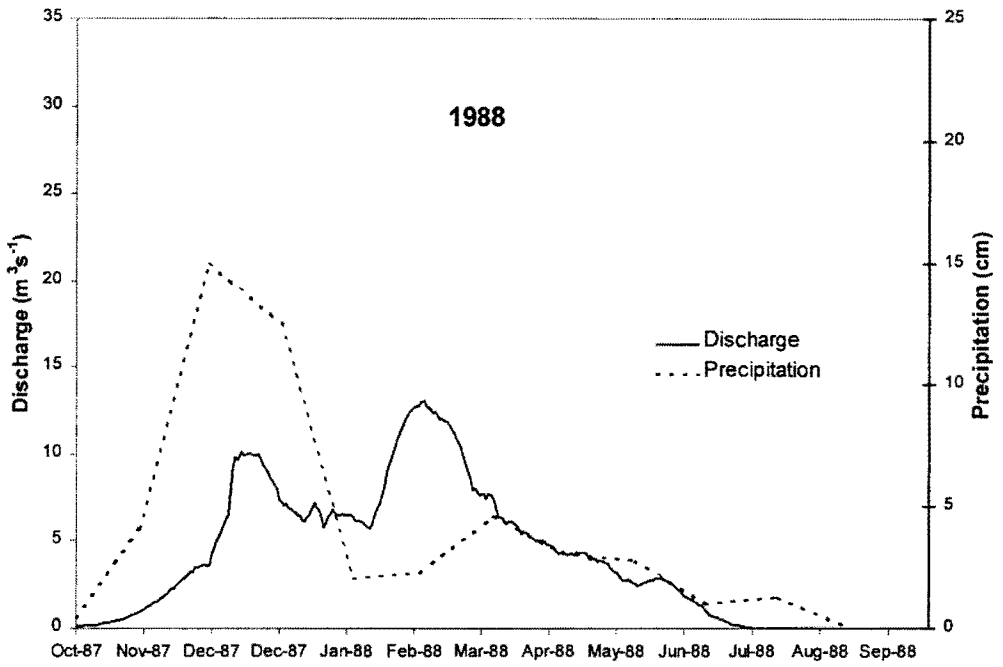
Zdanowicz, C. M., Zielinski, G. A., and Germani, M. S., 1999, Mount Mazama eruption: Calendrical age verified and atmospheric impact assessed: *Geology*, v. 27, no. 7, p. 621-624.

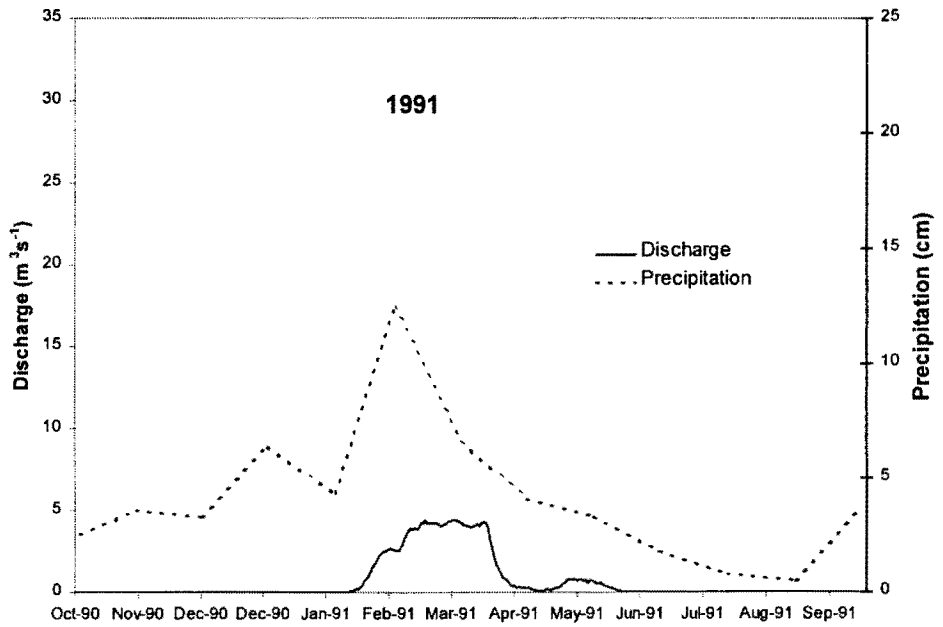
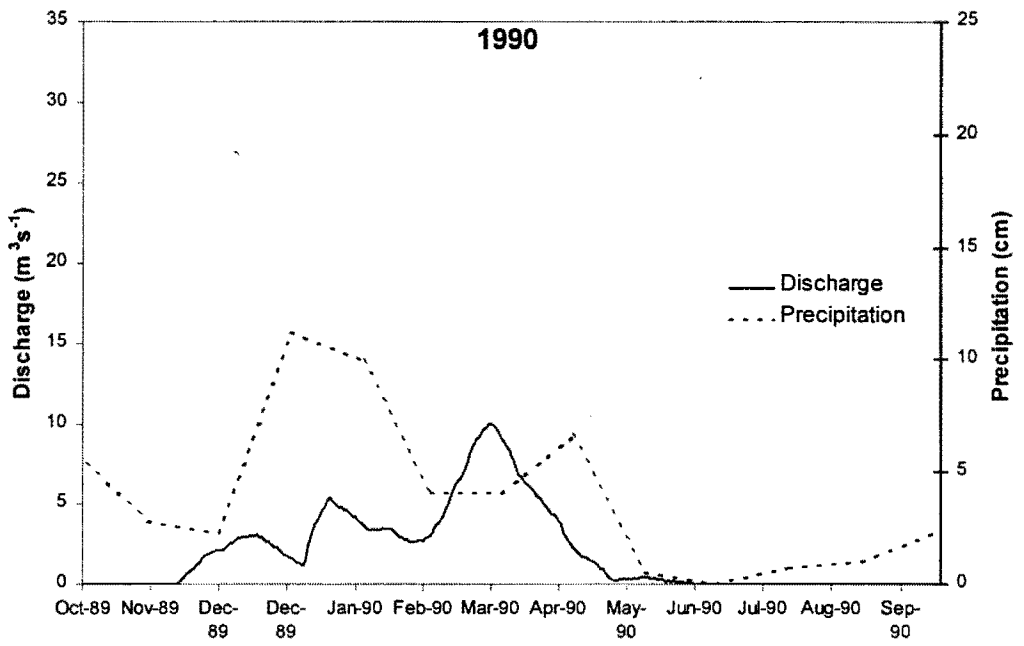
Appendix B: Discharge and Precipitation Plots

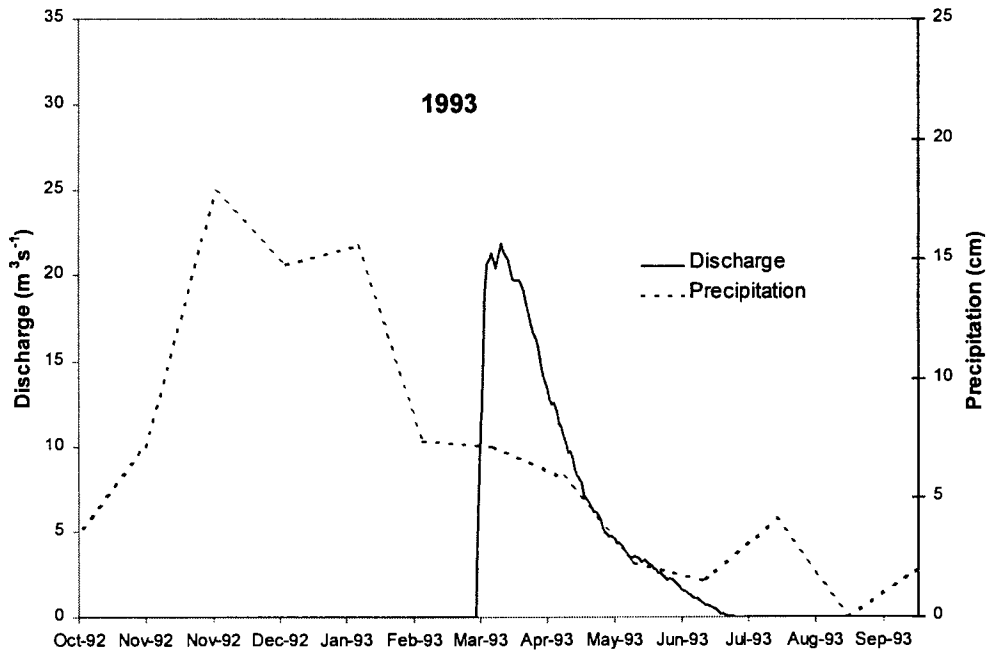
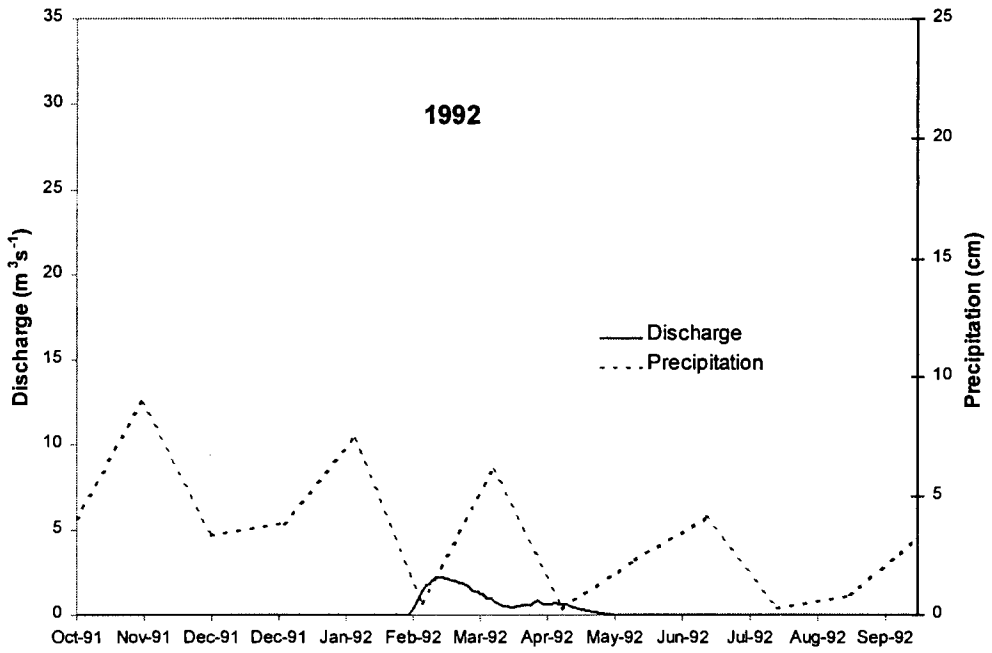


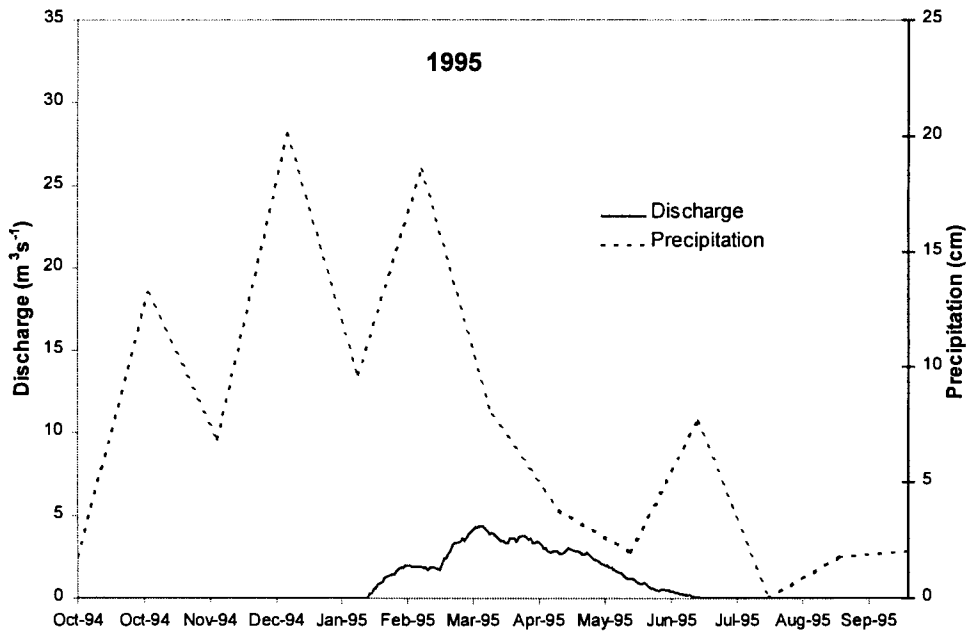
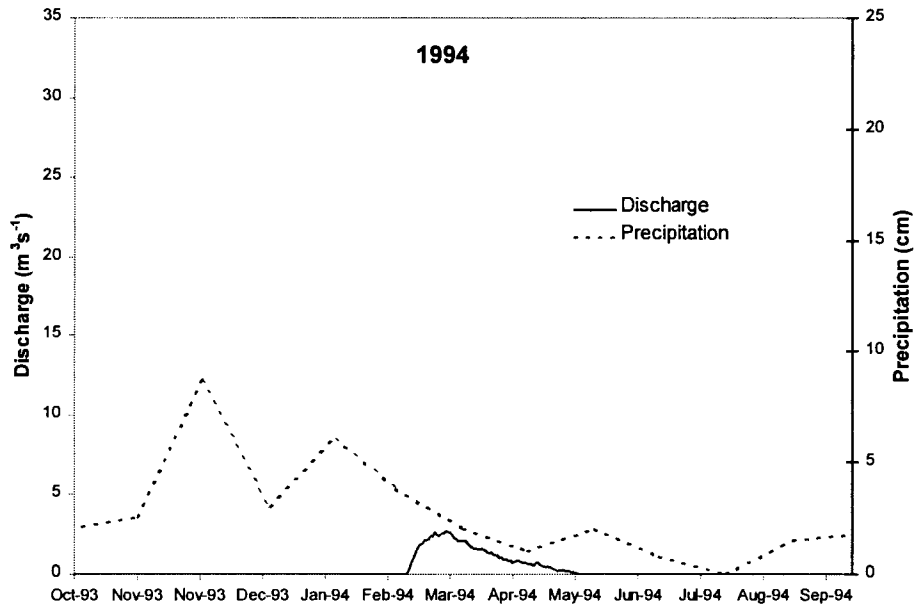


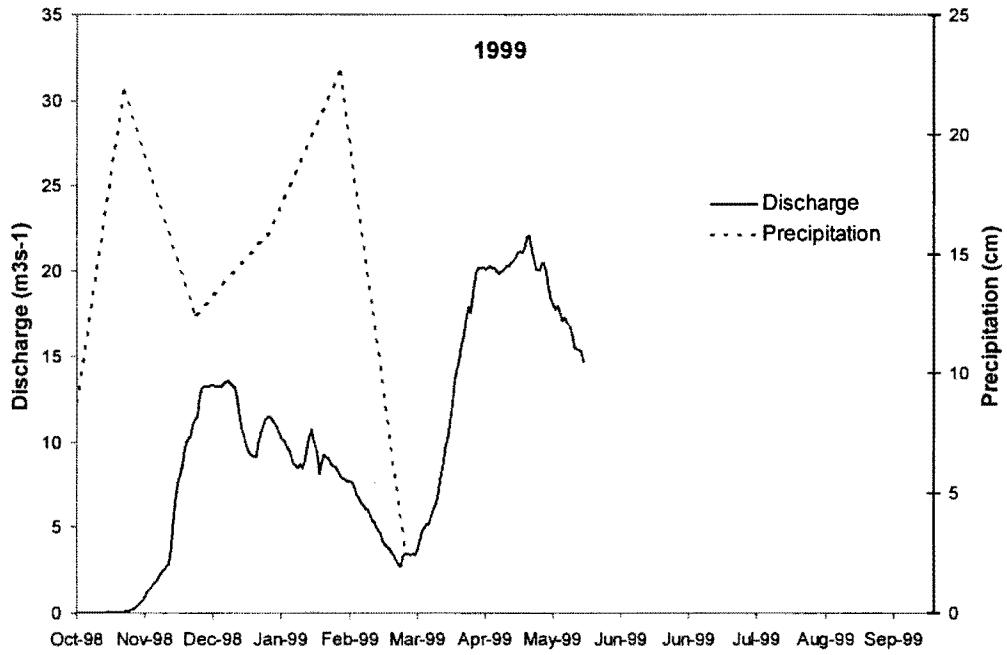












Appendix C: Selected well logs

State well No. 34S/7E-10

Location: NE ¼ NE ¼ Section: 10 T. 34S R.7E

Descriptive location: Southeast of Collier State Park

Year: 1976

Yield: 50 gal/min with 1 ft of drawdown after 1 hour

Static Level (ft): 5

Well Log (depths are in feet, SWL= static water level)

| <i>Material</i> | <i>From</i> | <i>To</i> | <i>SWL</i> |
|-----------------|-------------|-----------|------------|
| Top soil | 0 | 2 | |
| Pumice Sand | 2 | 5 | |
| Brown clay | 5 | 24 | |
| Blue clay | 24 | 48 | |
| Sandy blue clay | 48 | 90 | 5 |
| Blue clay | 90 | 140 | 5 |
| Sandy blue clay | 140 | 195 | 5 |
| Soft brown rock | 195 | 198 | 5 |

State well No. 34S/7E-10bb

Location: SE ¼ SE ¼ Section: 10 T. 34S R. 7E

Descriptive location: Southeast of Collier State Park

Year: 1980

Yield: 30 gal/min with 130 ft of drawdown after 1 hour

Static Level (ft): 1

Well Log (depths are in feet, SWL= static water level)

| <i>Material</i> | <i>From</i> | <i>To</i> | <i>SWL</i> |
|------------------|-------------|-----------|------------|
| Sandy top soil | 0 | 2 | |
| Pumice sand | 2 | 6 | |
| Brown clay | 6 | 10 | |
| Sandy brown clay | 10 | 12 | |
| Brown clay | 12 | 22 | |
| Blue clay | 22 | 28 | |
| Sandy blue clay | 28 | 30 | 1 |
| Blue claystone | 30 | 70 | |

| | | | |
|------------------------------------|-----|-----|---|
| Blue clay and streaks of sandstone | 70 | 78 | 1 |
| Claystone | 78 | 103 | |
| Sandstone | 103 | 105 | |
| Blue clay | 105 | 128 | |
| Black sand | 128 | 133 | 1 |
| Blue clay | 133 | 135 | |

State well No. :01109

Location: SE ¼ SW ¼ Section: 2 T. 34S R. 7E

Descriptive location: Near Collier State Park

Year: 1996

Yield: 10 gal/min with 35 ft of drawdown

Static Level (ft): 6

Well Log (depths are in feet, SWL= static water level)

| <i>Material</i> | <i>From</i> | <i>To</i> | <i>SWL</i> |
|--|-------------|-----------|------------|
| Top soil | 0 | 6 | |
| Brown clay and black sand | 6 | 10 | |
| Brown clay | 10 | 14 | |
| gray clay | 14 | 23 | |
| Gray clay with streaks of fine black sand | 23 | 32 | |
| Gray clay | 32 | 54 | |
| Gray clay with streaks of black sand and sandstone | 54 | 72 | 6 |
| Gray clay | 72 | 75 | |

State well No. 34S/7E-2dd

Location: SE ¼ SE ¼ Section: 2 T. 34S R. 7E

Descriptive location: South of Williamson River Canyon

Year: 1975

Yield: 16 gal/min with 60 ft of drawdown after 1 hour

Static Level (ft): 140

Well Log (depths are in feet, SWL= static water level)

| <i>Material</i> | <i>From</i> | <i>To</i> | <i>SWL</i> |
|-----------------|-------------|-----------|------------|
| Pumice top soil | 0 | 6 | |

| | | | |
|-------------------------|-----|-----|-----|
| Brown clay | 6 | 20 | |
| Pumice gravel | 20 | 30 | |
| Brown clay | 30 | 34 | |
| Blue clay | 34 | 46 | |
| Brown clay | 46 | 93 | |
| Blue clay | 93 | 197 | |
| Hard blue clay | 197 | 327 | |
| Blue clay | 327 | 370 | |
| Sandy clay | 370 | 380 | |
| Coarse sand | 380 | 385 | 140 |
| Rock and sand | 385 | 390 | |
| Blue clay | 390 | 420 | |
| Layers of rock and sand | 420 | 435 | 140 |

State well No.34S/7E-2od

Location: SW ¼ SE ¼ Section: 2 T. 34S R. 7E

Descriptive location: south of Williamson River Canyon

Year: 1978

Yield: 25 gal/min with ? ft of drawdown after 1 hour

Static Level (ft): 12

Well Log (depths are in feet, SWL= static water level)

| <i>Material</i> | <i>From</i> | <i>To</i> | <i>SWL</i> |
|--|-------------|-----------|------------|
| Pumice | 0 | 6 | |
| Yellow chalk or clay | 6 | 27 | |
| Grey clay | 27 | 50 | |
| Black semi hard sand | 50 | 90 | |
| Grey clay | 90 | 120 | |
| Black semi hard sand | 120 | 124 | 12 |
| Grey clay | 124 | 135 | |
| Semi hard sand with hard streaks of clay | 135 | 200 | 12 |

State well No. 33/7-35

Location: ¼ ¼ Section: 35 T. 33 R. 7E

Descriptive location: Mouth of Williamson River canyon

Year: 1967

Yield: 45 gal/min with 0 ft of drawdown after 2 hours

Static Level (ft): 15

Well Log (depths are in feet, SWL= static water level)

| Material | From | To | SWL |
|-------------------------------------|------|----|-----|
| Brown sandy topsoil | 0 | 3 | |
| Brownish pumice sand | 3 | 7 | |
| Basalt river boulders | 7 | 11 | |
| Brownish pumice stone | 11 | 15 | |
| Brown clay stone | 15 | 22 | |
| Coarse river boulders and gravel | 22 | 39 | 15 |
| Soft black sandstone | 39 | 44 | |
| Brown shale and gravel conglomerate | 44 | 77 | |

State well No. 34S/7E-2bb

Location: NW ¼ NW ¼ Section: 2 T. 34S R. 7E

Descriptive location: National Forest Campground

Year: 1984

Yield: 27 gal/min with drill stem at 50ft

Static Level (ft): 3

Well Log (depths are in feet, SWL= static water level)

| Material | From | To | SWL |
|----------------------------------|------|-----|-----|
| Brown sandy soil and pumice | 0 | 15 | |
| Pumice and streaks of green clay | 15 | 40 | |
| Gray shale | 40 | 85 | |
| Black sandstone | 85 | 110 | |
| Gray shale | 110 | 130 | |
| Black sandstone | 130 | 140 | |

State well No. 34

Location: ¼ SW ¼ Section: 2 T. 34S R. 7E

Descriptive location: South of Forest Service campground

Year: 1993

Yield: 20 gal/min with drill stem at 50 ft for 1 hour

Static Level (ft): 13

Well Log (depths are in feet, SWL= static water level)

| <i>Material</i> | <i>From</i> | <i>To</i> | <i>SWL</i> |
|--|-------------|-----------|------------|
| Brown pumice | 0 | 16 | |
| White pumice and black sand | 16 | 28 | 12 |
| White pumice and coarse gravel | 28 | 34 | 12 |
| Blue clay | 34 | 48 | |
| Blue clay with streaks of black sand | 48 | 75 | 13 |
| Gray clay | 75 | 94 | |
| Gray clay with streaks of black sand and sandstone | 94 | 196 | 13 |

State well No. 32S/8E-30ab

Location: NW ¼ NE ¼ Section: 30 T. 32S R. 8E

Descriptive location: East of Hwy 97 and north of Kirk Sill

Year: 1982

Yield: 20 gal/min with 4 ft of drawdown after 1 hour

Static Level (ft): 54

Well Log (depths are in feet, SWL= static water level)

| <i>Material</i> | <i>From</i> | <i>To</i> | <i>SWL</i> |
|---|-------------|-----------|------------|
| Top soil | 0 | 1 | |
| Lava rock | 1 | 2 | |
| Pumice boulders | 2 | 14 | |
| Layers of sand ,gravel, clay and pumice | 14 | 337 | 54 |

State well No. 32S/8E-32ba

Location: NE ¼ NW ¼ Section: 32 T. 32S R. 8E

Descriptive location: north end of Soloman Butte quadrangle

Year: 1988

Yield: 4 gal/min with drill stem at 100 ft for 1 hour

Static Level (ft): 67

Well Log (depths are in feet, SWL= static water level)

| <i>Material</i> | <i>From</i> | <i>To</i> | <i>SWL</i> |
|-----------------|-------------|-----------|------------|
| Top soil | 0 | 3 | |
| Pumice and clay | 3 | 18 | |
| Soft brown rock | 18 | 24 | |

| | | | |
|------------------------|-----|-----|----|
| Hard black rock | 24 | 43 | |
| Brown lava rock | 43 | 67 | |
| Black lava rock | 67 | 79 | 67 |
| Bubbly brown lava rock | 79 | 109 | |
| Black lava rock | 109 | 221 | |

State well No. 31s/8E-25dd

Location: SE ¼ SE ¼ Section: 25 T. 31S R. 8E

Descriptive location: Wocus Butte

Year: 1977

Yield: 40 gal/min with 20 ft of drawdown after 1 hour

Static Level (ft): 35

Well Log (depths are in feet, SWL= static water level)

| <i>Material</i> | <i>From</i> | <i>To</i> | <i>SWL</i> |
|-----------------|-------------|-----------|------------|
| Pumice | 0 | 5 | |
| Brown clay | 5 | 35 | |
| Blue clay | 35 | 120 | |
| Black rock | 120 | 135 | 35 |

State well No. 32S/8E-19cd

Location: SE ¼ SW ¼ Section: 19 T. 32S R. 8E

Descriptive location: East of Hwy 97 and North of Kirk Sill

Year: 1980

Yield: 15 gal/min with 13 ft of drawdown after 1 hour

Static Level (ft): 47

Well Log (depths are in feet, SWL= static water level)

| <i>Material</i> | <i>From</i> | <i>To</i> | <i>SWL</i> |
|--------------------|-------------|-----------|------------|
| Pumice top soil | 0 | 5 | |
| Brown conglomerate | 5 | 15 | |
| Crevised rock | 15 | 35 | |
| Hard rock | 35 | 37 | |
| Crevised rock | 37 | 45 | |
| Hard rock-black | 45 | 60 | |
| Fractured rock | 60 | 65 | 47 |

State well No. 31s/9e/10cc

Location: SW ¼ SW ¼ Section: 10 T. 31S R. 9E

Descriptive location: Silver lake Hwy in Military Crossing quad

Year: 1992

Yield: 30 gal/min with drill stem at 30 ft for 1 hour

Static Level (ft): 15

Well Log (depths are in feet, SWL= static water level)

| Material | From | To | SWL |
|----------------------------------|------|-----|-----|
| Brown clay | 0 | 3 | |
| Brown pumice | 3 | 22 | 11 |
| White pumice and brown sand | 22 | 35 | 11 |
| sandy brown clay and sandstone | 35 | 48 | |
| Brown sandstone and black sand | 48 | 70 | 15 |
| Sandy brown clay and fine gravel | 70 | 102 | 15 |
| Yellow clay and fine gravel | 102 | 120 | 15 |
| Brown sandstone and yellow clay | 120 | 127 | 15 |
| Black lava rock | 127 | 128 | 15 |

State well No. 31s/9e-10cad

Location: NE ¼ SW ¼ Section: 10 T. 31S R. 9E

Descriptive location: Silver lake Hwy in Military Crossing quad

Year: 1985

Yield: 30 gal/min with drill stem at 154 ft for 1 hour

Static Level (ft): 81

Well Log (depths are in feet, SWL= static water level)

| Material | From | To | SWL |
|----------------------|------|-----|-----|
| Light brown pumice | 0 | 9 | |
| Gray pumice | 9 | 16 | |
| Dark pumice, brown | 16 | 34 | |
| Reddish brown pumice | 34 | 61 | |
| Cemented gravel | 61 | 74 | |
| Brown and gray lava | 74 | 154 | 81 |

State well No. 34/7-4G

Location: SW ¼ NE ¼ Section: 4 T. 34S R. 7E

Descriptive location: Northwest of Collier State Park

Year: 1959

Yield: 20 gal/min artesian flow

Static Level (ft): 15

Well Log (depths are in feet, SWL= static water level)

| <i>Material</i> | <i>From</i> | <i>To</i> | <i>SWL</i> |
|--------------------|-------------|-----------|------------|
| Top soil loam | 0 | 3 | |
| Yellow hard pan | 3 | 4 | |
| Pumice | 4 | 7 | |
| Black mud and sand | 7 | 15 | |
| Burnt log | 15 | 16 | |
| Yellow clay | 16 | 21 | |
| Blue clay | 21 | 42 | |
| Blue sand (fine) | 42 | 43 | |
| Gray shale | 43 | 60 | |
| Brown sandstone | 60 | 63 | |
| Gray shale | 63 | 66 | |
| Brown shale | 66 | 71 | |
| Pink shale | 71 | 97 | |
| Black sand | 97 | 97.6 | |
| Pink clay | 97.6 | 165 | |
| Sand black (fine) | 165 | 167 | |
| Pink clay | 167 | 182 | |
| Sand | 182 | 188 | |
| Blue clay | 188 | 251 | |
| Blue sand | 251 | 251.6 | |
| Blue clay | 188 | 251 | |
| Blue sand | 251 | 251.6 | |
| Blue clay | 251.6 | 287 | |
| Blue sand | 287 | 304 | |
| Blue clay | 304 | 307 | |
| Blue sand | 307 | 311 | |
| Clay | 311 | 318 | |
| Black sand | 318 | 322 | |
| Blue clay | 322 | 341 | |

| | | | |
|---------------------|-----|-----|--|
| Black sand | 341 | 347 | |
| Blue clay | 347 | 364 | |
| Black sand | 364 | 365 | |
| Blue clay | 365 | 382 | |
| Blue sand (coarse) | 382 | 384 | |
| Blue clay | 384 | 400 | |
| Gray clay | 400 | 418 | |
| Lava sand (coarse) | 418 | 424 | |
| Gray(sticky) Clay | 424 | 452 | |
| Black sand | 452 | 453 | |
| Gray clay | 453 | 478 | |
| Black sand (coarse) | 478 | 487 | |
| Gray clay | 487 | 496 | |
| Black sand | 496 | 498 | |
| Gray clay | 498 | 518 | |
| Black sand | 518 | 519 | |
| Gray clay (sticky) | 519 | 581 | |
| Black sand | 581 | 583 | |
| Gray clay (sticky) | 583 | 609 | |
| Lava sand | 609 | 615 | |
| Gray clay | 615 | 621 | |
| Black sand (fine) | 621 | 638 | |

State well No. 32s/8e-17ab

Location: NW ¼ NE ¼ Section: 17 T. 32S R. 8E

Descriptive location: East of the Williamson River, North of Soloman Flat

Year: 1976

Yield: 4000 gal/min with 79 ft of drawdown after 4 hours

Static Level (ft): 4

Well Log (depths are in feet, SWL= static water level)

| <i>Material</i> | <i>From</i> | <i>To</i> | <i>SWL</i> |
|-----------------------------|-------------|-----------|------------|
| Top soil | 0 | 2 | |
| Pumice | 2 | 27 | 4 |
| Pea gravel, sand and pumice | 27 | 32 | 4 |
| Gray pumice and clay | 32 | 44 | 4 |

| | | | |
|---------------------------------|-----|-----|---|
| Brown sand and pumice | 44 | 64 | 4 |
| Sand, gravel and small boulders | 64 | 70 | 4 |
| Sand and gravel | 70 | 122 | 4 |
| Brown clay | 122 | 126 | 4 |
| Gray sandstone | 126 | 139 | 4 |
| Gray lava | 129 | 164 | 4 |
| Brown sandstone | 164 | 184 | 4 |
| Gray lava | 184 | 205 | 4 |
| Red and gray bubbly lava | 205 | 250 | 4 |
| Brown talc | 250 | 253 | 4 |
| Red lava | 253 | 264 | 4 |
| Red and gray lava | 264 | 278 | 4 |
| Gray lava | 278 | 316 | 4 |
| Brown lava | 316 | 326 | 4 |
| Brown clay and sand | 326 | 340 | 4 |

State well No. 34s/7e-4a

Location: ¼ NE ¼ Section: 4 T. 34S R. 7E

Descriptive location: Spring Creek Ranch Motel West of Hwy 97, N of Collier State Park

Year: 1981

Yield: 200 gal/min artesian flow

Static Level (ft): Artesian

Well Log (depths are in feet, SWL= static water level)

| <i>Material</i> | <i>From</i> | <i>To</i> | <i>SWL</i> |
|--|-------------|-----------|------------|
| Pumice | 0 | 26 | |
| Blue clay | 26 | 53 | |
| Sandy brown claystone with streaks of brown sand | 53 | 98 | Artesian |
| Blue clay | 98 | 145 | |
| Blue clay with streaks of black sand | 145 | 260 | Artesian |
| Brown clay | 260 | 262 | |
| Black rock | 262 | 263 | |

State well No. 33s/7e-35dc

Location: SW ¼ SE¼ Section: 35 T. 33S R. 7E

Descriptive location: Mouth of the Williamson River canyon

Year: 1978

Yield: 20 gal/min with 12 ft of drawdown after 1 hour

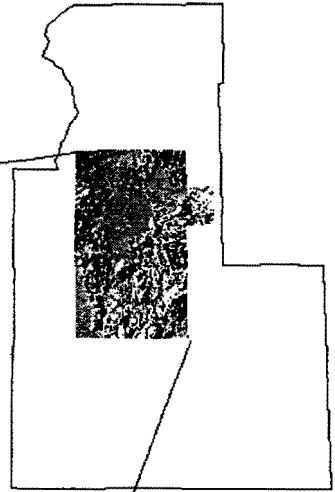
Static Level (ft): 14

Well Log (depths are in feet, SWL= static water level)

| <i>Material</i> | <i>From</i> | <i>To</i> | <i>SWL</i> |
|-------------------------------|-------------|-----------|------------|
| Pumice, top soil and boulders | 0 | 3 | |
| Boulders | 3 | 20 | |
| Gravel | 20 | 32 | 14 |

Appendix D

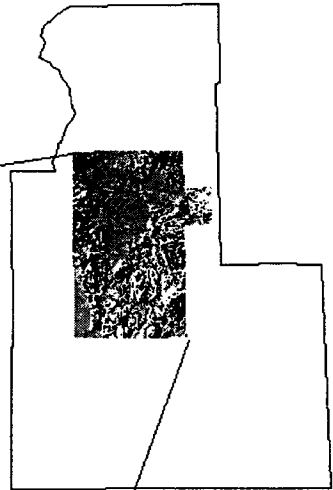
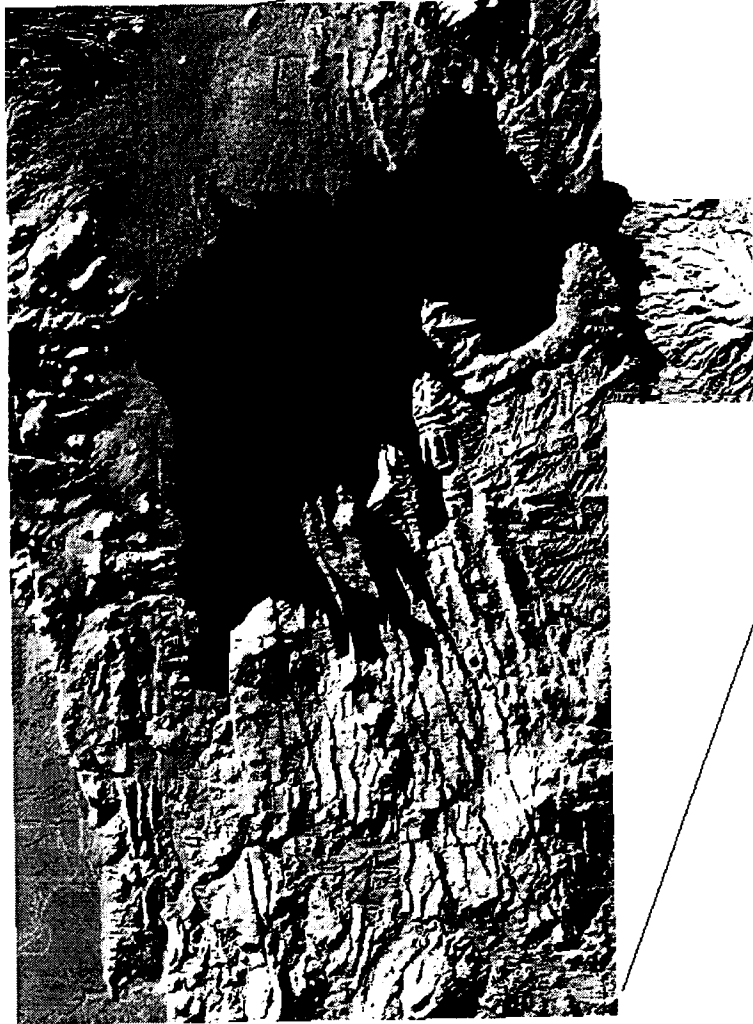
Projection of Pleistocene
terrace elevation



9 0 9 18 Kilometers

A horizontal scale bar with alternating black and white segments. The markings are labeled '9', '0', '9', and '18 Kilometers' from left to right, indicating a total length of 18 kilometers.

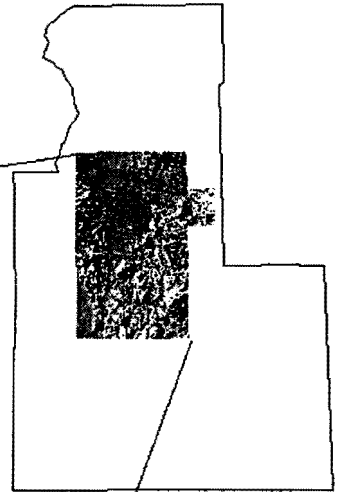
Projection of middle Holocene
terrace elevation



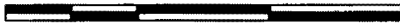
9 0 9 18 Kilometers

A scale bar with markings at 9, 0, 9, and 18 kilometers. The bar is divided into segments corresponding to these values.

Projection of late Holocene
terrace elevation



9 0 9 18 Kilometers

A horizontal scale bar with alternating black and white segments, used to indicate distance in kilometers.

Appendix E

Soloman Butte Hand Augers

| Auger | Easting (m) | Northing (m) | Depth cm | Description |
|---------|---|--------------|----------|--|
| SB01 | 594850 | 4724000 | 0-80 | pyroclastic fall deposits |
| | | | 80-85 | paleosol and basalt cobbles |
| SB02 | 595665 | 4730346 | 0-221 | pink pyroclastic fall deposits with 2-3% gravel sized pumice clasts |
| | | | 221-222 | lithic rich sand. Lithics are subangular and predominately quartz and feldspars |
| | | | 222-500 | greyish brown sandy ash with ~5% rounded pumice clasts up to 3.5 cm in diameter |
| SB03 | 594015 | 4724242 | 0-70 | pyroclastic flow deposits, unable to determine if they have been reworked |
| | | | 70 | water table |
| SB04 | 593924 | 4723849 | 0-50 | rounded pumice clasts within ash/sand matrix |
| | | | 50-200 | clasts are 1 cm in diameter ash with ~ 50% clasts that are up to 4 cm in diameter |
| | | | 200 | water table |
| SB05 | 593621 | 4723627 | 0-74 | rounded pumice clasts up to 1 cm in diameter in ash/sand matrix |
| | | | 74 | Cobbles |
| SB06 | 593508 | 4723641 | 0-20 | 2 cm rounded pumice clasts in ash/sand matrix |
| | | | 20-50 | up to 5 cm rounded pumice clasts in ash matrix |
| | | | 50-80 | rounded clasts up to 2 cm, thin lenses of sand |
| | | | 80-120 | rounded clasts of pumice up to 7 cm in ash/sand matrix |
| | | | 120-152 | 2-3 cm rounded pumice clasts in ash/sand matrix |
| | | | 152-170 | up to 5 cm rounded pumice clasts in ash/sand matrix |
| 170-185 | subrounded 3-4 cm basalt clast | | | |
| 185-256 | rounded pumice and basalt clasts up to 5 cm within an ash/sand matrix | | | |